

A11100 992883

NAT'L INST OF STANDARDS & TECH R.I.C.



A11100992883

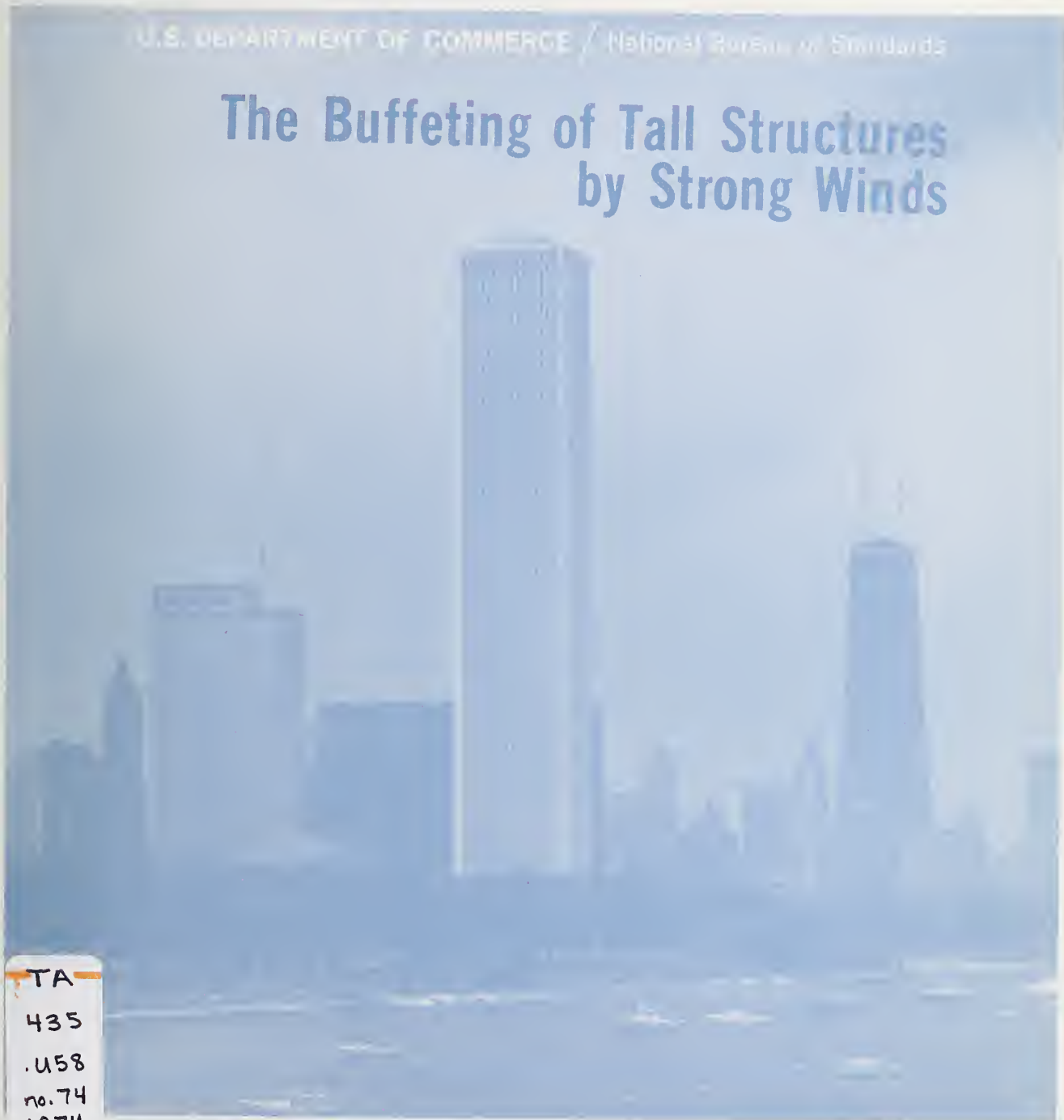
/NBS building science series
TA435 .U58 V74;1974 C.1 NBS-PUB-C 1974



NBS BUILDING SCIENCE SERIES 74

U.S. DEPARTMENT OF COMMERCE / National Bureau of Standards

The Buffeting of Tall Structures by Strong Winds



TA

435

.U58

no. 74

1974

c. 2

NATIONAL BUREAU OF STANDARDS

The National Bureau of Standards¹ was established by an act of Congress March 3, 1901. The Bureau's overall goal is to strengthen and advance the Nation's science and technology and facilitate their effective application for public benefit. To this end, the Bureau conducts research and provides: (1) a basis for the Nation's physical measurement system, (2) scientific and technological services for industry and government, (3) a technical basis for equity in trade, and (4) technical services to promote public safety. The Bureau consists of the Institute for Basic Standards, the Institute for Materials Research, the Institute for Applied Technology, the Institute for Computer Sciences and Technology, and the Office for Information Programs.

THE INSTITUTE FOR BASIC STANDARDS provides the central basis within the United States of a complete and consistent system of physical measurement; coordinates that system with measurement systems of other nations; and furnishes essential services leading to accurate and uniform physical measurements throughout the Nation's scientific community, industry, and commerce. The Institute consists of the Office of Measurement Services, the Office of Radiation Measurement and the following Center and divisions:

Applied Mathematics — Electricity — Mechanics — Heat — Optical Physics — Center for Radiation Research: Nuclear Sciences; Applied Radiation — Laboratory Astrophysics² — Cryogenics² — Electromagnetics² — Time and Frequency².

THE INSTITUTE FOR MATERIALS RESEARCH conducts materials research leading to improved methods of measurement, standards, and data on the properties of well-characterized materials needed by industry, commerce, educational institutions, and Government; provides advisory and research services to other Government agencies; and develops, produces, and distributes standard reference materials. The Institute consists of the Office of Standard Reference Materials, the Office of Air and Water Measurement, and the following divisions:

Analytical Chemistry — Polymers — Metallurgy — Inorganic Materials — Reactor Radiation — Physical Chemistry.

THE INSTITUTE FOR APPLIED TECHNOLOGY provides technical services to promote the use of available technology and to facilitate technological innovation in industry and Government; cooperates with public and private organizations leading to the development of technological standards (including mandatory safety standards), codes and methods of test; and provides technical advice and services to Government agencies upon request. The Institute consists of the following divisions and Centers:

Standards Application and Analysis — Electronic Technology — Center for Consumer Product Technology: Product Systems Analysis; Product Engineering — Center for Building Technology: Structures, Materials, and Life Safety; Building Environment; Technical Evaluation and Application — Center for Fire Research: Fire Science; Fire Safety Engineering.

THE INSTITUTE FOR COMPUTER SCIENCES AND TECHNOLOGY conducts research and provides technical services designed to aid Government agencies in improving cost effectiveness in the conduct of their programs through the selection, acquisition, and effective utilization of automatic data processing equipment; and serves as the principal focus within the executive branch for the development of Federal standards for automatic data processing equipment, techniques, and computer languages. The Institute consists of the following divisions:

Computer Services — Systems and Software — Computer Systems Engineering — Information Technology.

THE OFFICE FOR INFORMATION PROGRAMS promotes optimum dissemination and accessibility of scientific information generated within NBS and other agencies of the Federal Government; promotes the development of the National Standard Reference Data System and a system of information analysis centers dealing with the broader aspects of the National Measurement System; provides appropriate services to ensure that the NBS staff has optimum accessibility to the scientific information of the world. The Office consists of the following organizational units:

Office of Standard Reference Data — Office of Information Activities — Office of Technical Publications — Library — Office of International Relations — Office of International Standards.

¹ Headquarters and Laboratories at Gaithersburg, Maryland, unless otherwise noted; mailing address Washington, D.C. 20234.

² Located at Boulder, Colorado 80302.

The Buffeting of Tall Structures by Strong Winds

OF STANDARDS
LIBRARY

NOV 26 1975

OPS Building Science Series, No. 74.

Emil Simiu

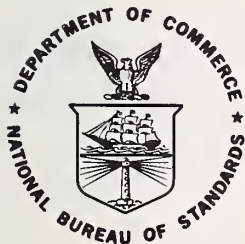
Center for Building Technology
Institute for Applied Technology
National Bureau of Standards
Washington, D.C. 20234

and

Daniel W. Lozier

Institute for Basic Standards
National Bureau of Standards
Washington, D.C. 20234

Front Cover: Standard Oil of Indiana Building, Chicago.
Courtesy of Standard Oil of Indiana. (Edward D. Stone,
Perkins and Will, Architects; Perkins and Will, Structural
Engineers; E. Alfred Picardi, Chief Engineer)



U.S. DEPARTMENT OF COMMERCE, Rogers C. B. Morton, Secretary

James A. Baker, III, Under Secretary

Dr. Betsy Ancker-Johnson, Assistant Secretary for Science and Technology

NATIONAL BUREAU OF STANDARDS, Ernest Ambler, Acting Director

Issued October 1975

Library of Congress Cataloging in Publication Data

Simiu, Emil.

The Buffeting of Tall Structures by Strong Winds.

(National Bureau of Standards Building Science Series; 74)

Includes bibliographical references.

Supt. of Docs. No.: C 13.29:2/74.

I. Wind-pressure. 2. Structural dynamics. 3. Tall buildings.
4. Buildings—Aerodynamics. I. Lozier, Daniel W., joint author.
II. Title. III. Series: United States. National Bureau of Standards. Building Science Series; 74.

TA435.U58 No. 74 [TA654.5] 690'.08s [690'.2] 75-30727

National Bureau of Standards Building Science Series 74

Nat. Bur. Stand. (U.S.), Bldg. Sci. Ser. 74, 90 pages (Oct. 1975)

CODEN: BSSNBV

U.S. GOVERNMENT PRINTING OFFICE
WASHINGTON: 1975

For sale by the Superintendent of Documents, U.S. Government Printing Office, Washington, D.C. 20402
(Order by SD Catalog No. C13.29:2/74). Price \$1.55 (Add 25 percent additional for other than U.S. mailing).

The Buffeting of Tall Structures by Strong Winds

Emil Simiu and Daniel W. Lozier

Certain shortcomings of current procedures for computing alongwind structural response have been shown to result in unrealistic estimates of tall building behavior under the action of strong winds. Differences between predictions of fluctuating response based on various such procedures may be as high as 200%. In recent years, advances in the state of the art have been made which provide a basis for significantly improved alongwind response predictions. The purpose of the present work is to present a procedure for calculating alongwind response which incorporates and utilizes these advances. The basic structural, meteorological and aerodynamic models employed are described, and expressions for the alongwind deflections and accelerations, consistent with those models, are derived. A computer program is presented for calculating the alongwind response of structures with unusual modal shapes or for which the contribution of the higher modes to the response is significant. For more common situations, a simple procedure is presented which makes use of graphs and on the basis of which rapid manual calculations of the alongwind deflections and accelerations can be performed. Numerical examples are given to illustrate the use of the computer program and of the graphs. Results of numerical calculations are used to discuss some of the approximations and errors inherent in the models employed.

KEY WORDS: Accelerations; buffeting; building codes; buildings; deflections; dynamic response; gust factors; structural engineering; wind engineering; wind loads.

ACKNOWLEDGMENTS

The writers wish to acknowledge useful comments and suggestions by R. D. Marshall, R. A. Crist and R. A. Grot of the Center for Building Technology. They also wish to express their appreciation to S. Haber of the Applied Mathematics Division for his advice on the numerical techniques employed in the computer program.

TABLE OF CONTENTS

Page

Abstract.	iii
Acknowledgments	iii
List of Symbols	vi
List of Figures	ix
List of Tables.	x
1. Introduction.	1
2. Structural, Meteorological and Aerodynamic Models. Alongwind Deflections and Accelerations	2
2.1 Structural Behavior.	2
2.2 The Atmospheric Boundary Layer	3
2.2.1 Horizontally Homogeneous Flow	3
2.2.2 Mean Wind Profiles.	4
2.2.3 Relation between Wind Speeds in Different Roughness Regimes	6
2.2.4 The Power Law Model	7
2.2.5 Longitudinal Velocity Fluctuations.	8
2.3 Mean and Fluctuating Pressures	10
2.3.1 Relation between Wind Pressures and Wind Speeds	10
2.3.2 Cross-Spectra of Fluctuating Pressures.	12
2.3.3 Results of Pressure Measurements.	14
2.4 Alongwind Deflections and Accelerations.	16
2.4.1 Mean Response	18
2.4.2 Fluctuating Response: Deflections and Accelerations.	19
3. Computer Program for Calculating Alongwind Deflections and Accelerations.	20
3.1 Description of the Computer Program.	20
3.2 Integration Procedure.	23
4. Simplified Procedure for Calculating Alongwind Deflections and Accelerations.	25
4.1 Introduction	25
4.2 Basic Assumptions.	26
4.3 Total Fluctuating Response as a Sum of Background and Resonant Contributions.	26
4.4 Alongwind Deflections and Accelerations.	29
4.4.1 Mean Response	29
4.4.2 Fluctuating Response: Deflections and Accelerations.	30
4.5 Numerical Example.	40
4.6 Comparison between Gust Response Factors Calculated Using Various Current Procedures	43
5. Approximations and Errors in the Estimation of the Alongwind Response	54
5.1 Contribution of Higher Vibration Modes to the Response	54
5.2 Influence upon Calculated Response of the Deviation from a Straight Line of Fundamental Modal Shape.	56
5.3 Influence upon Calculated Response of Errors in the Estimation of the Roughness Length	56
5.4 Spectra in the Lower Frequency Range and Alongwind Response.	56
5.5 Acrosswind Correlation of the Pressures and Alongwind Response	58
6. Conclusions	61
References	62
APPENDIX: Computer Program Listing. Sample Input and Output	67

LIST OF SYMBOLS

\bar{a}, a', \ddot{a}	= Mean deflection, fluctuating deflection, acceleration of structure, respectively.
$a_{\max}, \ddot{a}_{\max}$	= Maximum probable deflection, maximum probable acceleration, respectively.
A	= Area
A_w, A_ℓ	= Area of windward, of leeward side, respectively.
B	= Building width
\mathcal{B}	= Function defined by Eqs. 4.19, 4.27.
C_D	= Drag coefficient ($C_D = C_w + C_\ell$)
C_p	= Mean pressure coefficient
C_w, C_ℓ	= Mean pressure coefficient on windward, on leeward side, respectively.
$C_{lw}, C_w', C_{\ell l}, C_\ell'$	= Pressure coefficients defined by Eqs. 2.27a, 2.27b.
C_y, C_z	= Exponential decay coefficients (Eq. 2.18)
D	= Depth (alongwind dimension) of building
f, f_s, f_1	= Similarity (Monin) coordinate (Eq. 2.12), value of f beyond which Eq. 2.11 holds, peak similarity coordinate, respectively.
$\gamma, \gamma_f, \gamma_r$	= Nondimensionalized frequencies (Eq. 2.55 and 2.48)
$F_{P_1}(t)$	= Force acting at point P_1
g	= Acceleration of gravity = 9.81 m/s^2
$g_a(z), g_{\ddot{a}}(z)$	= Peak deflection, peak acceleration factor, respectively (Eqs. 2.36, 2.40).
$G(z), G_r$	= Functions defined by Eqs. 2.43, 2.45.
G.F.	= Gust factor (ratio of maximum probable deflection to mean deflection).
H	= Building height.
$H(z, P_1, n)$	= Mechanical admittance.
$H^*(z, P_1, n)$	= Complex conjugate of $H(z, P_1, n)$
I_{rrL}	= Function defined by Eq. 2.54
J	= Function defined by Eq. 4.17
J_L	= Function defined by Eq. 2.53
L_x	= Turbulence scale
M	= Point of ordinate z
m	= Mass of building per unit height

M_r	= Generalized mass (Eq. 2.4)
\tilde{M}_r	= Nondimensional generalized mass (Eq. 2.44)
n, n_r	= Frequency, natural frequency in the rth mode, respectively
$N_u(p_1, p_2, n)$	= Alongwind velocity cross-correlation coefficient
$N(p_1, p_2, n)$	= Alongwind pressure cross-correlation coefficient
$p, \bar{p}, p', p'_w, p'_\ell$	= Pressure, mean pressure, fluctuating pressure, fluctuating pressure on the windward, on the leeward side, respectively
r_w, r_ℓ	= Ratios defined by Eqs. 2.28a, 2.28b
r_i, \tilde{r}_i	= Ratios defined in Section 5.5
P_i	= Point of coordinates y_i, z_i
R_u, R_p	= Square root of acrosswind coherence function for longitudinal velocity fluctuations for pressure fluctuations, respectively.
\mathcal{R}	= Function defined by Eqs. 4.20, 4.28
$S_a, S_{\ddot{a}}, S_F, S_p, S_u$	= Spectral density of fluctuating response, of acceleration, of force, of pressure, of longitudinal velocity fluctuations, respectively
T, t	= Time
u	= Longitudinal velocity fluctuation
U	= Mean wind speed
u_*	= Friction velocity
\tilde{U}	= Nondimensionalized mean wind speed (Eq. 2.46)
v_f	= Fastest mile wind
w	= Weight of building per unit volume
y	= Horizontal coordinate in plane perpendicular to wind direction
Y	= y/B (Nondimensionalized coordinate)
Y_{rr}	= Function defined by Eq. 2.57
z	= Height above ground
Z	= z/H (Nondimensionalized coordinate)
z_o	= Roughness length
z_d	= Zero plane displacement
α	= Power law exponent (Eq. 2.9)
β	= Square of ratio between r.m.s of velocity fluctuation and friction velocity (Eq. 2.13)
γ	= Constant defining modal shape in Eq. 5.2

η_r	= Damping ratio in rth mode
$\mu_r(z)$	= Modal shape in r-th mode
ω_r	= Circular frequency in r-th mode (Eq. 2.3)
ρ	= Air density $\approx 1.25 \text{ kg/m}^3$
$v_a, v_{\ddot{a}}$	= Quantities defined by Eqs. 2.37, 2.41, 4.22, 4.24
ξ, ξ_1	= Quantities defined by Eq. 2.26b, Eq. 4.30, respectively.

LIST OF FIGURES

	<u>Page</u>
2.1	Flow downwind of a surface roughness discontinuity (after Peterson [17]). . . 5
2.2	Ratios u_*/u_{*1} 6,31
2.3a,b	Spectra of longitudinal velocity fluctuations and spectra of fluctuating pressures at stagnation point [34] 13
4.1a,b,c	White noise spectrum, square of modulus of mechanical admittance, decaying spectral curve 27
4.2	Function $\tilde{\gamma}$ 33
4.3	Function $\tilde{\beta}$, $C_z = 10$, $C_y = 16$ 34
4.4	Function $\tilde{\gamma}_{11}$, $B/H = 0$, $C_z = 10$, $C_y = 16$ 35
4.5	Function $\tilde{\gamma}_{11}$, $B/H = 0.167$, $C_z = 10$, $C_y = 16$ 36
4.6	Function $\tilde{\gamma}_{11}$, $B/H = 0.4$, $C_z = 10$, $C_y = 16$ 37
4.7	Function $\tilde{\gamma}_{11}$, $B/H = 1.0$, $C_z = 10$, $C_y = 16$ 38
4.8	Function $\tilde{\gamma}_{11}$, $B/H = 3.0$, $C_z = 10$, $C_y = 16$ 39
4.9	Function $\tilde{\beta}$, $C_z = 6.3$, $C_y = 10$ 44
4.10	Function $\tilde{\gamma}_{11}$, $B/H = 0$, $C_z = 6.3$, $C_y = 10$ 45
4.11	Function $\tilde{\gamma}_{11}$, $B/H = 0.4$, $C_z = 6.3$, $C_y = 10$ 46
4.12	Function $\tilde{\gamma}_{11}$, $B/H = 1.0$, $C_z = 6.3$, $C_y = 10$ 47
4.13	Function $\tilde{\gamma}_{11}$, $B/H = 3.0$, $C_z = 6.3$, $C_y = 10$ 48
4.14	Function $\tilde{\beta}$, $C_z = 4.0$, $C_y = 6.4$ 49
4.15	Function $\tilde{\gamma}_{11}$, $B/H = 0$, $C_z = 4.0$, $C_y = 6.4$ 50
4.16	Function $\tilde{\gamma}_{11}$, $B/H = 0.4$, $C_z = 4.0$, $C_y = 6.4$ 51
4.17	Function $\tilde{\gamma}_{11}$, $B/H = 1.0$, $C_z = 4.0$, $C_y = 6.4$ 52
4.18	Function $\tilde{\gamma}_{11}$, $B/H = 3.0$, $C_z = 4.0$, $C_y = 6.4$ 53
5.1	Modal Shapes 55

LIST OF TABLES

	<u>Page</u>
2.1 Suggested Values of z_o for Various Types of Exposure.	4
2.2 Approximate Ratios of Probable Maximum Speed Averaged over Period t to that Averaged over One Hour (in Open Terrain).	5
2.3 Estimated Ratios of Design Pressures to Measured Pressures near the Stagnation Point for Various Buildings	16
4.1 Values of k_1, k_2, k_3	32
4.2 Values of $\frac{z_o}{H}, \frac{z_d}{H}$ Corresponding to Various γ_{11} Curves	32
5.1 Description of Buildings Selected as Case Studies	54
5.2 Percent Contribution of Higher Modes of Vibration to Root Mean Square of Fluctuating Response	55
5.3 Deflections and Accelerations for Various Roughness Lengths	57
5.4 Ratios $[a_{max}]_{f_1} / [a_{max}]_{0.03}$	58
5.5 Ratios of Response for Various Values C_z, C_y to Response Calculated Using $C_z = 10, C_y = 16$	60

Chapter 1. INTRODUCTION

Following an increasing recognition of the importance in tall building design of the dynamic effects due to the gustiness of wind, several procedures for computing alongwind response have been proposed in the last decade [1, 2, 3]. ^{1/} The purpose of these procedures is to calculate equivalent static wind loads whose effect upon the structure is the same as that of the gusty wind.

As part of an effort aimed at evaluating and improving building code provisions on design for wind loads, an analysis of current procedures for computing alongwind structural response - including the procedures described in the American National Standard A58.1 [4] and in the National Building Code of Canada [5, 6] - has been presented in Ref. 7. From this analysis, the following points emerged. First, the alongwind cross-correlation of the fluctuating pressures is represented in current procedures by models which are fundamentally inadequate: in Ref. 6 it is assumed that pressures on the windward and leeward faces are perfectly correlated to each other, whereas in Ref. 4 the reduction factor expressing the alongwind correlation of these pressures, rather than being applied to their cross-spectrum alone, is in effect applied to the entire response [8]. It is primarily for this reason that the differences between the values of the fluctuating part of the response calculated in accordance with the A58.1 Standard, on the one hand, and the National Building Code of Canada, on the other hand, may in certain cases be as high as 200% [7]. Second, current procedures do not take into account the dependence of the longitudinal wind velocity spectra upon height above ground. This was shown to result in significant overestimates of the components of the fluctuating velocity which produce resonant excitation in wind-sensitive structures [7, 9]. Third, current procedures do not enable the analyst to estimate the contribution of the higher vibration modes to the structural response. Fourth, most of the existing procedures do not provide an estimate of the alongwind accelerations induced in structures by gusty winds.

In the years following the development of the procedures described in Refs. 1, 2, 3, 4 and 6, developments of significance in the context of determining structural response to wind have taken place notably in the area of boundary layer meteorology. Progress has also been made in understanding and evaluating the effect of the alongwind pressure cross-correlations upon building response. Finally, efficient numerical methods have been developed, from which economical computer programs, suitable for the analysis of structures subjected to wind loads, could evolve. The purpose of this paper is to present a procedure which incorporates and utilizes these advances and thus results in improved estimates of alongwind response.

In the following chapters, the basic structural, meteorological and aerodynamic models employed in this work are discussed, and expressions for the alongwind deflections and accelerations, consistent with these models, are presented. An efficient procedure for carrying out the required integrations, and the main features of the computer program developed for the calculation of the alongwind response, are described. A complete listing of the computer program, and a sample input and output for the program, are included in an Appendix.

^{1/} Figures in brackets indicate the literature references at the end of the paper.

The use of the computer program is required in the case of structures with unusual modal shapes or for which the contribution of the higher modes to the response is significant. For more common situations, in which the fundamental modal shape may be approximated by a straight line and the contribution of the second and higher vibration modes may be neglected, a simple procedure is presented, which makes use of graphs and on the basis of which rapid manual calculations of the alongwind deflections and accelerations can be performed. Numerical examples are given to illustrate the use of the computer program and of the graphs. Results of numerical calculations are then used to discuss some of the approximations and errors inherent in the models employed.

Chapter 2. STRUCTURAL, METEOROLOGICAL AND AERODYNAMIC MODELS. ALONGWIND DEFLECTIONS AND ACCELERATIONS.

This chapter presents a description of the structural, meteorological and aerodynamic models required for the calculation of the alongwind structural response. Questions related to the definition of the wind climate for engineering design purposes are beyond the scope of this work and will therefore not be discussed herein.

2.1 Structural Behavior

The structure is assumed to be linear and elastic. Its deformation may then be expressed as a sum of products of modal shapes and generalized coordinates. To each of the r vibration modes, where $r = 1, 2, 3, \dots$ there corresponds a modal shape $\mu_r(z)$, where $z =$ height above ground, a natural frequency ω_r and a mechanical damping ratio η_r . The deformation $y(z,t)$ at point M (or ordinate z) of the structure under the action of a force $F(P_1,t)$ acting at point P_1 (or ordinate z_1) can then be written as

$$y(z,t) = \sum_r \mu_r(z) y_r(t) \quad (2.1)$$

in which the generalized coordinates $y_r(t)$ are the solutions of the equations

$$\ddot{y}_r(t) + 2\omega_r \eta_r \dot{y}_r(t) + \omega_r^2 y_r(t) = \frac{1}{M_r} \mu_r(z_1) F(P_1,t) \quad (2.2)$$

$$\text{where } \omega_r = 2\pi n_r \quad (2.3)$$

$$M_r = \int_0^H \mu_r^2(z) m(z) dz \quad (2.4)$$

and $m(z) =$ mass of structure per unit of height.

Methods for calculating the modal shapes and the natural frequencies of structures are described, for example, in Ref. 10. Suggested values for the mechanical damping ratios for steel frames and reinforced concrete frames are 0.01 and 0.02, respectively [4,6]. Lower values of the mechanical damping ratios may have to be used, for example in the case of welded steel stacks or of certain prestressed concrete structures or of structures of the

framed tube type [6, 62]. In addition to the mechanical damping, the aerodynamic damping may, in principle, also be taken into account. The aerodynamic damping is associated with changes in the relative velocity of the air with respect to the building as the latter oscillates about its mean deformed position (see Ref. 32). It appears that it may be unconservative to rely upon the effect of the aerodynamic damping; for this reason, the latter is not taken into account in Refs. 4,6 and will also be neglected in this work.

2.2 The Atmospheric Boundary Layer

2.2.1 Horizontally Homogeneous Flow

For the purpose of estimating alongwind response it is useful and convenient to consider the model of a horizontally homogeneous boundary layer flow. Implicit in this model are the following assumptions:

1. At a sufficiently large height above ground, where the effects of the ground friction become negligibly small (i.e., at the level of the so-called gradient wind), the flow is horizontally homogeneous.
2. The terrain is horizontal.
3. The roughness of the terrain is uniform over a sufficiently large fetch.

The first of these assumptions may be applied in the case of large-scale, extratropical storms, but does not, strictly speaking, hold in the case of mature hurricanes or severe local storms such as thunderstorms. Indeed, in mature hurricanes, in the region of highest winds the curvature of the isobars is relatively large and the wind speeds depend upon distance from the center of the storm. It is presumably for these reasons that the hurricane mean wind profiles implicit in the Southern Building Code [11] (non-dimensionalized with respect to the mean speed at 10m above ground) differ markedly - on the unconservative side - from profiles associated with other types of storms. Recent research of a preliminary nature suggests, however, that in the lowest few hundred meters of the atmosphere, the differences between profiles corresponding to mature hurricanes, on the one hand, and to extratropical storms (i.e., to horizontally homogeneous flow), on the other hand, are relatively small and may be neglected in structural engineering applications [12].

Thunderstorm winds are caused by strong, localized downdrafts which spread over the ground in the manner of a wall jet [57]. The intensity of thunderstorm winds is therefore highly dependent upon distance from the center of the downdraft. Since the model which best describes the thunderstorm wind flow is of the wall jet, rather than of the parallel boundary layer type, it is likely that differences exist between mean wind profiles typical of thunderstorms, on the one hand, and of large-scale extratropical storms, on the other hand. It is also noted in this connection that the notion of gradient wind has no meaning in the case of thunderstorms. Nevertheless, in current building codes, it is tacitly assumed that the wind structure may be considered to be the same in thunderstorms as in large-scale, extratropical storms. The question as to whether this assumption is acceptable from an engineering viewpoint is one to which no clear answers are currently available and which merits careful research. Also, little information is available regarding the structure of the flow in non-horizontal terrain. Research into this question has been recently reported by Sacré [14].

The effect upon the flow of a change in roughness of terrain has been investigated by various writers, among whom Panofsky and Townsend [15], Taylor [16] and Peterson [17]; however, the results obtained so far do by no means appear to be definitive. A tentative result derived by Peterson [17] will be presented subsequently herein.

2.2.2 Mean Wind Profiles

It can be shown, on the basis of both theoretical and experimental results, that for high wind speeds the mean wind profile in the boundary layer of horizontally homogeneous flows may be described throughout the height range of interest to the structural engineer, by the relation [18,19,20,21,22]:

$$U(z) = 2.5 u_* \ln \frac{z - z_d}{z_o} \quad (2.5)$$

where $U(z)$ = mean speed at height z above ground, z_d = zero plane displacement, z_o = roughness length and u_* = friction velocity, given by

$$u_* = \frac{U(z_R)}{2.5 \ln \frac{z_R - z_d}{z_o}} \quad (2.6)$$

in which z_R is any given reference height. In meteorological work, the standard reference height is $z_R = 10\text{m}$. Eq. 2.5 is commonly referred to as the logarithmic law. Suggested values of the roughness length z_o are given in Table 2.1 (see Refs. 20,22,24). For example, at Sale, Australia, for terrain described as open grassland with few trees, at Cardington, England, for open farmland broken by a few trees and hedgerows, and at Heathrow Airport in London, $z_o \approx 0.08\text{m}$ [20,22,58,59]. At Cranfield, England, where the ground upwind of the anemometer is open for a distance of half a mile across the corner of an airfield, and where neighboring land is broken by small hedged fields, $z_o = 0.095\text{m}$ [20,60].

Table 2.1 - Suggested Values of z_o for
Various Types of Exposure

Type of Exposure	Coastal ^a	Open	Outskirts of Towns, Suburbs	Center of Towns	Centers of Large Cities
z_o (meters)	0.005-0.01	0.03-0.10	0.20-0.30	0.35-0.45	0.60-0.80

^aApplicable to structures directly exposed to winds blowing from open water.

The zero plane displacement may in all cases be assumed to be zero, except that in centers of large cities the smaller of the values $z_d = 20\text{m}$ and $z_d = 0.75\bar{h}$, where \bar{h} = average height of buildings in the surrounding area, may be used.

It has been estimated [19,20] and verified experimentally [21] that the logarithmic law is valid up to a height

$$z_{\log} \approx 0.03 \frac{u_*}{f}$$

where f is the Coriolis parameter. In terrain for which $z_0 \approx 0.07\text{m}$ and $U(10) = 26.8 \text{ m/s}$ (hourly mean), $u_* = 2.16 \text{ m/s}$ and, with $f \approx 10^{-4} \text{ s}^{-1}$, $z_{\log} \approx 650 \text{ m}$.

According to the National Building Code of Canada [6] the assumption that the exposure is suburban or urban may not be used in design unless the appropriate terrain roughness persists in the upwind direction for at least one mile. In the ANSI A58.1 Standard [4] it is suggested that the type of exposure corresponding to centers of large cities may be assumed only if the terrain is heavily built-up for at least one-half mile upwind of the structure, with at least 50% of the buildings being in excess of six stories. It can be seen that these criteria do not contain any provisions relating height above ground to length of fetch required for the assumption of horizontal homogeneity to hold. In this connection, Peterson [17] suggests that the flow downwind of a discontinuity can be divided into three zones, as shown in Fig. 2.1. In zone I, the velocity is essentially equal to the velocity upwind from the discontinuity. In zone III it may be assumed that the flow is adjusted to the new roughness conditions, i.e., is determined by the same parameters z_{02} , u_{*2} that would control the flow if the roughness length were everywhere z_{02} . In zone II, the flow varies gradually from line AB, where it is presumably nearly the same as upwind of the discontinuity, to line AC, where it may be described in terms of the parameters z_{02} , u_{*2} . Peterson's results were obtained on the basis of theoretical considerations alone and have not been verified experimentally. Further research into the question of the flow transition due to a change of terrain roughness is therefore believed to be necessary.

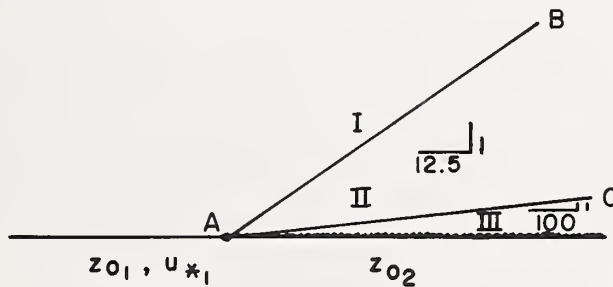


Fig. 2.1 - Flow downwind of a surface roughness discontinuity (after Peterson [17])

In designing tall buildings it is reasonable to use mean wind speeds averaged over a period of one hour [4,6]. If the mean winds U^t are averaged over periods t different from one hour, the mean winds U^h averaged over one hour may be obtained using Table 2.2 [56].

Table 2.2. Approximate Ratios of Probable Maximum Speed Averaged over Period t to that Averaged over One Hour (at 10m Above Ground in Open Terrain)

t (Seconds)	2	5	10	30	60	100	200	500	1000	3600
$\frac{U^t}{U^h}$	1.53	1.47	1.42	1.28	1.24	1.18	1.13	1.07	1.03	1.00

For values of t not included in Table 2.2, linear interpolation is permissible. If the wind speeds are given in terms of fastest miles, the averaging period t in seconds is given by $t = 3600/v_f$, where v_f is the fastest mile speed in miles per hour.

2.2.3 Relation between Wind Speeds in Different Roughness Regimes

Consider two adjacent terrains, each of sufficiently large fetch, the roughness lengths of which are denoted z_{o1} , z_o , respectively, and over which the mean wind speeds may be described, respectively, by Eqs. 2.7a and 2.7b:

$$U_1 = 2.5 u_{*1} \ln \frac{z - z_{d1}}{z_{o1}} \quad (2.7a)$$

$$U = 2.5 u_* \ln \frac{z - z_d}{z_o} \quad (2.7b)$$

It can be shown that the relation between the friction velocities u_{*1} , u_* can be written as:

$$\frac{u_*}{u_{*1}} = \left\{ \frac{A^2 + \left(\ln \frac{u_{*1}}{f z_{o1}} - C \right)^2}{A^2 + \left(\ln \frac{u_*}{f z_o} - C \right)^2} \right\}^{1/2} \quad (2.8)$$

in which f is the Coriolis parameter and A , C are meteorological constants determined experimentally [18,20]. For the purpose of calculating the ratios u_{*2}/u_{*1} , it may be assumed $A = 4.5$, $C = 0$; the error involved if these values are used can be shown to be negligibly small [20]. Since the dependence of Eq. 2.8 upon u_{*1} and f is very weak, the ratio u_{*2}/u_{*1} may be determined, for practical purposes, simply as a function of the roughness lengths z_{o1} , z_{o2} , as shown in Fig. 2.2. The following numerical example, in which the data are excerpted from Refs. 20, 22, illustrates the use of Fig. 2.2.

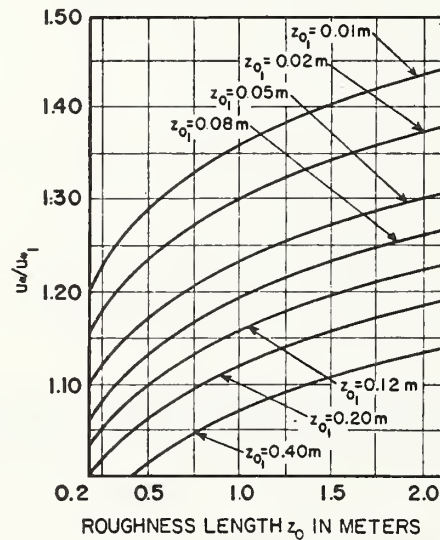


Fig. 2.2 - Ratios u_*/u_{*1}

At Heathrow airport (near London) $z_{o1} = 0.08\text{m}$, $z_{d1} = 0$, and the measured wind speed at 10m above ground was $U_1(10) = 11.7\text{m/s}$. Using Eq. 2.7a,

$$u_{*1} = \frac{11.7}{2.5 \ln \frac{10}{0.08}} = 0.968 \text{ m/s}$$

At the Post Office Tower (in the center of London) $z_o = 0.78\text{m}$ and $z_d = 21\text{m}$. From Fig. 2.2, $u_*/u_{*1} = 1.17$, i.e., $u_* = 1.13 \text{ m/s}$. The calculated value of the wind speed at $z = 195\text{m}$ at the Post Office Tower is then,

$$U(195) = 2.5 \times 1.13 \ln \frac{195-21}{0.78} = 15.3 \text{ m/s}$$

which coincides with the measured wind speed reported in Ref. 22.

It is also possible to obtain from Fig. 2.2 ratios u_*/u_{*1} for the case, $z_{o1} > z_o$. Thus, let $z_{o1} = 0.08\text{m}$ and $z_o = 0.01\text{m}$. Let $z_{o2} = 0.20\text{m}$. Then, for Fig. 2.2, $u_{*2}/u_* = 1.20$, $u_{*2}/u_{*1} = 0.06$. It follows that $u_*/u_{*1} = 1.06/1.20 \approx 0.88$.

2.2.4 The Power Law Model

Historically, the first representation of the mean wind profile in horizontally homogeneous terrain has been the so-called power law:

$$U(z) = U(z_R) \left(\frac{z}{z_R} \right)^\alpha \quad (2.9)$$

in which z_R is any given reference height and α is an exponent dependent upon the roughness of the terrain.

To calculate the relation between wind speeds over terrains with different exposures, an empirical model has been proposed according to which there corresponds to each of three standard exposures a given exponent in Eq. 2.9 and a given gradient height, independent of wind speed [1,2,3,4,6]. Criticisms of this model by various authors have been summarized in Ref. 20.

On the basis of recent experimental and theoretical atmospheric boundary layer research, it is now widely recognized that for high winds the logarithmic law is a superior representation of mean wind profiles in the lowest few hundred meters of the atmosphere [19,20,21, 22,23,24]. It is therefore the logarithmic law that will be used in the calculations performed herein. The logarithmic law has, in addition, the advantage of being consistent with the expression of the longitudinal velocity spectra. Indeed, as will be shown subsequently, the spectra are defined in terms of the friction velocity u_* and are thus implicit functions of z_o , z_d . Thus, if the power law is used, it is necessary that some approximate relation between the parameter, α , describing the mean wind profile, and the parameters z_o , z_d , characterizing the wind spectra, be assumed, since no unique relation between α and z_o , z_d , independent of z , z_R , exists. On the other hand, no such approximations are required - and the errors inherent in them are thus eliminated - if the mean profiles are described by the logarithmic law.

2.2.5 Longitudinal Velocity Fluctuations

In the methods for determining gust factors described in the ANSI A58.1 Standard [4] and in the National Building Code of Canada [6], the validity of the following expression for the wind spectrum is assumed:

$$\frac{n S_u(z, n)}{u_*^2} = 4 \frac{x^2}{(1 + x^2)^{4/3}} \quad (2.10)$$

in which n is the frequency in Hz, $S_u(z, n)$ = spectrum of longitudinal wind fluctuations, $x = 1,200n/U(10)$, $U(10)$ = mean speed at $z = 10$ m. (Some authors use the notation $\kappa U^2(10+z_d) = u_*^2$, where $\kappa = [0.4/\ln(10/z_0)]^2$ and z_0 is expressed in meters.) According to Eq. 2.10, $S_u(z, n)$ is independent of height. On the basis of both theoretical and experimental results, it has been established, however, that Eq. 2.10 does not reproduce correctly the dependence on z in the higher frequency part of the spectrum (see, for example, Ref. 25, p. 399), and that an excellent representation of this dependence is given by the relation [24,26,27,28]:

$$\frac{n S_u(z, n)}{u_*^2} = 0.26 f^{-2/3} \quad (2.11)$$

in which

$$f = n(z-z_d)/U(z) \quad (2.12)$$

is known as the Monin, or similarity, coordinate. For engineering purposes it may be assumed conservatively that Eq. 2.11 is valid for $f > 0.2$ [26].

In the lower frequency range, similarity breaks down and the spectra are not capable of being described by a universal relation [24,25,27]. A useful description may, however, be obtained, if it is remembered that (1) the one dimensional spectrum approaches a non-zero value as the frequency approaches zero; (2) the product $n S_u(n)$ reaches a maximum at some value $0 < f_1 < f_s$ (in which f_s is the value of f beyond which Eq. 2.11 is valid), i.e., the derivative of $n S_u(n)$ with respect to f vanishes at $f = f_1$; (3) the relation

$$\overline{u^2} = \int_0^\infty S_u(n) dn = \beta u_*^2 \quad (2.13)$$

in which $\overline{u^2}$ = mean square value of longitudinal velocity fluctuations, with $\beta \approx 6.0$ [1,3,4,29], holds.

The above requirements are satisfied by the curve

$$\frac{n S_u(n)}{u_*^2} = \frac{200f}{(1+50f)^{5/3}} \quad (2.14)$$

which also approximates very closely (from a designer's viewpoint, on the slightly conservative side) the spectrum in the higher frequency range (Eq. 2.11), and may therefore be used as a representation of the entire spectrum. Eq. 2.14 differs from a similar expression proposed by Kaimal et al [28] in that it satisfies Eq. 2.13 with $\beta \approx 6.0$, rather than $\beta = 4.75$ as in Ref. 28, and yields therefore more conservative estimates of the dynamic response.

In Eq. 2.14, $f_1 = 0.03$. In reality, the spectra in the low frequency range, and therefore the peak similarity coordinate f_1 , appear to vary strongly [27], indeed quite erratically [25], between sites and between atmosphere and laboratory. According to Owen [25], this unpredictable variation may be caused by meso-scale phenomena. Also, f_1 varies with height. According to available results of measurements [27,30], for neutral stratification--which prevails in strong winds-- $f_1 \approx 0.02-0.03$ at $z = 3-6m$, $f_1 \approx 0.025-0.04$ at $z = 15/20m$, $f_1 \approx 0.04-0.08$ at $z = 30-60m$, $f_1 \approx 0.1$ at $z = 90 m$. The question therefore arises as to whether the assumption $f_1 = 0.03$, which is implicit in Eq. 2.14, might not be the source of significant errors in the estimates of structural response. To answer this question, it is necessary to study the influence upon response of the variation of f_1 .

For this purpose, an alternative expression of the longitudinal spectra was developed which is consistent with the requirements previously described, but in which f_1 is a parameter that may be varied, rather than being a given constant as in Eq. 2.14. It is convenient, and as will be shown subsequently, sufficiently accurate for engineering purposes, to represent the spectra in the low frequency range as,

$$\frac{nS_u(z,n)}{u_*^2} = \frac{c_1 + a_1 f + b_1 f^2}{c_2 + a_2 f + b_2 f^2} \quad 0 \leq f < f_1 \quad (2.15)$$

$$\frac{nS_u(z,n)}{u_*^2} = \frac{c_1 + a_1 f + b_1 f^2}{c_2 + a_2 f + b_2 f^2} \quad f_1 < f \leq f_2 \quad (2.16)$$

The coefficients in Eqs. 2.15 and 2.16 result from the three conditions stated just before Eq. 2.13, and from the condition that Eqs. 2.15, 2.16, and 2.11 form a curve continuous at $f = f_1$ and $f = f_s$. Thus,

$$c_1 = 0$$

$$a_1 = 2b_1 f_1$$

$$a_2 = 2b_2 f_1$$

$$c_2 = \frac{(f_s - 2f_1)(\beta - \beta_1) - 2/3 \beta_1 (f_s/2 - 2f_1)}{(3/2 + \ln \frac{f_s}{f_1})(f_s - 2f_1) - (f_s/2 - 2f_1)}$$

$$b_2 = \frac{2/3 \beta_1 - c_2}{f_s (f_s - 2f_1)} \quad (\text{for } f_s \neq 2f_1)$$

$$b_2 = 2 \frac{2/3 \beta_1 (3/2 + \ln 2) - (\beta - \beta_1)}{f_s^2} \quad (\text{for } f_s = 2f_1)$$

$$b_1 = b_2 - c_2/f_1^2$$

in which

$$\beta_1 = 0.39 f_s^{-2/3}$$

To summarize: the spectra of the longitudinal velocity fluctuations may be described by Eq. 2.14, in which case it is implied that $f_1 = 0.03$, or, alternatively, by Eqs. 2.15, 2.16, 2.11, in which case the values of f_1 and f_s may be chosen as design parameters. It is reasonable (i.e., slightly conservative) to assume $f_s = 0.2$. Then, to assess the influence of the variation of f_1 upon the structural response, calculations may be carried out based on values of f_1 within the range $0 < f_1 < 0.2$.

The cross-spectrum of the longitudinal fluctuating velocities at two points P_1, P_2 may be expressed in the form:

$$S_u(P_1, P_2, n) = S_u^{1/2}(P_1, n) S_u^{1/2}(P_2, n) R_u(y_1, y_2, z_1, z_2, n) N_u(P_1, P_2, n) \quad (2.17)$$

in which y_i, z_i are the coordinates of point P_i ($i = 1, 2$) in a plane perpendicular to the direction of the mean wind. The functions R_u and N_u are defined as the acrosswind and the alongwind cross-correlation coefficient, respectively. By definition, if the points P_1, P_2 are in the same plane perpendicular to the mean wind direction, $N_u(P_1, P_2, n) \equiv 1$. Otherwise, $N_u(P_1, P_2, n) < 1$; its magnitude decreases as the alongwind separation between P_1, P_2 increases and as the frequency n increases. The acrosswind cross-correlation coefficient is a complex quantity, the modulus of which is known as the square root of the acrosswind coherence function [31]. However, its imaginary part has been determined by measurements to be negligible for wind engineering purposes [1,2,3,32]. The following expression for the acrosswind cross-correlation coefficient has been proposed by Davenport [3]:

$$R_u(y_1, z_1, y_2, z_2, n) = \exp \frac{-2n[C_z^2(z_1 - z_2)^2 + C_y^2(y_1 - y_2)^2]^{1/2}}{U(z_1) + U(z_2)} \quad (2.18)$$

On the basis of wind tunnel measurements, Vickery [3] suggested that it is reasonable to assume in engineering calculations $C_z = 10$, $C_y = 16$. Expressions for the acrosswind cross-correlation equivalent in practice to Eq. 2.18 with $C_z = 10$, $C_y = 16$ are presently used in building codes. It appears, however, that the exponential decay coefficients depend on surface roughness conditions [13], on height above ground and, quite strongly, on wind speed [63,64]. In open terrain, C_y may decrease by a factor of three if $U(10)$ decreases from 30m/s to 10m/s. C_z was also found to decrease as $U(10)$ decreases, although less than C_y . C_z also decreases as the height above ground increases. For example, for $z_1 = 110m$, $z_2 = 150m$, measured values of C_z were about one half as much as for $z_1 = 30m$, $z_2 = 80m$ (see Table 1 and Figs. 4 and 9 of Ref. 64). The dependence of the exponential decay coefficients upon terrain roughness, height above ground and wind speed is insufficiently documented and therefore represents a source of uncertainty in engineering calculations. Additional research in this area - both theoretical and experimental - is therefore believed to be necessary.

2.3 Mean and Fluctuating Pressures

2.3.1 Relation between Wind Pressures and Wind Speeds

The pressure acting at a point P of elevation z on the surface of a building immersed in a flow which has a steady velocity $U(z)$ may be expressed as

$$p(P) = 1/2 \rho C_p(P) U^2(z) \quad (2.19)$$

In this expression $U(z)$ = undisturbed mean velocity of the flow, i.e., its velocity at a sufficiently large distance upwind from the building, and C_p is a dimensionless mean pressure coefficient. For blunt bodies in turbulent flow, $C_p(P)$ must be determined by experiment.

In the case of an unsteady velocity, the pressure may be expressed as follows:

$$p(P) = \bar{p}(P) + p'(P) = 1/2 \rho C_p(P) [U(z) + u(z)]^2 + \rho C_M(P) B(z) \dot{u}(z, t) \quad (2.20)$$

in which $\bar{p}(P)$ = mean pressure, $p'(P)$ and $u(z)$ = pressure and velocity fluctuations, $C_M(P)$ = added mass coefficient and $B(z)$ = width of structure. Such an expression is reasonable under the assumption that the transverse building dimension is small compared to the scale of the energy containing eddies of the turbulence.

The question of the relative importance of the added mass term (the last term in Eq. 2.20) has been examined by Vickery and Kao [32]. On the basis of wind tunnel pressure measurements [33], these writers showed that in determining pressures on bluff bodies in turbulent flow the added mass term may be neglected. The same result was obtained in wind tunnel tests reported by Bearman [34] and by Petty [35]. Neglecting the added mass term, it follows from Eq. 2.20 and the definition of average values that

$$p' = 1/2 \rho C_p U^2 \left[2 \frac{u}{U} + \frac{u^2 - \overline{u^2}}{U^2} \right] \quad (2.21)$$

and

$$\bar{p} = 1/2 \rho C_p U^2 \left[1 + \frac{\overline{u^2}}{U^2} \right] \quad (2.22)$$

If $u(z)/U(z)$ is small (i.e., $\overline{u^2(z)}^{1/2}/U(z) < 0.1$) and the linear dimensions of the body are small compared with the length characteristics of turbulence, the assumption that the non-linear term in Eq. 2.21 may also be neglected is confirmed by experimental evidence [36].

In the atmosphere it may be assumed that $\overline{u^2(z)}^{1/2}/U(z) \approx 2.45u_*/2.5u_* \ln [(z-z_d)/z_o]$, in which u_* , z_d , z_o = frictional velocity, zero plane displacement, roughness length, respectively (Eqs. 2.5 and 2.13). For tall buildings this ratio is of the order of 0.05 to 0.3, depending upon building height and roughness of terrain. Also, except in the case of slender, line-like structures, the ratio of building dimension to scale of turbulence is not necessarily very small. Questions may thus arise as to whether the non-linear term may be neglected in the case of buildings with typical widths in atmospheric flow. Practical difficulties have prevented so far the carrying out of simultaneous full-scale measurements of $p'(P)$, $U(z)$ and $u(z)$. However, wind tunnel measurements have been performed [32,33] and appear to confirm the assumption that Eq. 2.21 may be linearized. Also, the effect of the non-linear term was analyzed in Ref. 37, according to which the contribution of this term to the fluctuating alongwind response of a 300m tall structure appears to be of the order of 5% (i.e., a contribution to the total alongwind response of about 3%). It thus appears that the linearization of Eq. 2.21 is acceptable and that

$$p'(P) = \rho C_p U(z) u(z) \quad (2.23a)$$

$$\bar{p} = 1/2 \rho C_p U^2 \quad (2.23b)$$

This simplified model of the relation between alongwind fluctuating pressures and velocities represented by Eq. 2.23a is used in all existing procedures for calculating dynamic alongwind response [1, 2, 3, 4, 6]. Eq. 2.23a is applied in these procedures to express the pressures on both the windward and the leeward sides of the building:

$$p'_w(P) = \rho C_w U(z) u(z) \quad (2.23c)$$

$$p'_\ell(P) = \rho C_\ell U(z) u(z) \quad (2.23d)$$

in which

$$C_w = \frac{\bar{p}_w(z)}{1/2 \rho U^2(z)} \quad (2.24a)$$

$$C_\ell = \frac{\bar{p}_\ell(z)}{1/2 \rho U^2(z)} \quad (2.24b)$$

\bar{p}_w , \bar{p}_ℓ are the average values of the mean pressure at elevation z on the windward and the leeward faces of the building, respectively. Attempts to verify by measurements the validity of Eqs. 2.23, 2.24 are further discussed in Section 2.3.3.

It is implicit in Eq. 2.23d that the pressure fluctuations on the leeward side are proportional to the velocity fluctuations in the upstream flow. As noted in Ref. 8, in reality the flow in the wake of the building is quite dissimilar from that in the oncoming flow. Measurements suggest that the fluctuating pressures on the leeward side are small compared to those on the windward side and, therefore, that Eq. 2.23d may be slightly conservative [8,38,39].

2.3.2 Cross-Spectra of Fluctuating Pressures

If Eq. 2.23 is used,

$$S_p(P_1, P_2, n) = C_p(P_1) C_p(P_2) \rho^2 U(z_1) U(z_2) S_u(P_1, P_2, n) \quad (2.25a)$$

in which the cross-spectral density of the velocity fluctuations can be written as

$$S_u(P_1, P_2, n) = S_u^{1/2}(P_1, n) S_u^{1/2}(P_2, n) R_u(P_1, P_2, n) N_u(P_1, P_2, n) \quad (2.25b)$$

and in which $C_p(P_i) = C_w$ or C_ℓ according as P_i ($i = 1, 2$) is on the windward or leeward side. Useful information regarding the magnitude of $N_u(P_1, P_2, n)$ is provided by results of measurements of cross-spectra of pressures on the windward and leeward sides of structures. Such measurements, carried out on full-scale buildings, have been reported by Lam Put [40] and by

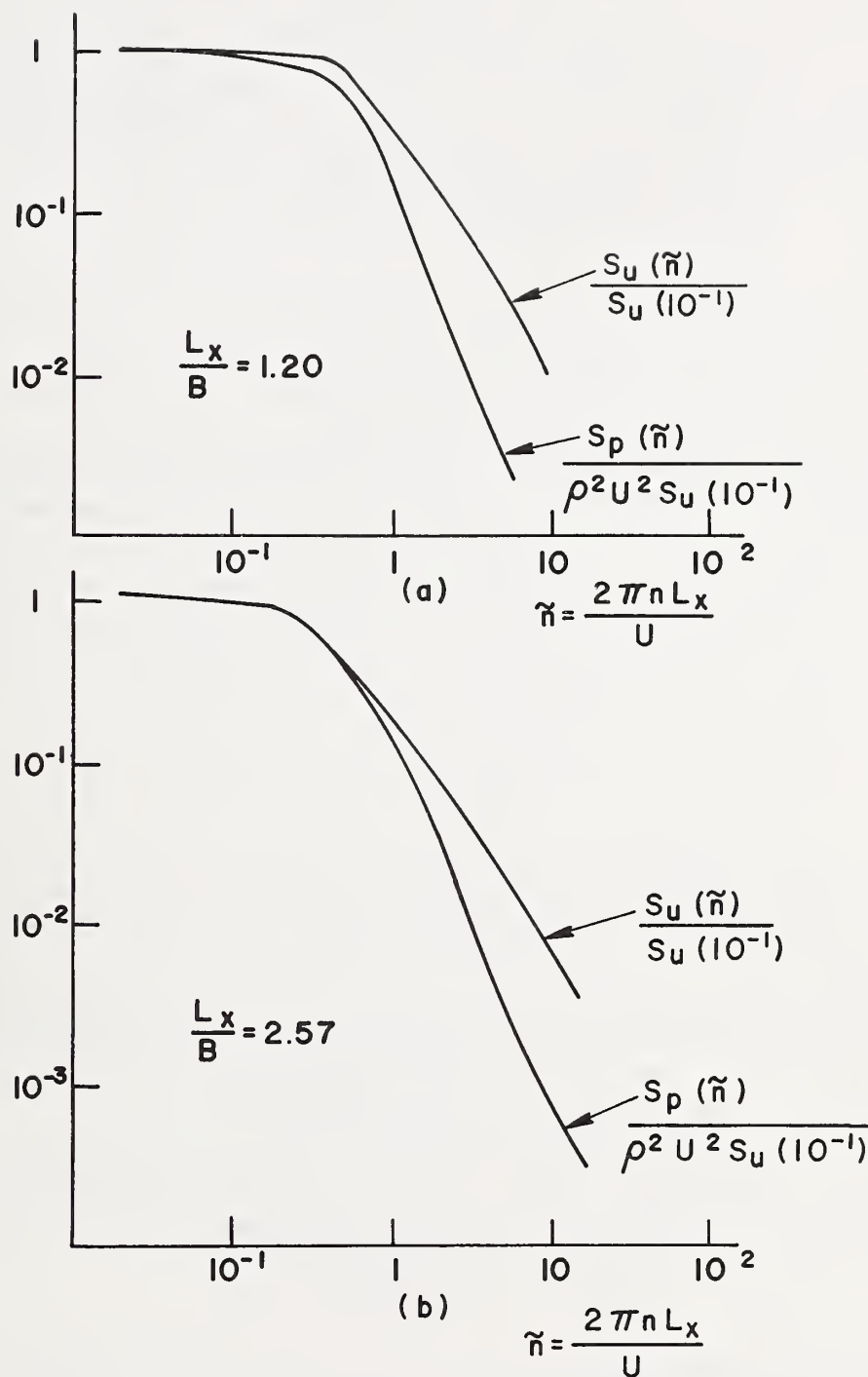


Fig. 2.3 - Spectra of longitudinal velocity fluctuations and spectra of fluctuating pressures at stagnation point: (a) $L_x/B = 1.20$; (b) $L_x/B = 2.57$ [34]

Van Koten [29] who found that except for very low frequencies, $N_u(P_{1w}, P_{2l}, n) < 0.2$ (the subscripts w, l indicate that the points P_1, P_2 are on the windward and leeward sides, respectively; points P_{1w}, P_{1l} and P_{2w}, P_{2l} have coordinates y_1, z_1 and y_2, z_2 , respectively). From results of wind tunnel measurements reported by Kao (Figs. 5.1, 5.19, 5.21 of Ref. 33) it also follows that, except for extremely low frequencies corresponding to eddies of negligible energy, $N(P_{1w}, P_{2l}, n)$ is nearly zero. More recently, Holmes [61] reported full-scale measurements which suggest that it is reasonable to assume

$$N_u(P_{1w}, P_{2l}, n) = \frac{1}{\xi} - \frac{1}{2\xi^2} (1 - e^{-2\xi}) \quad (2.26a)$$

where

$$\xi = \frac{3.85n \Delta x}{\bar{U}} \quad (2.26b)$$

$$\bar{U} = 2.5 u_* \left(\ell n \frac{H-z_d}{z_o} - 1 \right) \quad (2.26c)$$

In Eq. 2.5b, Δx is the smaller of the quantities $4H, 4B$ or $4D$, where H, B, D are the height, the width and the depth of the building, respectively [2].

The presence of a body in a turbulent flow produces, around that body, changes in the mean flow and boundary layer effects which result in a distortion of the oncoming turbulence [34, 40, 42, 43, 44]. This distortion is not reflected by Eqs. 2.23, 2.25a, 2.25b. The extent to which the turbulence distortion may affect the pressures on a body immersed in an isotropic turbulent flow has been investigated by Bearman for a two-dimensional bluff body with a flat windward face [34], by Marshall for a circular disk [42] and by Petty for a circular cylinder [35]. These authors' results show that, at low frequencies, the pressure spectra at the stagnation point are indeed proportional to the velocity spectra, i.e., may be predicted by Bernoulli's equation, even for ratios L_x/B of turbulence scale to transverse body dimension considerably smaller than those typical of buildings in atmospheric flows (in the atmosphere L_x is of the order of a few hundred meters [31]). However, at higher frequencies, due to fluid strain effects, the pressure fluctuations are attenuated and the pressure spectra drop off approximately 1.75 times as fast as the spectra of the oncoming turbulence [34] (see Figure 2.3). It has also been observed that the intensity of high frequency surface pressure fluctuations tends to increase with distance from the stagnation point but that this increase is generally insufficient to offset the attenuation along the stagnation streamline [42]. Thus, at higher frequencies, estimates of the pressure fluctuation components at the stagnation point based upon Bernoulli's equation appear to be conservative. The differences between such estimates and the measured values decrease, however, as the ratio L_x/B becomes larger. Bearman also suggests that the attenuated higher frequency components of the pressure fluctuations are better correlated than the corresponding components of fluctuating velocities in the oncoming flow.

2.3.3 Results of Pressure Measurements

Measurements of pressures on the surface of a high-rise building model and of mean and fluctuating velocities were carried out by Sadeh, Cermak and Hsi [44] in a shear flow simulating the atmospheric boundary layer. On the basis of these measurements (p. 50 and Fig. 4.8, p. 77, Ref. 33), the ratio

$$\frac{\overline{p'^2(P)}^{1/2} U(z)}{2p(P) \overline{u^2(z)}^{1/2}}$$

which is unity if Eq. 2.25a holds - was calculated along the centerline of the windward face and found to have the values .97, 1.07, .85, 1.16, 1.16 at $z/H = 0.45, 0.55, 0.65, 0.75$ and 0.85 , respectively, where z = height above ground and H = building height.

In the writers' opinion, research aimed at developing an improved model of the relation between alongwind fluctuating pressures and velocities is clearly desirable. It appears, however, that in the absence of such a model, Eqs. 2.23c, 2.23d may be used for engineering purposes, the ensuing errors in estimating of the response being on the conservative side. That this is the case is suggested by results of full-scale pressure measurements on buildings reported in Refs. 46,47,48,49,50, as will be subsequently shown.

For the windward and leeward sides of a tall building, the mean pressure coefficients specified by the A58.1 Standard are $C_w = 0.8$ and $C_\ell = -0.6$, respectively. These values appear to be confirmed by wind tunnel tests [44,51]. However, measurements suggest that pressure coefficients for full-scale buildings are smaller than those obtained in wind tunnel tests, i.e., are slightly decreasing functions of Reynolds number. It is therefore of interest to compare pressures calculated using eqs. 2.23c, 2.23d (with $C_w = 0.8$, $C_\ell = -0.6$) - which will be referred to herein as design pressures - to pressures estimated from measurements reported in the literature. The measurement results are given in the form

$$C_{lw} = \frac{[\overline{p_w(z)}]_{\text{meas}}}{1/2 \rho U^2(z_a)} \quad (2.27a)$$

$$C'_w = \frac{\overline{[p'^2(z)]_{\text{meas}}}^{1/2}}{1/2 \rho U^2(z_a)} \quad (2.27b)$$

where z_a is the anemometer height. It follows from Eq. 2.24a and the definitions of C_{lw} , C'_w

$$r_w = \frac{[\overline{p_w(z)}]_{\text{design}}}{[\overline{p_w(z)}]_{\text{measured}}} = \frac{0.8}{C_{lw} \left(\frac{U(z_a)}{U(z)} \right)^2} \quad (2.28a)$$

$$r'_w = \frac{\overline{[p'^2_w(z)]_{\text{design}}}^{1/2}}{\overline{[p'^2_w(z)]_{\text{measured}}}^{1/2}} = \frac{0.8 \rho U(z) \overline{u^2(z)}^{1/2}}{1/2 \rho C'_w U(z_a)^2} \quad (2.28b)$$

with similar expressions for the quantities r_ℓ , r'_ℓ corresponding to the leeward side. To estimate the ratios r'_w , r_w , r'_ℓ , r_ℓ it was assumed that $\overline{u^2(z)}^{1/2}/U(z) \approx 1/\ln[(z-z_d)/z_o]$ and $U(z_a)/U(z) = \ln[(z_a-z_d)/z_o]/\ln[(z-z_d)/z_o]$ (see Eqs. 2.5 and 2.13). The roughness parameters

used in the calculations were $z_o = 0.7$ m, $z_d = 10$ m for centers of large cities, $z_o = 0.40$ m, $z_d = 0$ for towns, $z_o = 0.25$ m, $z_d = 0$ for suburban areas. The results of the calculations, which are given in Table 2.3, were quite insensitive to even large differences in the assumed values of z_o and z_d . To the extent that the measurements reported are reliable and that the assumptions used in estimating the ratios r_w , r_ℓ , r'_w , r'_ℓ are correct, the results of Table 2.3 suggest that the values of the pressures calculated in accordance with Eqs. 2.23c, 2.23d, in which $C_w = 0.8$, $C_\ell = -0.6$, are indeed conservative.

Table 2.3 - Estimated Ratios of Design Pressures to Measured Pressures near the Stagnation Point for Various Buildings

Ref.	Location	Exposure	Building Height	Pressure Transducer Elevation	Anemometer Elevation								
			meters			C_{lw}	$-C_{l\ell}$	C'_w	C'_ℓ	r_w	r_ℓ	r'_w	r'_ℓ
50	London	Large city	66	47	50	.42	.14	.30	.08	1.80	4.00	1.25	3.50
48	Kobe	Town	107	75	120	.69	.50	.20	.15	1.01	0.84	1.36	1.22
49	Tokyo	Large city	152	136	164	.80	.13	.20	-	0.94	4.20	1.45	-
46	Tokyo	Large city	120	95	124	.45	.40	.29	.14	1.57	1.20	1.00	1.55
47	Monash U.	Suburban	43	33	53	.74	-	.14	.40	1.57	1.20	1.00	1.55

2.4 Alongwind Deflections and Accelerations

Consider a linearly elastic structure subjected to the action of a stationary random force $F_{P_1}(t)$ of known spectral density $S_F(n)$ and applied at a point P_1 . The spectral density of the fluctuating deflection $a'(M,t)$ at some point M (of ordinate z) of the structure can be shown to be [52]:

$$S_a(z,n) = H^*(z,P_1,n)H(z,P_1,n)S_F(n) \quad (2.29)$$

in which $H(z,P_1,n)$ is the mechanical admittance, i.e., the structural response divided by $e^{i2\pi nt}$, and $H^*(z,P_1,n)$ is the complex conjugate of $H(z,P_1,n)$. From Eq. 2.2, in which $F(P_1,t) = e^{i2\pi nt}$, and Eq. 2.1, it follows,

$$H(z,P_1,n) = \sum_r \frac{\mu_r(z)\mu_r(z_1)}{4\pi^2 M_r (1 - \frac{n^2}{n_r^2} + i\eta_r \frac{n}{n_r})} \quad (2.30)$$

where M_r is given by Eq. 2.4.

If the structure is acted upon by two stationary random forces $F_{P_1}(t)$ and $F_{P_2}(t)$ applied at points P_1, P_2 , respectively, the spectral density of the response $a'(M, t)$ depends not only upon the spectral densities, but also on the cross-spectral densities of the two forces, i.e. [52]:

$$S_a(z, n) = H^*(z, P_1, n)H(z, P_1, n)S_{F_{P_1}}(n) + H^*(z, P_2, n)H(z, P_2, n)S_{F_{P_2}}(n) + H^*(z, P_1, n)H(z, P_2, n)S_{F_{P_1} F_{P_2}}(n) + H^*(z, P_2, n)H(z, P_1, n)S_{F_{P_1} F_{P_2}}(n) \quad (2.31)$$

If a distributed stationary random loading is applied to an area A , Eq. 2.31 may be generalized:

$$S_a(z, n) = \int_A \int_A H^*(z, P_1, n)H(z, P_2, n)S_p(P_1, P_2, n)dA_1 dA_2 \quad (2.32)$$

in which P_1, P_2 are the centers of elemental areas dA_1, dA_2 ; $S_p(P_1, P_2, n)$ = cross-spectral density of pressures at points P_1, P_2 .

It can be shown that if the damping is small and the peaks are well separated, the imaginary part of the product $H^*(M, P_1, n) H(M, P_2, n)$ is negligible [52], and

$$H^*(z, P_1, n)H(z, P_2, n) = \sum_r \sum_s \frac{\mu_r(z)\mu_s(z)\mu_r(z_1)\mu_s(z_2)}{16\pi^4 M_r M_s n_r^2 n_s^2} \quad (2.33)$$

$$\frac{(1-n^2/n_r^2)(1-n^2/n_s^2) + 4\eta_r \eta_s (n/n_r)(n/n_s)}{[(1-n^2/n_r^2)^2 + 4\eta_r^2 n^2/n_r^2][(1-n^2/n_s^2)^2 + 4\eta_s^2 n^2/n_s^2]}$$

The cross-spectrum $S_p(P_1, P_2, n)$ used in Eq. 2.32 is described by Eqs. 2.25a, 2.25b and 2.18. It was indicated in Section 2.2.5 that, by definition, if P_1, P_2 are both on either the windward or the leeward side of a building $N(P_1, P_2, n) \equiv 1$. In view of the results reported in Refs. 33, 38, 39, 40, 61 and quoted in Section 2.3.2, if P_1, P_2 are points on opposite sides of a building, it is reasonable and conservative to assume

$$N(P_1, P_2, n) \equiv 1 \quad 0 \leq n < n_a \quad (2.34)$$

$$N(P_1, P_2, n) \equiv N_u(P_{1w}, P_{2l}, n_1) \quad n_a \leq n < \infty \quad (2.35)$$

where $N_u(P_{1w}, P_{2l}, n_1)$ is given by Eqs. 2.25 with $n = n_1$, and n_a is a sufficiently large frequency which may be assumed to be equal to, say, $0.9n_1$ (see also Section 4.3).

The peak factor for the deflections, i.e., ratio between the maximum probable value and the root mean square of the fluctuating deflections, may be written, approximately, as [1]:

$$g_a(z) = (2 \ln v_a(z)T)^{1/2} + 0.577/(2 \ln v_a(z)T)^{1/2} \quad (2.36)$$

in which T = duration of wind loading, assumed to be one hour (3,600 sec) and

$$v_a^2(z) = \int_0^\infty n^2 S_a(z, n) / \overline{a'^2(z)} \quad (2.37)$$

The spectral density and the mean square value of the alongwind acceleration of the building may be written as:

$$S_{\ddot{a}}(z, n) = (2\pi n)^4 S_a(z, n) \quad (2.38)$$

$$\overline{\ddot{a}^2(z)} = \int_0^\infty S_{\ddot{a}}(z, n) dn \quad (2.39)$$

The peak factor for the acceleration may be written as:

$$g_{\ddot{a}}(z) = (2 \ln v_{\ddot{a}}(z) T)^{1/2} + 0.577 / (2 \ln v_{\ddot{a}}(z) T)^{1/2} \quad (2.40)$$

in which,

$$v_{\ddot{a}}(z) = \int_0^\infty n^2 S_{\ddot{a}}(z, n) / \overline{\ddot{a}^2(z)} \quad (2.41)$$

If, as is typically the case for modern tall buildings, the intervals between natural frequencies in successive vibration modes are sufficiently large and the damping is light, the terms involving cross-products may be neglected [52], and the following relations are obtained:

2.4.1 Mean Response

in which

$$\bar{a}(z) = \frac{1}{2} (C_w + C_\ell) \rho B H^2 G(z) / 4\pi^2 m \quad (2.42)$$

$$G(z) = \sum_r [\tilde{\mu}(z) G_r / M_r \tilde{f}_r^2] \quad (2.43)$$

$$M_r = \int_0^1 \tilde{\mu}_r^2(z) dz \quad (2.44)$$

$$G_r = \int_0^1 \tilde{U}^2(z) \tilde{\mu}_r(z) dz \quad (2.45)$$

$$\tilde{U}(z) = U(z) / u_* \quad (2.46)$$

$$z = z/H \quad (2.47)$$

$$\tilde{f}_r = nrH/u_* \quad (2.48)$$

2.4.2 Fluctuating Response: Deflections and Accelerations

$$\overline{a'^2(z)}^{1/2} = \rho B H^2 J_0(z) / 4\pi^2 m \quad (2.49)$$

$$v_a(z) = \frac{u_*}{H} \frac{J_1(z)}{J_0(z)} \quad (2.50)$$

$$\overline{\ddot{a}^2(z)}^{1/2} = \rho B u_*^2 J_2(z) / m \quad (2.51)$$

$$v_{\ddot{a}}(z) = \frac{u_*}{H} \frac{J_3(z)}{J_2(z)} \quad (2.52)$$

in which

$$J_L(z) = [\sum_r^2 I_{rrL} / \tilde{f}_r^4 M_r^2]^{1/2} \quad (L = 0, 1, 2, 3) \quad (2.53)$$

$$I_{rrL} = \int_0^\infty \tilde{f}^{2L} \phi_{rr}^*(\tilde{f}) Y_{rr}(\tilde{f}) d\tilde{f} \quad (2.54)$$

$$\tilde{f} = nH/u_* \quad (2.55)$$

$$\phi_{rr}^*(\tilde{f}) = \frac{1}{[1 - (\tilde{f}/\tilde{f}_r)^2]^2 + [2\eta_r (\tilde{f}/\tilde{f}_r)]^2} \quad (2.56)$$

$$Y_{rr}(\tilde{f}) = \int_0^1 \int_0^1 \int_0^1 \int_0^1 [C_w^2 + 2C_w C_\ell N(u_* \tilde{f}/H) + C_\ell^2] \mu_r(Z_1) \mu_r(Z_2) U(Z_1) U(Z_2) \left[\frac{nS(Z_1, n)}{u_*^2} - \frac{nS(Z_2, n)}{u_*^2} \right]^{1/2} dZ_1 dZ_2 dY_1 dY_2 \quad (2.57)$$

$$R_u(Y_1, Y_2, Z_1, Z_2, n) = \exp \left(\frac{-2C_z [(Z_1 - Z_2)^2 + (C_y B/C_z H)^2 (Y_1 - Y_2)^2]^{1/2}}{U(Z_1) + U(Z_2)} \tilde{f} \right) \quad (2.58)$$

$$Z = z/H; Y = y/B \quad (2.59)$$

$$N(u_* \tilde{f}/H) \equiv 1 \quad 0 \leq \tilde{f} < 0.9\tilde{f}_1 \quad (2.60)$$

$$N(u_* \tilde{f}/H) \equiv \frac{1}{\xi_1} - \frac{1}{2\xi_1^2} (1 - e^{-2\xi_1}) \quad 0.9\tilde{f}_1 \leq \tilde{f} < \infty \quad (2.61)$$

$$\xi = \frac{3.85n_1 \Delta x}{\bar{U}} \quad (2.62)$$

$$\bar{U} = 2.5u_* (\ln \frac{H - z_d}{z_o} - 1) \quad (2.63)$$

In Eq. 2.61, Δx is the smaller of the quantities $4B$, $4D$ or $4H$. The peak factors $g_a(z)$, $g_{\ddot{a}}(z)$ are given by Eqs. 2.36, 2.40.

3.1 Description of the Computer Program

A Fortran program has been written to compute the integral I_{rrL} (Eq. 2.54) and the mean deflection response (Eq. 2.42), the fluctuating deflection and acceleration (Eqs. 2.49 and 2.51), and the peak factors (Eqs. 2.36 and 2.40). The program consists of a main program, called MAIN, and eight subprograms, called INPUT, INIT, TRIPLE, F, UTILDA, XMU, STILDA and FISTAR. Listings and a sample run appear in the Appendix. The program may be obtained on magnetic tape from the National Technical Information Service, Springfield, Va. 22151.

MAIN contains the quadrature method for the integral I_{rrL} . The integrand for I_{rrL} , which is itself a triple integral, is computed by the subprogram TRIPLE. MAIN also contains the coding for the mean and fluctuating responses, and the peak factors. MAIN calls the subroutines INPUT and INIT, which control the reading of input parameters from cards and the setting of parameters for the numerical integration, respectively. After INPUT and INIT have been called, MAIN completes the calculation with the aid of the other subroutines, and the cycle is begun again with another call to INPUT. If there is no more input, a blank card will cause a normal program exit.

The card deck read by INPUT has the following form:

Card 1, format (3I2)

IREP	Selects one of two spectral representations of longitudinal wind fluctuations. Representation 1 corresponds to Eq. 2.14. Representation 2 is given by Eqs. 2.15 and 2.16 and is devised to study dependence of the solution on the peak similarity coordinate $\tilde{\gamma}_1$.
IPRINT	Selects one of two options for output printing by the main program. As the approximate integration of I_{rrL} progresses from $\tilde{\gamma} = 0$ to $\tilde{\gamma} = \text{some cutoff value}$, option 1 causes running information to be printed at each sample value of $\tilde{\gamma}$ in the quadrature. Option 2 suppresses this printing. Output formats will be described below.
RLIM	The number of vibrational modes to use in the calculation, between 1 and 8.

Card 2, format (3F6.0)

H	Height of building, H, in meters.
BCON	Width of building, B, in meters.
XMASS	Mass of building per unit height, m, in kilograms per meter.

Card 3, format (8F6.0)

EN(1) Natural frequencies n_1, n_2, \dots , of the building in modes 1, 2, . . in cycles per second.

Card 4, format (8F6.0)

ZETA(1) Damping ratios η_1, η_2, \dots , in modes 1, 2,...

Card 5, format (7F6.0)

ZO Roughness length, z_o , in meters.
CZ Exponential decay coefficient, C_z .
CY Exponential decay coefficient, C_y .
DCON Zero plane displacement, z_d , in meters.
BETACN Coefficient β in Eq. 2.13.
F1 Peak similarity coordinate, f_1 , used only for spectral representation 2 (see input parameter IREP).
FS Value of similarity coordinate beyond which Eq. 2.11 is valid, used only for spectral representation 2.

Card 6, format (2F6.0)

USTAR Friction velocity, u_* , in meters per second (for calculation of u_* , see Section 4.4, steps 1 through 4).
T Duration of storm in seconds.

Card 7, format (4F6.0)

CW Mean pressure coefficient on windward side, C_w .
CL Mean pressure coefficient on leeward side, C_l .
XN Alongwind cross-correlation coefficient, N , for large values of the frequency, n (Eq. 2.61).
RHO Air density, $\rho \approx 1.25 \text{ kg/m}^3$.

All of these values are printed by subroutine INPUT, after being read in. For details on the selection of input parameters, the reader is referred to Sections 2.2, 4.2, 4.4.

The subprograms for the computation of the integrals which appear in the expressions of the alongwind response will now be described. Further details on the integration procedure are given in Section 3.2.

The subprogram INIT determines the quadrature sample points and weights (program variables FTILDA and ATILDA) for the integration with respect to \tilde{f} (Eq. 2.54) from NF_1, NF_2, NF_3 and NF_4 ; these parameters specify the number of subintervals to take in each of four special subranges of the semi-infinite range $(0, \infty)$. In the r -th vibration mode, these subranges are determined by the three points $(\tilde{f}_r - 2)/30, \tilde{f}_r - 2$ and $\tilde{f}_r + 2$, and the points 0 and ∞ , where \tilde{f}_r is given by Eq. 2.55. The program variable FPEAK stands for \tilde{f}_r . This scheme allows smaller subintervals to be taken in the numerical integration for \tilde{f} close to zero and \tilde{f}_r , which are points at which the integrand becomes large. Numbers NN_1, NN_2, NN_3 and NN_4 are also specified in INIT. These give the number of subdivisions to take on each edge of the "unit cube" (after an appropriate transformation of the physical problem variables, see Sec. 3.2) in the evaluation of the triple integral that is involved in the integrand of I_{rrL} . Subroutine INIT must be recompiled to change the values of the NF or NN.

The subprogram TRIPLE computes the triple integral $Y_{rr}(\tilde{f})$, given by Eq. 3.4, that occurs in the integrand of I_{rrL} . This is the same as the quadruple integral of Eq. 2.57 after a change of variable. The integrand for the triple integral is computed by the FORTRAN function F. Values of the functions $\mu_r(Z), \tilde{U}(Z)$ (see Eq. 2.46 and Eqs. 4.1, 4.2) and $S(Z, n)$ which occur in the integrand of the triple integral are computed by the Fortran functions XMU, UTILDA and STILDA. These functions represent modal shapes, the non-dimensionalized mean speed and the spectrum of longitudinal wind fluctuations, respectively. One of two different spectral representations is selected in STILDA according to the value of the input parameter IREP, as has already been described. Finally, the function FISTAR computes the function $\phi_{rr}^*(\tilde{f})$ (Eq. 2.56) that also enters into the integrand of I_{rrL} .

The printed output will now be described. The first step lists the input values read from cards by subroutine INPUT. For each mode, R , in succession, the following information is printed. First, the input parameters determined by subroutine INIT are listed. If the output print parameter IPRINT is one, subsequent pages will contain, for each value of \tilde{f} used in the numerical quadrature of Eq. 2.56, the following:

A line containing the calculated value of $Y_{rr}(\tilde{f})$, (named "avg. of integrals") and an estimate of the error in calculating it.

A table of four rows and nine columns, containing the following quantities (denote the quantity in the i -th row and the j -th column by $A_{i,j}$):

$$A_{1,1} = \tilde{f}; A_{i,1} = \tilde{f}^{2(i-1)}, i = 2, 3, 4$$

$$A_{1,2} = \phi_{rr}^*(\tilde{f}); A_{i,2} = A_{i,1} \phi_{rs}^*(\tilde{f}), i = 2, 3, 4$$

$A_{i,3} = \tilde{a} A_{i,2}, i = 1, \dots, 4; \tilde{a}$ is the coefficient used by the quadrature formula in connection with the abscissa \tilde{f} .

$A_{i,4} = A_{i,3} \cdot Y_{rr}(\tilde{f})$ (The "term" in the quadrature sum).

$A_{i,5}$ = the sum of the current and all preceding (i.e., for preceding values of \tilde{f}) values of $A_{i,4}$. (The "partial sum" of the quadrature sum; its value for the last \tilde{f} is the calculated approximation to the integral I_{rrL} .)

$A_{i,6}$ = an estimate of the variance of $A_{i,4}$, due to the random factors in the calculation of $Y_{rr}(\tilde{f})$.

$A_{i,7}$ = a similar estimate of the standard deviation of $A_{i,5}$.

$A_{i,8}$ = same as $A_{i,3}$ but with the factor unity in lieu of $\phi_{rr}^*(\tilde{f})$.

$A_{i,9}$ = same as $A_{i,5}$ but using $A_{i,8}$ instead of $A_{i,3}$. Its value for the last \tilde{f} is the calculated approximation to the first term in the sum of Eq. 4.13 and corresponds to the so-called background response (see Sections 4.2 and 4.3).

If IPRINT is set equal to two the printout is modified to print the information about $Y_{rr}(\tilde{f})$, and the table, only for the last value of \tilde{f} .

Finally, the values at the top of the building are printed of the mean alongwind deflection (in m), the root mean square of the fluctuating deflections (in m) and accelerations (in m/s^2), and the peak factors for the deflections and accelerations as computed from the modes so far encountered (i.e., from the first mode on the page with the output for $R,S = 1,1$, from the first and second modes on the page with the output for $R,S = 2,2$, etc.).

3.2 Integration Procedure

The integrals being evaluated are:

$$I_{rsL} = \int_0^\infty \tilde{f}^{2L} \phi_{rs}(z, \tilde{f}) Y_{rs}(\tilde{f}) d\tilde{f} \quad (3.1)$$

where

$$\phi_{rs}(z, \tilde{f}) = \frac{\mu_r(z/H) \mu_s(z/H)}{\tilde{M}_r \tilde{M}_s \tilde{f}^{2\gamma_r} \tilde{f}^{2\gamma_s}} \phi_{rs}^*(\tilde{f}) \quad (3.2)$$

$$\phi_{rs}^* = [C_w^2 + 2C_w C_\ell N(u_* \tilde{f}/H) + C_\ell^2] \frac{[1 - (\tilde{f}/\tilde{f}_r)^2][1 - (\tilde{f}/\tilde{f}_s)^2] + [2\eta_r(\tilde{f}/\tilde{f}_r)][2\eta_s(\tilde{f}/\tilde{f}_s)]}{([1 - (\tilde{f}/\tilde{f}_r)^2]^2 + [2\eta_r(\tilde{f}/\tilde{f}_r)]^2)([1 - (\tilde{f}/\tilde{f}_s)^2]^2 + [2\eta_s(\tilde{f}/\tilde{f}_s)]^2)} \quad (3.3)$$

$$\begin{aligned} Y_{rs}(\tilde{f}) &= \int_0^1 \int_0^1 \int_0^1 \mu_r(z_1) \mu_s(z_2) \tilde{U}(z_1) \tilde{U}(z_2) [\tilde{F}(\tilde{f}, z_1) \tilde{F}(\tilde{f}, z_2)]^{1/2} \\ &\quad \exp\left(\frac{-2C_z \tilde{f} [(z_1 - z_2)^2 + (C_y B/C_z H)^2 (Y_1 - Y_2)^2]^{1/2}}{\tilde{U}(z_1) + U(z_2)}\right) dY_1 dY_2 dz_1 dz_2 \\ &= \int_0^1 \int_0^1 \mu_r(z_1) \mu_s(z_2) \tilde{U}(z_1) \tilde{U}(z_2) [\tilde{F}(\tilde{f}, z_1) \tilde{F}(\tilde{f}, z_2)]^{1/2} \\ &\quad \exp\left(\frac{-2C_z \tilde{f} [(z_1 - z_2)^2 + (C_y B/C_z H)^2 t^2]^{1/2}}{\tilde{U}(z_1) + \tilde{U}(z_2)}\right) dz_1 dz_2 dt \end{aligned} \quad (3.4)$$

$$\tilde{F}(\tilde{f}, z) = \frac{nS(z, n)}{u_*^2} \quad (3.5)$$

The basic integration scheme has two parts. The integration with respect to f is done by a form of trapezoid rule, as follows: four numbers, called NF_1 , NF_2 , NF_3 and NF_4 , are specified, and a trapezoid rule using NF_1 subintervals is applied on the interval $[0, \frac{f_r - 2}{30}]$, one using NF_2 subintervals is applied on the interval $[-\frac{f_r - 2}{30}, f_r - 2]$, one using NF_3 subintervals is applied on the interval $[f_r - 2, f_r + 2]$, and one using NF_4 subintervals on $[f_r + 2, 2f_r - \frac{f_r - 2}{NF_4}]$. Finally, a correction is made to compensate for discarding the rest of $[0, \infty]$: the coefficient of the last integrand value is modified by adding to it,

$$\frac{3}{20}(f_r - \frac{f_r - 2}{NF_4})$$

This corrects properly when $L = 0$, and of course also whenever the resulting last term in the quadrature sum is negligible compared to the sum itself. That last term is one of the auxiliary quantities pointed out by the program. If it is not negligible, and L is not zero, a correction should be made by adding

$$\frac{6L}{20 - 6L}$$

times the last term (as printed out) to the sum.

(The source of these corrections is a simple extrapolation of the integrand,

$$f^{2L} \phi_{rs}(z, f) Y_{rs}(f)$$

from the highest value of f used, to infinity. The extrapolation assumes that this function can be represented, on that interval, by its asymptotic form,

$$C \bar{X}_{r,s}(z) f^{2L - (23/3)}$$

to all the accuracy needed.)

The procedure just outlined for integrating with respect to f is applicable in the case $r = s$. For the $r \neq s$ case, where there is cross-mode coupling, the procedure must be suitably modified.

For each of the four intervals of f values mentioned above, an integer N is specified. (In the FORTRAN program, these 4 values of N are denoted by $NN(1)$, $NN(2)$, $NN(3)$, $NN(4)$, respectively.) The unit cube is divided into N^3 congruent subcubes by dividing the interval $[0,1]$ on each axis into N equal subintervals. In each subcube, two points R and R' are chosen at random, independently of each other. The point S that is opposite R - with respect to the center of the subcube - is determined, as is the point S' that is opposite R' . The values of the integrand at the points R and S , in all the N^3 subcubes, are summed; and the sum is divided by $2N^3$, to form an average that we shall call "Y". The same is done with the points R' and S' , to form a second average, "Y'". Y and Y' can both be regarded as approximations to the desired triple integral $Y_{rs}(f)$; their average, $(Y + Y')/2$, is a better approximation and is used as the value of $Y_{rs}(f)$.

The randomness in the selection of R and R', if nothing else, insures that there will be some error in Y, Y', and (Y + Y')/2. (There are, of course, other sources of error; the randomness is introduced in order to decrease the total error. The theory behind this integration procedure is given in Ref. 53). The program calculates, as an estimate of the likely size of the error of (Y + Y')/2, the quantity,

$$E = \frac{1}{4N^3} \left[\sum_{k=1}^{N^3} (F(R_k) + F(S_k) - F(R'_k) - F(S'_k))^2 \right]^{1/2}$$

where "f" denotes the integrand and the summation indicated is over the N^3 subcubes - k being the number of the subcube for each particular summand. E is a positive quantity; the absolute value of the error of (Y + Y')/2 is likely to be about as big as E - only occasionally greater than 2E and seldom greater than 3E.

The random points used in thus calculating $Y_{rs}(\bar{f})$ for one particular value of \bar{f} should not be the same as those used for other values of \bar{f} . New random points should be generated for each \bar{f} , in a manner as independent as possible of the points used for the other values of \bar{f} . Doing that generally results in some cancelling of the errors of the individual $Y_{rs}(\bar{f})$ when they are combined in the integration with respect to \bar{f} .

One remark must be made about the use of the term "random" in the above description. The points R and R' are not found by using any "genuinely random" physical process - such as coin-tossing or observing radioactive decay - but are generated by a determinate mathematical process whose results are thought to mimic those of random processes. The numbers so generated should perhaps be called "pseudorandom" rather than "random"; but it is customary to call them "random". The particular random numbers used in the present version of the program are generated in the subroutine TRIPLE, under the names X(I) and XPRIME(I). The mathematical "random number generator" used there is an unusual one; any standard one could probably be used in its place.

Chapter 4. A SIMPLIFIED PROCEDURE FOR CALCULATING ALONGWIND DEFLECTIONS AND ACCELERATIONS

4.1 Introduction

The computer program described in Chapter 3 may be used to calculate the response of structures with any modal shapes and natural frequencies. The purpose of this chapter is to present a simplified procedure for calculating alongwind response, applicable to structures for which it may be assumed, first, that the fundamental modal shape is linear and, second, that the response to wind loading is dominated by the fundamental mode. The first of these assumptions is acceptable in a large number of situations of practical interest, such as in the case of typical multistory framed structures (see, for example, Ref. 10, p. 428 or Ref. 55, p. 60 and p. 242); moreover, as will be shown in Chapter 5, even if it deviates rather significantly from a straight line, the fundamental modal shape may be assumed to be linear without introducing errors in the estimated ratio of fluctuating to mean response that exceed a few percent. The second of these assumptions will generally hold if the ratios of natural

frequencies in the second and higher modes to the fundamental frequency are sufficiently large (see Chapter 5).

4.2 Basic Assumptions

In developing the procedure presented in this chapter, the following assumptions were used:

1. The behavior of the structure is linear. Its fundamental mode of vibration is a linear function of height above ground, i.e., $\mu_1(z) = C \frac{z}{H}$, where C is an arbitrary constant. The graphs developed herein are based upon the value $C = 0.26$.
2. The contribution of the second and higher modes of vibration to the response is negligible.
3. The mean velocity profile is described by the relations,

$$U(z) = 2.5 u_* \ln \frac{z - z_d}{z_o} \quad z \geq z_d + 10 \quad (4.1)$$

$$U(z) = 2.5 u_* \ln \frac{10}{z_o} \quad z \leq z_d + 10 \quad (4.2)$$

where z , z_o , z_d are expressed in meters.

The use of the logarithmic profile above elevation $(z+10)$ meters implies the assumption of horizontal homogeneity of the flow (see Chapter 1). Eq. 4.2 is used, conservatively, on account of the uncertainty regarding the actual nature of the flow near a building for $z < z_d + 10$ or so. The mean velocity $U(z)$ used in Eqs. 4.1, 4.2 is averaged over a period of one hour.

4. The spectral density of the longitudinal wind speed fluctuations is described by Eq. 2.14. The justification of this assumption was presented in Section 2.2.
5. The mean and fluctuating pressures are described by Eqs. 2.23c, 2.23d, 2.24a, 2.24b. (For tall buildings it is commonly assumed $C_w = 0.8$, $C_\ell = 0.5$, $C_D = C_w + C_\ell = 1.3$.)
6. The spatial cross-correlation of the fluctuating pressures in the acrosswind and alongwind directions may be described by Eq. 2.58 and 2.60, 2.61, respectively. For design purposes, the values recommended for the exponential decay coefficients are $C_z = 10$, $C_y = 16$ [3,7]; comparable values are used in Refs. 1,2,4,6. However, to permit the evaluation of possible errors due to uncertainties with regard to the actual values of the coefficients C_z, C_y , (see Sect. 2.2.5) calculations can also be carried out using different sets of values. Thus, graphs were developed that correspond, in addition to the values $C_z = 10$, $C_y = 16$, to the values $C_z = 6.4$, $C_y = 10$ and $C_z = 4.0$, $C_y = 6.4$.

4.3 Total Fluctuating Response as a Sum of Background and Resonant Contributions

Consider a single degree of freedom linearly elastic system with natural frequency n_1 and damping ratio η . Let this system be subjected to the action of a forcing function with a

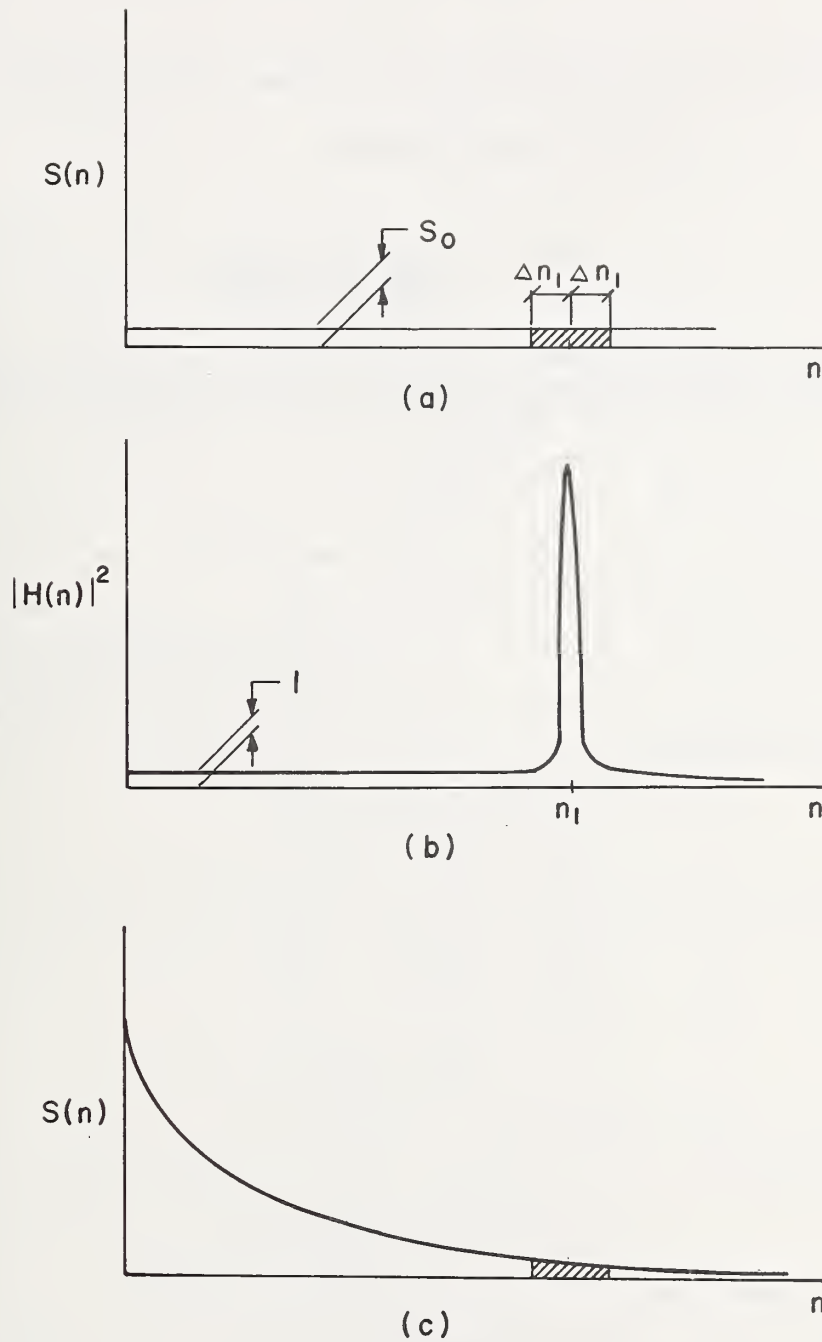


Fig. 4.1 - (a) White noise spectrum, (b) Square of modulus of mechanical admittance, (c) Decaying spectral curve

spectrum $S(n)$ such that (Fig. 4.1a)

$$S(n) \equiv S_0 \quad n \geq 0 \quad (4.3)$$

where S_0 is a constant. The mean square value of the response can be written as

$$\overline{x^2} = S_0 \int_0^\infty |H(n)|^2 dn \quad (4.4)$$

where

$$|H(n)|^2 = \frac{1}{[1 - (\frac{n}{n_1})^2]^2 + (2\eta \frac{n}{n_1})^2} \quad (4.5)$$

The quantity $|H(n)|^2$, which is represented in Fig. 4.1b, is an analytic function; therefore, the integral in Eq. 4.4 can be evaluated by means of the residue theorem to yield (see Ref. 10, p. 501):

$$\overline{x^2} = \frac{\pi n_1}{4\eta} S_0 \quad (4.6)$$

If the damping ratio η is small, the bulk of the contributions to the total value $\overline{x^2}$ is due to the forcing function components of frequencies $n_1 - \Delta n_1 < n < n_1 + \Delta n_1$, where $\frac{\Delta n_1}{n_1}$ is a small number (hatched area in Fig. 4.1a). If, as in the case of atmospheric turbulence, the spectral curve $S(n)$ has the shape of a decaying curve (Fig. 4.1c), $\overline{x^2}$ may be written as the sum of three contributions:

$$\overline{x^2} = (\overline{x^2})_1 + (\overline{x^2})_2 + (\overline{x^2})_3 \quad (4.7)$$

in which

$$(\overline{x^2})_1 = \int_0^{n_1 - \Delta n_1} S(n) |H(n)|^2 dn \quad (4.8)$$

$$(\overline{x^2})_2 = \int_{n_1 - \Delta n_1}^{n_1 + \Delta n_1} S(n) |H(n)|^2 dn \quad (4.9)$$

$$(\overline{x^2})_3 = \int_{n_1 + \Delta n_1}^\infty S(n) |H(n)|^2 dn \quad (4.10)$$

Assuming again that η is small, $(\overline{x^2})_2 \approx \frac{\pi n_1}{4\eta} S(n_1)$; for $0 < n < n_1 - \Delta n_1$, $|H(n)|^2 \approx 1$; and $(\overline{x^2})_3$ is negligibly small. Thus,

$$\overline{x^2} \approx \int_0^{n_1 - \Delta n_1} S(n) dn + \frac{\pi n_1}{4\eta} S(n_1) \quad (4.11)$$

or

$$\overline{x^2} \approx \int_0^\infty S(n) dn + \frac{\pi n_1}{4\eta} S(n_1) \quad (4.12)$$

The first and the second term of the sum in Eq. 4.12 are usually referred to as the background part and the resonant part of the response, respectively.

The above relation can similarly be applied to Eq. 2.54, i.e.,

$$I_{11L} = \int_0^\infty \phi_{11}^* (\gamma) \gamma^{2L} Y_{11}(\gamma) d\gamma \quad (4.13)$$

$$\approx \int_0^\infty \gamma^{2L} Y_{11}(\gamma) d\gamma + \frac{\pi f_1^2}{4\eta} \gamma_1^{2L} Y_{11}(\gamma_1)$$

where $\gamma_1 = n_1 H / u_*$

The first and the second term of the sum in Eq. 4.13 correspond to the background and resonant parts of the response, respectively.

To verify the extent to which the approximation involved in Eq. 4.13 is acceptable, numerical computations were carried out - using the program described in Chapter 3 - for about 120 cases corresponding to a wide range of typical buildings and terrain roughness conditions. The calculations showed that the approximation is of the order of 1%. It was also verified that, for $L = 1, 2, 3$, the background term may be neglected and that

$$I_{11L} \approx \frac{\pi f_1^2}{4\eta} \gamma_1^{2L} Y_{11}(\gamma_1) \quad (L = 1, 2, 3) \quad (4.14)$$

4.4 Alongwind Deflections and Accelerations

4.4.1 Mean Response

From Eqs. 2.42, 2.43, 2.44, 2.45 it follows that the mean deflection may be written as:

$$\bar{a}(z) = 0.238 \frac{\rho u_*^2}{mn_1} C_D J\left(\frac{z_0}{H}, \frac{z_d}{H}, H\right) B \frac{z}{H} \quad (4.15)$$

or, with $\rho = 1.25 \text{ kg/m}^3$, $C_D = 1.3$ and all quantities being expressed in SI units (m, kg, s):

$$\bar{a}(z) = 0.387 \frac{u_*^2}{mn_1} J\left(\frac{z_0}{H}, \frac{z_d}{H}, H\right) B \frac{z}{H} \quad (4.16)$$

where

$$J\left(\frac{z_0}{H}, \frac{z_d}{H}, H\right) = \frac{1}{(2.5 u_*^2)} \int_0^1 Z U^2(Z) dZ \quad (4.17)$$

The function $J\left(\frac{z_0}{H}, \frac{z_d}{H}, H\right)$ defined by Eq. 4.17 may be expressed as,

$$J\left(\frac{z_0}{H}, \frac{z_d}{H}, H\right) = \mathcal{J}\left(\frac{z_0}{H}, \frac{z_d}{H}\right) + \frac{1}{H^2} [k_1(z_0) + z_d k_2(z_0) + z_d^2 k_3(z_0)] \quad (4.18)$$

where all dimensions are in meters. \mathcal{J} can be obtained from Fig. 4.2 and k_1, k_2, k_3 are given in Table 4.1.

4.4.2 Fluctuating Response: Deflections and Accelerations

Let the quantities \mathfrak{B} and \mathfrak{R} be defined as follows:

$$\mathfrak{B} = \frac{1}{C_D^2} \int_0^\infty Y_{11}(\xi) d\xi \quad (4.19)$$

$$\mathfrak{R} = \frac{1}{C_D^2} \frac{\pi f_1}{4\eta} Y_{11}(\xi_1) \quad (4.20)$$

where $\xi_1 = \frac{n_1 H}{u_*}$. It follows from Eqs. 2.49 through 2.54 and Eqs. 4.19, 4.20, that

$$\frac{\overline{a'^2(z)}^{1/2}}{\bar{a}(z)} = 1.23 \frac{(\mathfrak{B} + \mathfrak{R})^{1/2}}{J} \quad (4.21)$$

$$v_a(z) = \left(\frac{\mathfrak{R}}{\mathfrak{B} + \mathfrak{R}} \right)^{1/2} n_1 \quad (4.22)$$

$$\frac{\overline{\ddot{a}^2(z)}^{1/2}}{\bar{a}(z)} \approx 50 n_1^2 \frac{\mathfrak{R}^{1/2}}{J} \quad (4.23)$$

$$v_{\ddot{a}}(z) = n_1 \quad (4.24)$$

where $\overline{a'^2(z)}^{1/2}$ and $\overline{\ddot{a}^2(z)}^{1/2}$ are the root square mean of the fluctuating deflection and of the acceleration, respectively. The peak factors associated with these quantities are

$$g_a(z) = [2 \ln 3,600 v_a]^{1/2} + \frac{0.577}{[2 \ln 3,600 v_a]^{1/2}} \quad (4.25a)$$

$$g_{\ddot{a}}(z) = [2 \ln 3,600 n_1]^{1/2} + \frac{0.577}{[2 \ln 3,600 n_1]^{1/2}} \quad (4.25b)$$

respectively, i.e., the maximum probable value of the fluctuating deflection and of the acceleration are $g_a(z) \overline{a'^2(z)}^{1/2}$ and $g_{\ddot{a}}(z) \overline{\ddot{a}^2(z)}^{1/2}$, respectively, and the gust response factor is

$$G.F. = 1 + g_a(z) \frac{\overline{a'^2(z)}^{1/2}}{\bar{a}(z)} \quad (4.26)$$

The quantity \mathfrak{B} may be obtained as follows:

$$\mathfrak{B} = \left(1 - \frac{z_d}{H} \right) \tilde{\mathfrak{B}} \left(\frac{B}{H}, \frac{z_o}{H} \right) \quad (4.27)$$

in which the value of $\tilde{\mathfrak{B}}$ - corresponding to the values of the exponential decay coefficients $C_z = 10$, $C_y = 16$, and calculated using the conservative assumption $N \equiv 1$ - can be found in Fig. 4.3. For $z_d \neq 0$, Eq. 4.27 is approximate; the approximation was verified by numerical calculations to be of the order of 1%.

Table 2.1 - Suggested Values of z_o for
Various Types of Exposure

Type of Exposure	Coastal ^a	Open	Outskirts of Towns, Suburbs	Center of Towns	Centers of Large Cities
z_o (meters)	0.005-0.01	0.03-0.10	0.20-0.30	0.35-0.45	0.60-0.80

^aApplicable to structures directly exposed to winds blowing from open water.

Table 2.2 - Approximate Ratios of Probable Maximum Speed
Averaged over Period t to that Averaged
over One Hour (at 10m Above Ground in Open Terrain)

t (Seconds)	2	5	10	30	60	100	200	500	1000	3600
$\frac{U^t}{U^h}$	1.53	1.47	1.42	1.28	1.24	1.18	1.13	1.07	1.03	1.00

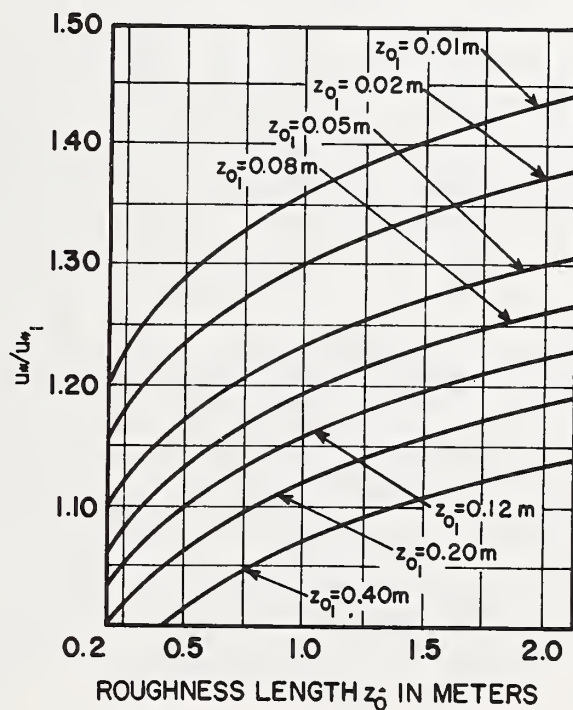


Fig. 2.2 - Ratios u_m/u_{*1}

Table 4.1 - Values of k_1, k_2, k_3

z_o (meters)	0.01	0.05	0.07	0.10	0.20	0.30	0.40	0.60	0.80	1.00	1.20
k_1	320	240	223	204	171	150	135	115	101	90	86
k_2	-	-	-	-	-	-	-	36	33	26	22
k_3	-	-	-	-	-	-	-	3.95	3.20	2.65	2.25

Table 4.2 - Values $z_o/H, z_d/H$ Corresponding to
Various \hat{Y}_{11} Curves

CURVE	z_o/H	z_d/H	CURVE	z_o/H	z_d/H
A	1.3×10^{-5}	0.	J'	3.4×10^{-3}	0.04
B	3.4×10^{-5}	0.	K	5.4×10^{-3}	0.
C	8.3×10^{-5}	0.	K'	5.4×10^{-3}	0.15
D	1.1×10^{-4}	0.	L	8.0×10^{-3}	0.
E	1.9×10^{-4}	0.	L'	8.0×10^{-3}	0.10
F	4.7×10^{-4}	0.	M	1.3×10^{-2}	0.
G	1.0×10^{-3}	0.	M'	1.3×10^{-2}	0.20
H	1.6×10^{-3}	0.	N	1.8×10^{-2}	0.
I	2.2×10^{-3}	0.	N'	1.8×10^{-2}	0.45
I'	2.2×10^{-3}	0.06	O	2.7×10^{-2}	0.
J	3.4×10^{-3}	0.	O'	2.4×10^{-2}	0.30

Note: If z_d/H is of the order of 0.1 or less and $z_o/H < 10^{-2}$, in determining \hat{Y}_{11} it may be assumed $z_d = 0$.

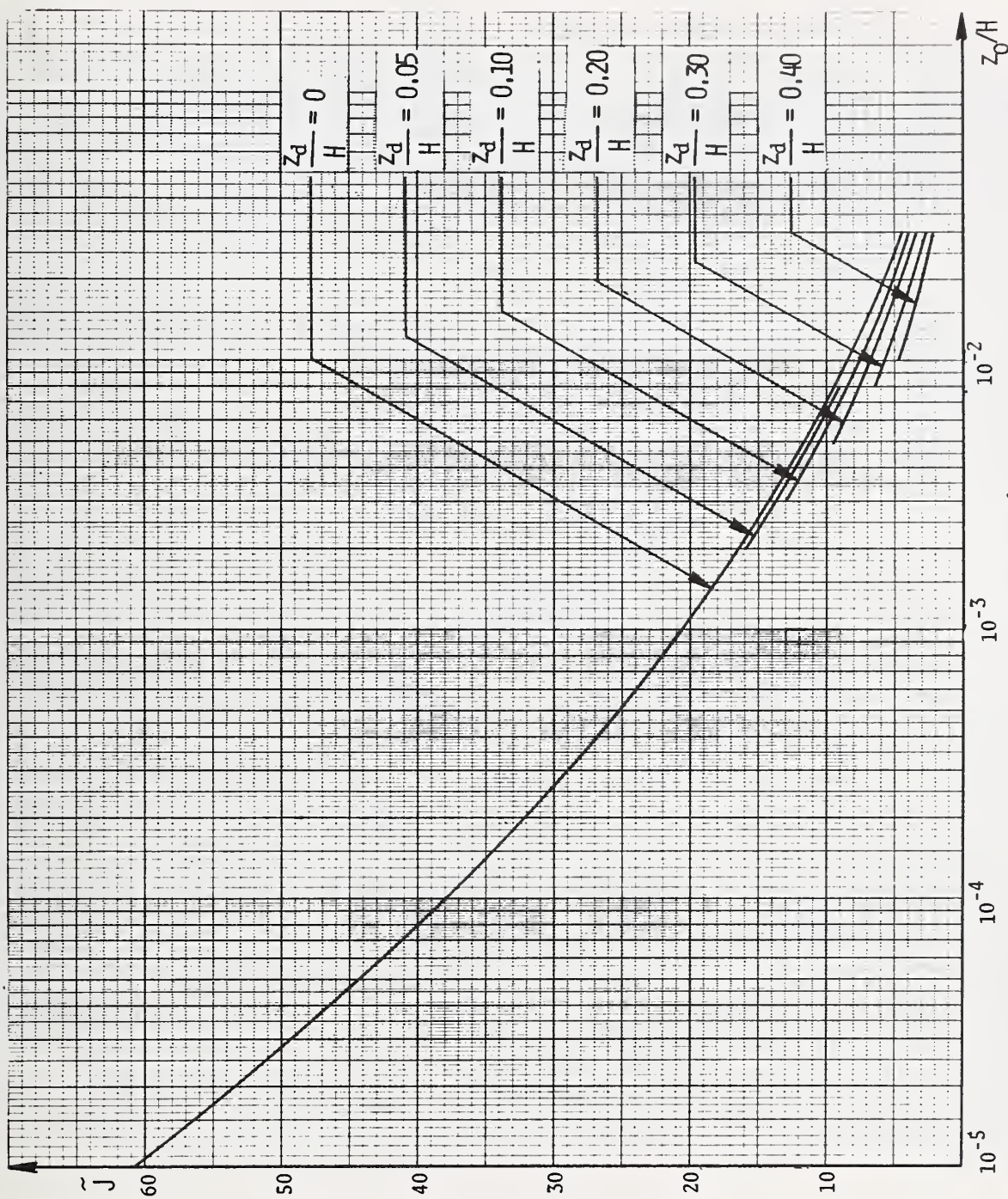


Fig. 4.2 Function J

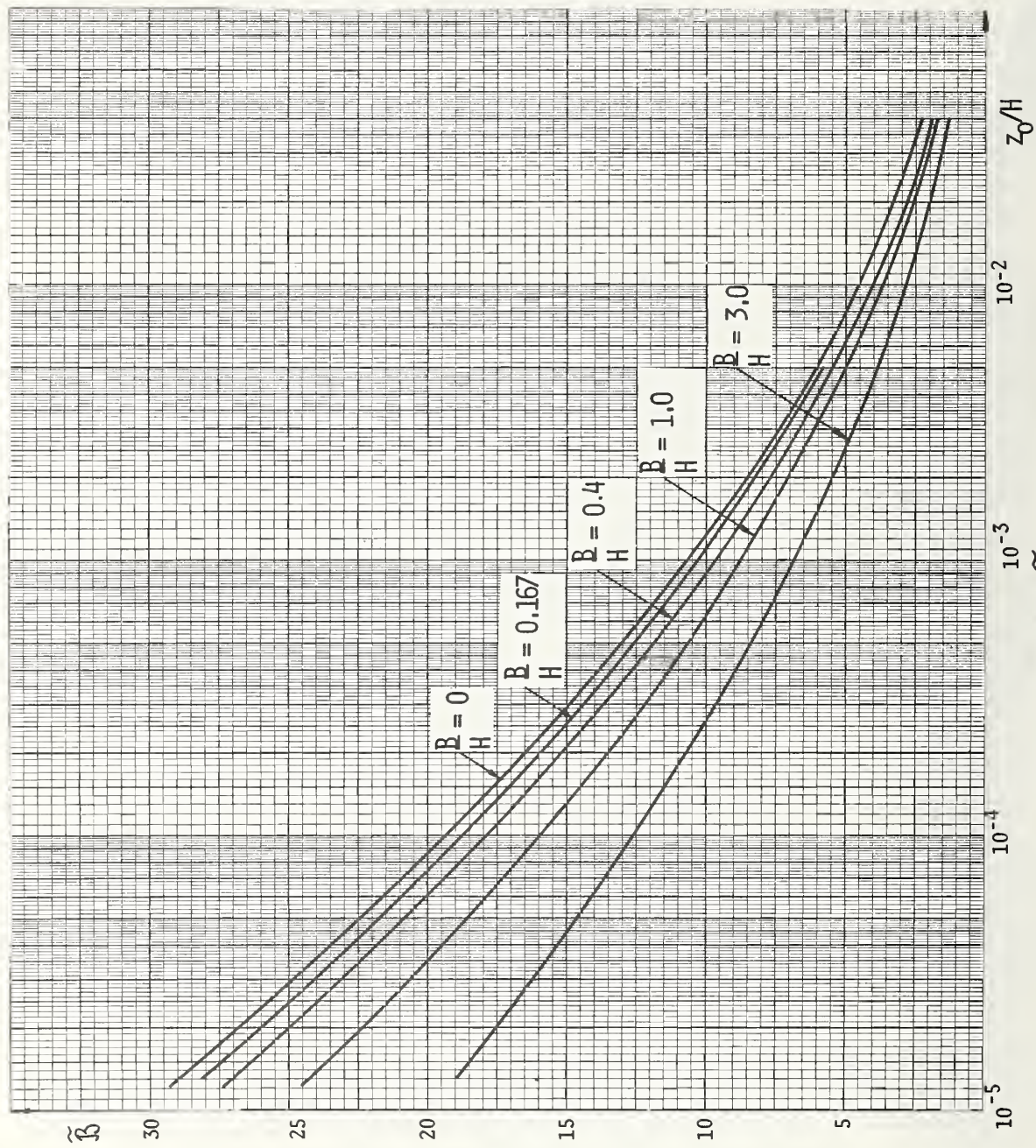


Fig. 4.3 Function \tilde{B} , $C_z = 10$, $C_y = 16$

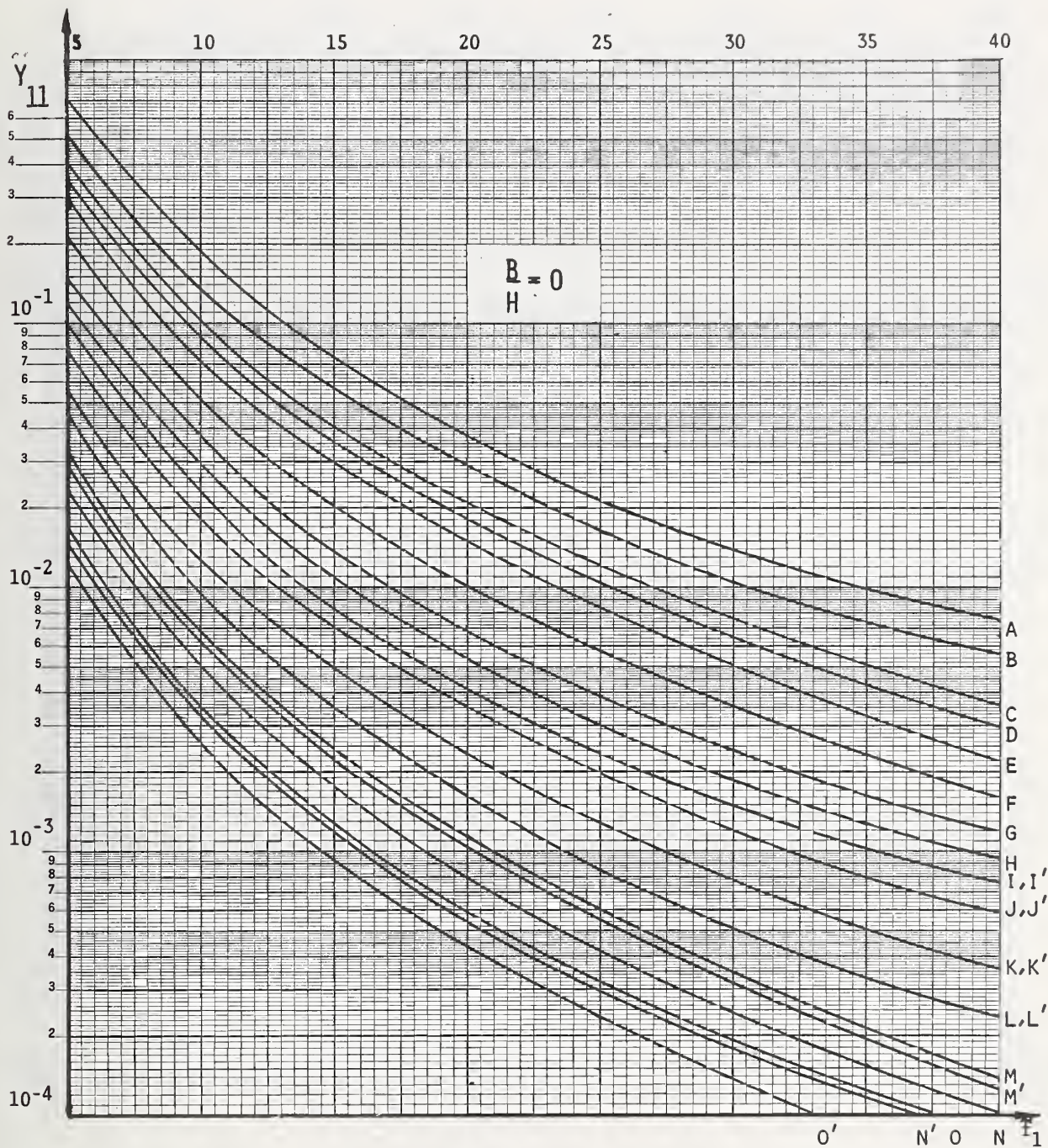


Fig. 4.4 Function Y_{11} , $B/H = 0$, $C_z = 10$, $C_y = 16$

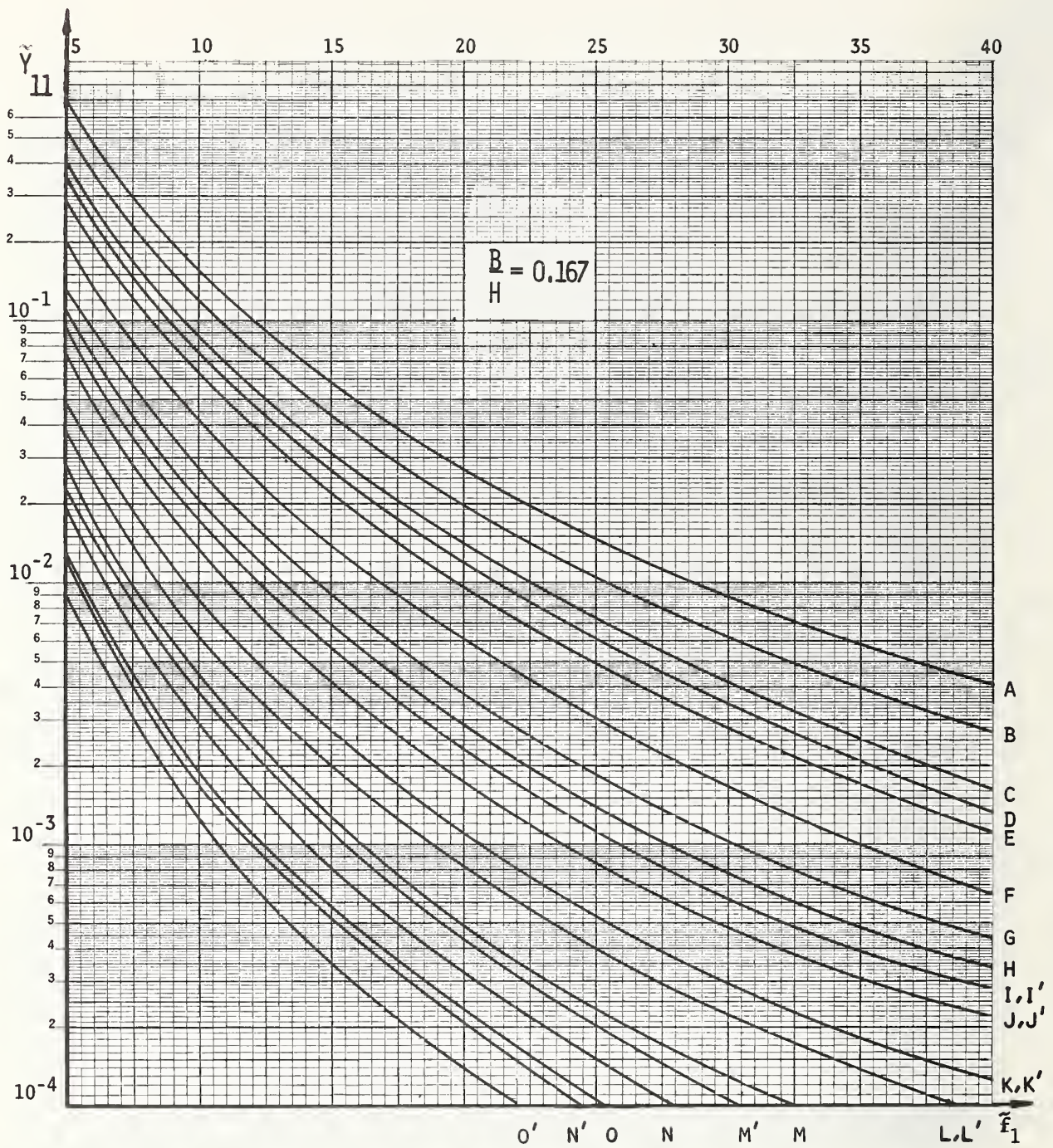


Fig. 4.5 Function \tilde{Y}_{11} , $B/H = 0.167$, $C_z = 10$, $C_y = 16$

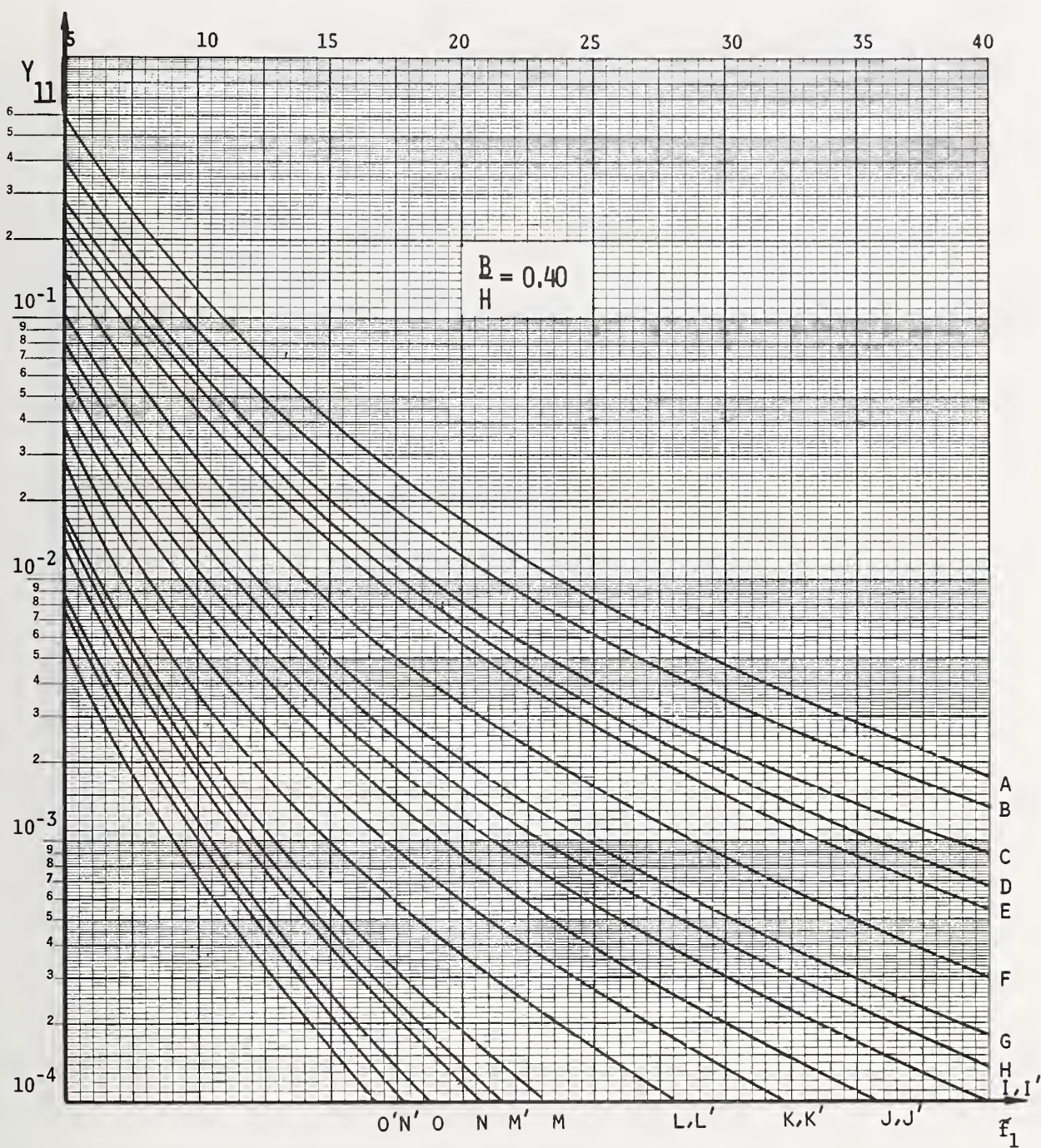


Fig. 4.6 Function γ_{11} , $B/H = 0.4$, $C_z = 10$, $C_y = 16$

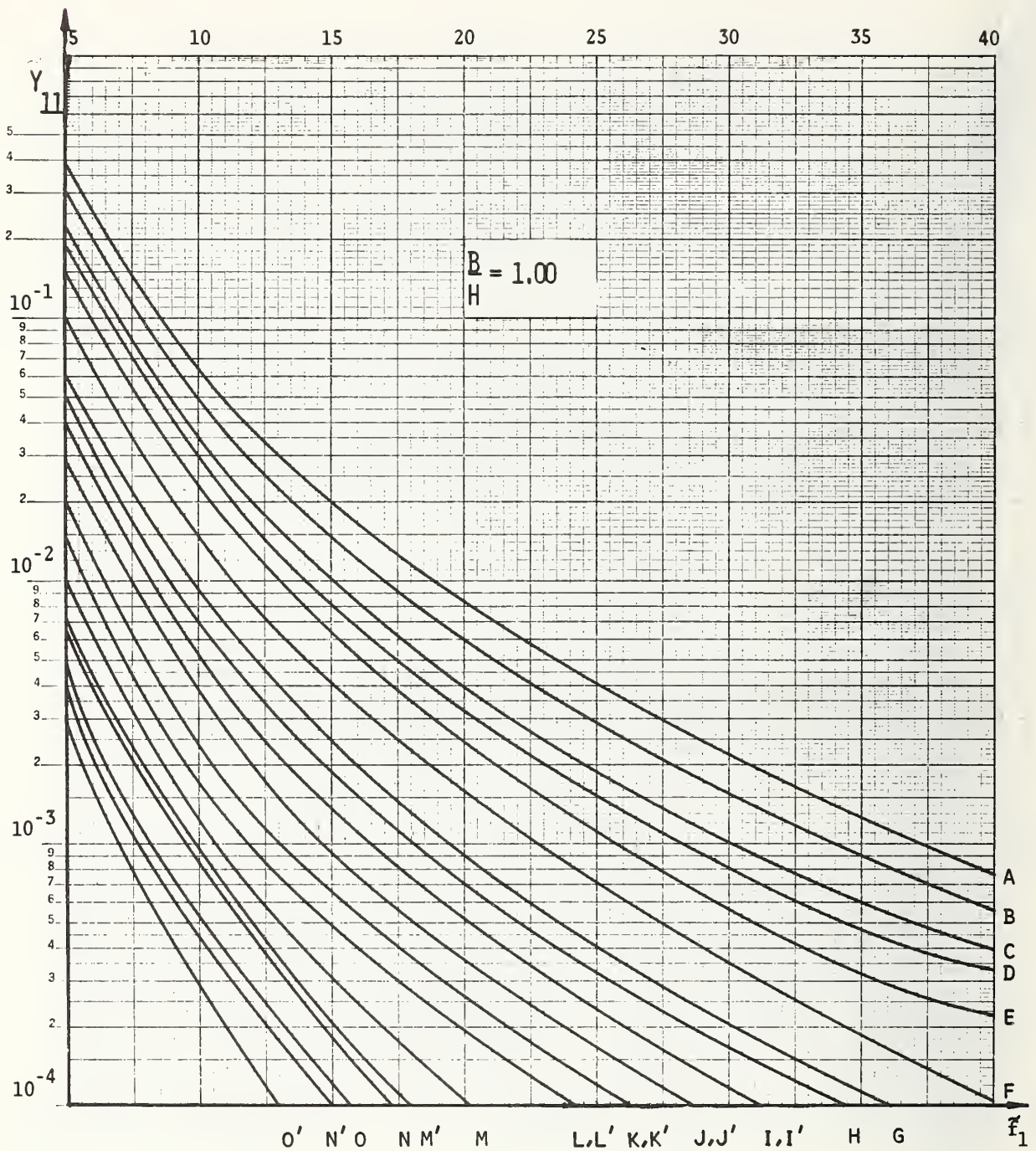


Fig. 4.7 Function Y_{11} , $B/H = 1.0$, $C_z = 10$, $C_y = 16$

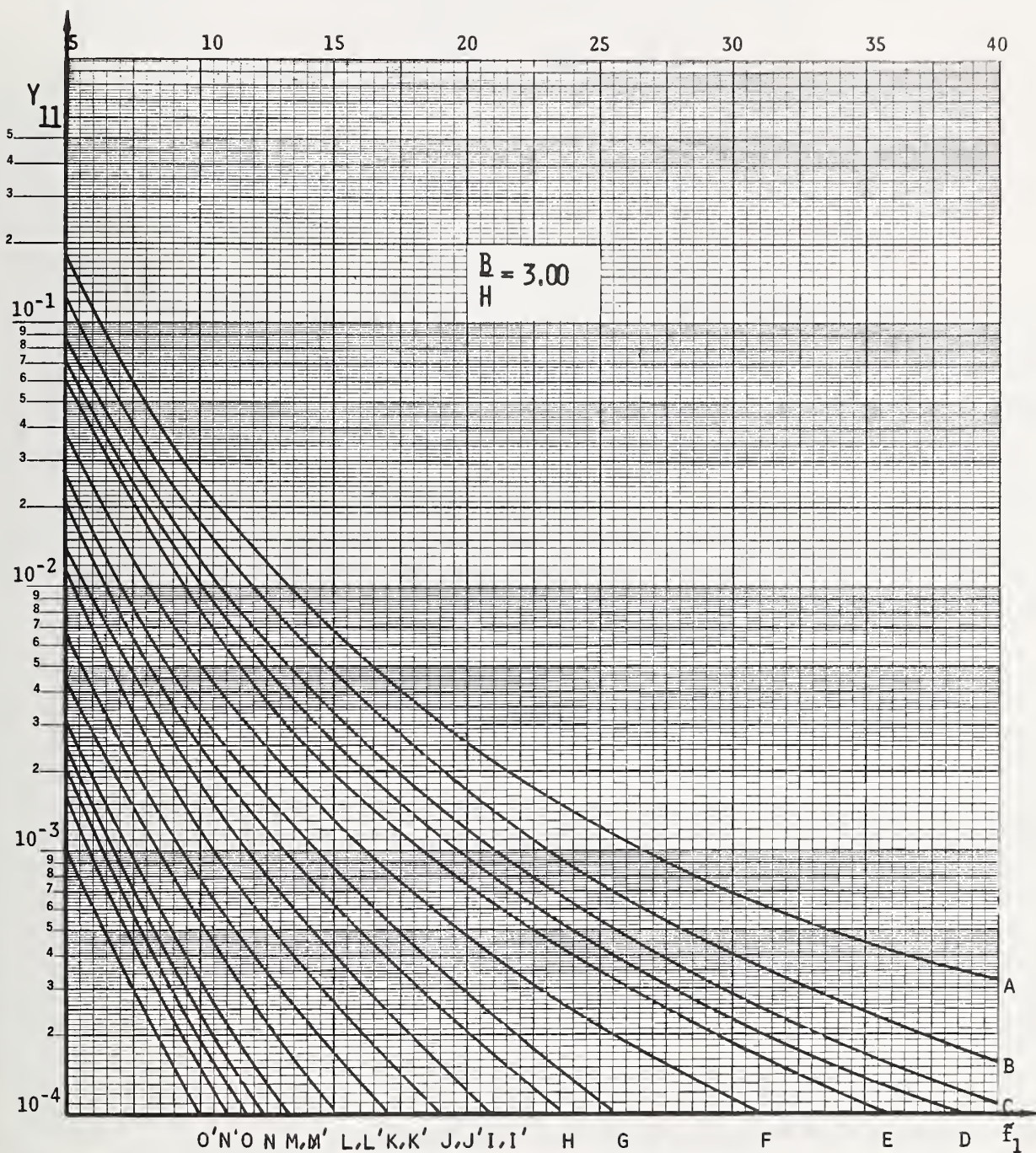


Fig. 4.8 Function Y_{11} , $B/H = 3.0$, $C_z = 10$, $C_y = 16$

The quantity \mathcal{R} may be obtained as follows

$$\mathcal{R} = \frac{C_w^2 + 2C_w C_\ell N + C_\ell^2}{(C_w + C_\ell)^2} \frac{\pi f_1^2}{4\eta} \tilde{Y}_{11} \left(\frac{B}{H}, \frac{z_o}{H}, \frac{D}{H}, \gamma_1 \right) \quad (4.28)$$

$$N = \frac{1}{\xi_1} - \frac{1}{2\xi_1^2} (1 - e^{-2\xi_1}) \quad (4.29)$$

$$\xi_1 = \frac{3.85 n_1 \Delta x}{\bar{U}} \quad (4.30)$$

$$\bar{U} = 2.5 u_* \left(\ln \frac{H - z_d}{z_o} - 1 \right) \quad (4.31)$$

The values of \tilde{Y}_{11} corresponding to the values of the exponential decay coefficients $C_z = 10$, $C_y = 16$ can be found in Figs. 4.4 through 4.8. Linear interpolation in and between Figs. 4.3 through 4.8 is permissible.

To evaluate possible errors due to uncertainties with regard to the actual values of C_z, C_y , the quantities \tilde{Y}_{11} corresponding to $C_z = 6.3$, $C_y = 10$ and $C_z = 4.0$, $C_y = 6.4$ are given in Figs. 4.9 through 4.13 and 4.14 through 4.18, respectively.

The \tilde{Y}_{11} curves are identified by capital Roman letters to which there correspond ratios z_o/H , z_d/H , listed in Table 4.2. For convenience, Tables 2.1, 2.2 and Fig. 2.2 have also been included in this chapter.

4.5 Numerical Example

Consider a building for which the height $H = 400\text{m}$, the width $B = 66\text{m}$, the depth (i.e., the dimension in the alongwind direction) $D = 45\text{m}$, the damping ratio $\eta = 0.01$, the fundamental frequency $n_1 = 0.09\text{ Hz}$, the weight per unit volume $w = 1,500\text{ N/m}^3$ ($1\text{N} \approx \frac{1}{4.45}\text{ lb}$). The basic wind speed (i.e. the fastest mile wind at 10 m above ground in open terrain) is $v_f = 75\text{mph}$ ($1\text{ mph} = 0.4474\text{ m/s}$). The building is located in the center of a large city for which it may be assumed $z_o = 0.65\text{m}$, $z_d = 20\text{m}$ (see Table 2.1). It is assumed, in addition, that the air density $\rho = 1.25\text{ kg/m}^3$, the acceleration of gravity $g = 9.81\text{ m/s}^2$, the mean pressure coefficients on the windward and leeward sides are $C_w = 0.8$, $C_\ell = 0.5$ and thus the drag coefficient $C_D = C_w + C_\ell = 1.3$, the acrosswind correlation coefficients $C_z = 10$, $C_y = 16$. [In view of the uncertainty with respect to the actual values of C_z , C_y (see Sect. 2.2.5) it is advisable that calculations be also carried out corresponding to lower values of C_z , C_y (see Sect. 5.5)].

Step 1. Averaging time for the given fastest mile wind speed (see Section 1.2.2):

$$T = \frac{3600}{v_f} = \frac{3600}{75} = 48\text{ s}$$

Step 2. Mean hourly speed at 10 m above ground in open terrain corresponding to the given fastest mile wind (see Table 2.2):

$$U_1(10) = \frac{v_f}{1.26} = 59.6\text{ mph} = 26.8\text{ m/s}$$

Step 3. Friction velocity in open terrain (for which it is assumed $z_{o1} = 0.07\text{m}$ (See Eq. 2.6);

$$u_{*1} = \frac{U_1(10)}{2.5 \ln \frac{10}{z_{o1}}} = \frac{26.8}{12.4} = 2.16 \text{ m/s}$$

Step 4. Ratio between friction velocities over terrains with $z_{o1} = 0.07\text{m}$ and $z_o = 0.65\text{m}$, respectively (see Fig. 2.2):

$$\frac{u_*}{u_{*1}} = 1.17$$

i.e., $u_* = 1.17 \times 2.16 = 2.54 \text{ m/s}$.

Step 5. Determine the following quantities:

$$\frac{B}{H} = \frac{66}{400} = 0.165$$

$$\frac{z_o}{H} = \frac{0.65}{400} = 1.6 \times 10^{-3}$$

$$\frac{z_d}{H} = \frac{20}{400} = 0.05$$

$$\gamma_1 = \frac{n_1 H}{u_*} = \frac{0.09 \times 400}{2.53} = 14.2$$

$$k_1 = 111.5$$

$$k_2 = 35.25$$

(Table 4.1)

$$k_3 = 3.76$$

$$\gamma = 17.1 \text{ (Fig. 4.2)}$$

$$\tilde{\beta} = 8.9 \text{ (Fig. 4.3)}$$

$$\gamma_{11} = .8 \times 10^{-2} \text{ (Table 4.2 and Fig. 4.5)}$$

$$m = B \times D \times w/g = 445,000 \text{ kg/m (mass of building per unit height)}$$

Step 6. Determine the quantities

$$\bar{U} = 2.5 u_* \left(\ln \frac{H - z_d}{z_1} - 1 \right) = 34.0 \text{ m/s} \quad (\text{Eq. 4.31})$$

$$\xi_1 = \frac{3.85 n_1 \Delta x}{\bar{U}} = 1.83 \quad (\text{Eq. 4.30})$$

(In Eq. 4.30, Δx is the smaller of the quantities $4B$, $4D$ and $4H$)

$$N = \frac{1}{\xi_1} - \frac{1}{2\xi_1^2} (1 - e^{-2\xi_1}) = 0.4 \quad (\text{Eq. 4.29})$$

Step 7 Calculate quantity J (Eq. 4.18)

$$\begin{aligned} J &= \gamma + \frac{1}{H^2} (k_1 + z_d k_2 + z_d^2 k_3) = \\ &= 17.1 + \frac{1}{(400)^2} [111.5 + 20 \times 35.25 + (20)^2 \times 3.76] \approx 17.1 \end{aligned}$$

Step 8 Calculate quantity β (Eq. 4.27)

$$\beta = (1 - \frac{z_d}{H}) \gamma = 8.45$$

Step 9 Calculate quantity \mathcal{R} (Eq. 4.29)

$$\mathcal{R} = .562 \frac{\gamma}{f_1} \frac{\gamma}{Y_{11}} / \eta = 6.4$$

Step 10 Mean Response

$$\bar{a}(z) = 0.387 \frac{u_*^2}{mn_1^2} J \beta \frac{z}{H} = 0.76 \frac{z}{H} \text{ (meters)}$$

where z is the height above ground of the point considered. The maximum mean deflection occurs at the top of the building and is $\bar{a}(H) = 0.76$ m.

Step 11 Ratio of root mean square of fluctuating deflections to mean deflection (Eq. 4.21)

$$\frac{\overline{a'^2(z)}^{1/2}}{\bar{a}(z)} = 1.23 \frac{(\beta + \mathcal{R})^{1/2}}{J} = 0.278$$

Step 12 Peak factor for fluctuating deflections (eqs. 4.22 and 4.25a)

$$\begin{aligned} v_a &= (\frac{\mathcal{R}}{\beta + \mathcal{R}})^{1/2} n_1 = 0.059 \\ [2 \ln 3600 v_a]^{1/2} &= [2 \ln (3600 \times 0.059)]^{1/2} = 3.28 \\ g_a &= 3.28 + \frac{0.577}{3.28} = 3.46 \end{aligned}$$

Step 13 Gust Response Factor (Eq. 4.26)

$$G.F. = 1 + g_a \frac{\overline{a'^2(z)}^{1/2}}{\bar{a}(z)} = 1.96$$

The maximum probable deflection is:

$$a_{\max}(H) = (G.F.) \bar{a}(H) = 1.96 \times 0.76 = 1.49m$$

Step 14 Root mean square of accelerations (Eq. 4.23)

$$\overline{\ddot{a}^2(z)}^{1/2} \approx 50 n_1^2 \frac{\mathfrak{R}^{1/2}}{J} \overline{a(z)} = 0.045 \frac{z}{H} m/s^2 \approx 0.0047 \frac{z}{H} g$$

Step 15 Peak factor for accelerations (Eq. 4.24, 4.25b):

$$(2 \ln 3,600 n_1)^{1/2} = 3.40$$

$$g_{\ddot{a}} = 3.40 + \frac{0.577}{3.40} = 3.57$$

Step 16 Maximum probable acceleration $a_{\max} = g_{\ddot{a}} \overline{\ddot{a}^2(H)}^{1/2}$:

$$g_{\ddot{a}} \overline{\ddot{a}^2(H)}^{1/2} = 3.57 \times 0.047 = 0.17 m/s^2 \approx 0.017 g$$

4.6 Comparison between Gust Response Factors Calculated Using Various Current Procedures

For the building just considered, the values of the gust response factors calculated in accordance with the procedures described in the ANSI A58.1 Standard [4], Ref. 6 and Ref. 3 are 1.53, 2.83 and 3.38, respectively, versus 1.96, as calculated herein. As noted in Ref. 7, the gust factors calculated using Refs. 3 and 6 are **larger, first, because the pressures** on the windward and leeward sides are conservatively assumed to act in phase (i.e., to be perfectly correlated) and second, because the variation with height of the spectrum of the longitudinal velocity fluctuations is ignored. Gust factors are underestimated by the procedure of Ref. 4 because the alongwind pressure correlation coefficient, rather than being applied as a reduction factor to just the cross-spectra of pressures acting on opposite sides of the building, is applied to the entire alongwind response, in violation of basic random vibration theory (see Ref. 8).

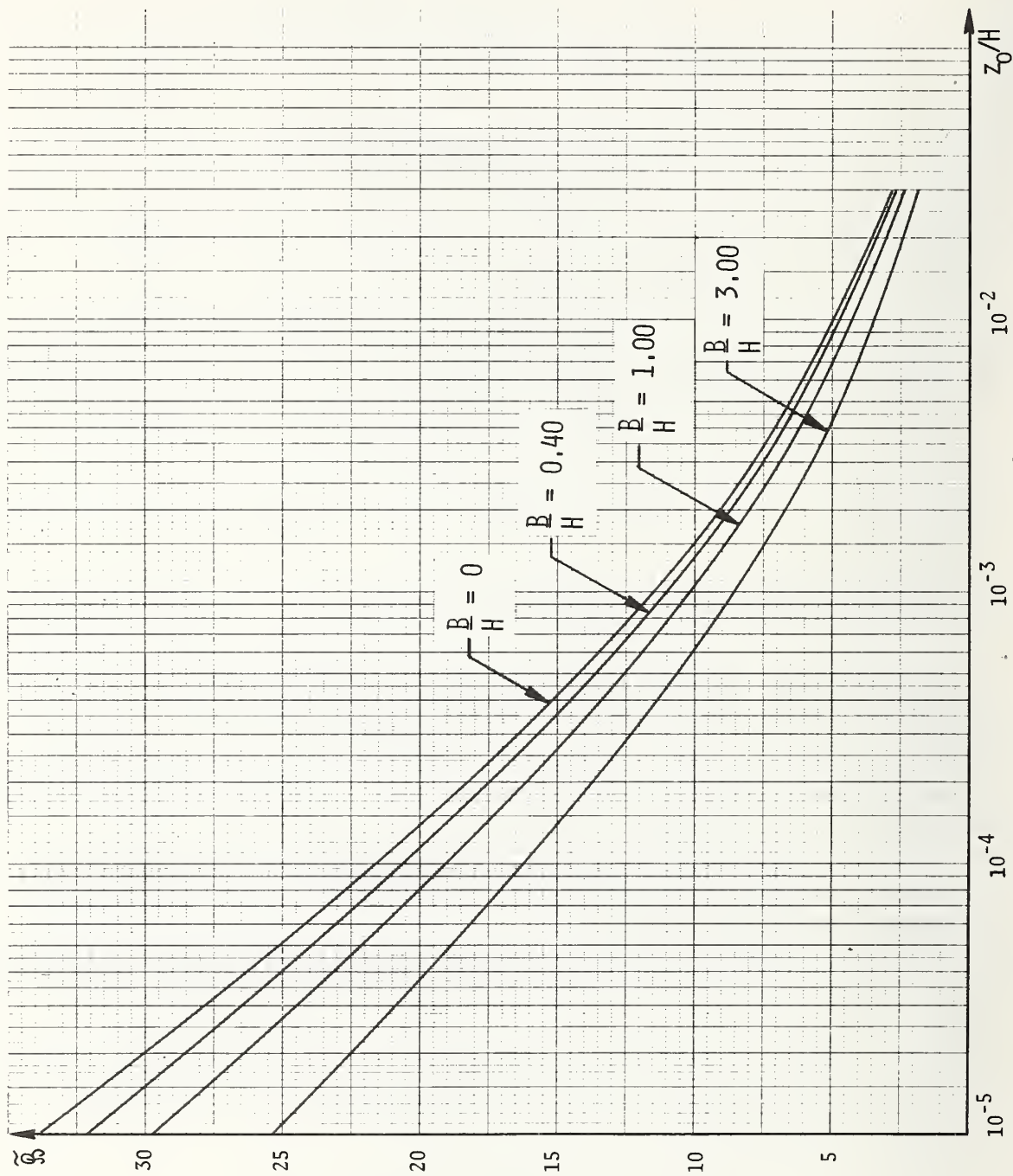


Fig. 4.9 Function $\tilde{\beta}$, $C_z = 6.3$, $C_y = 10$

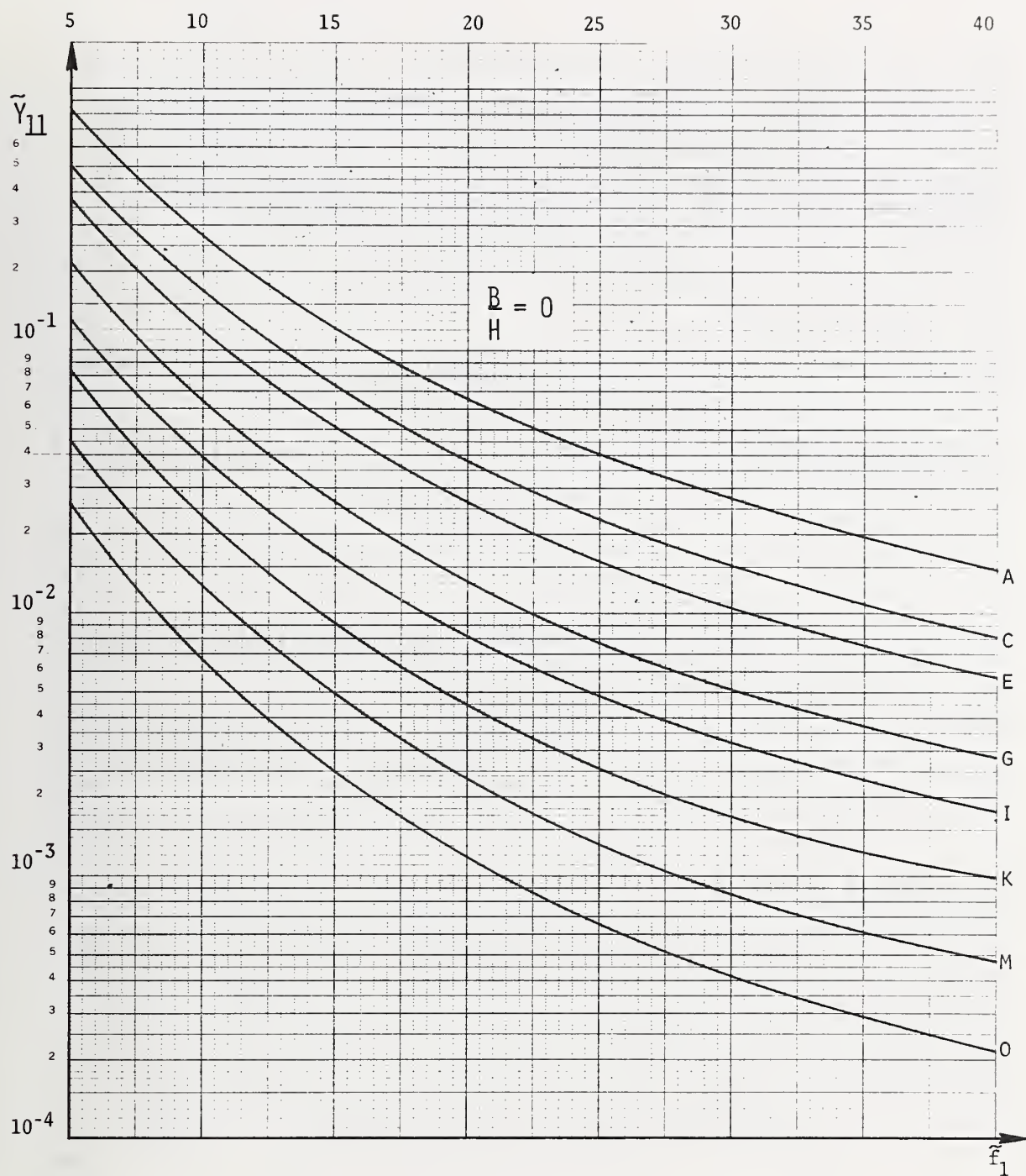


Fig. 4.10 Function \tilde{Y}_{11} , $B/H = 0$, $C_z = 6.3$, $C_y = 10$

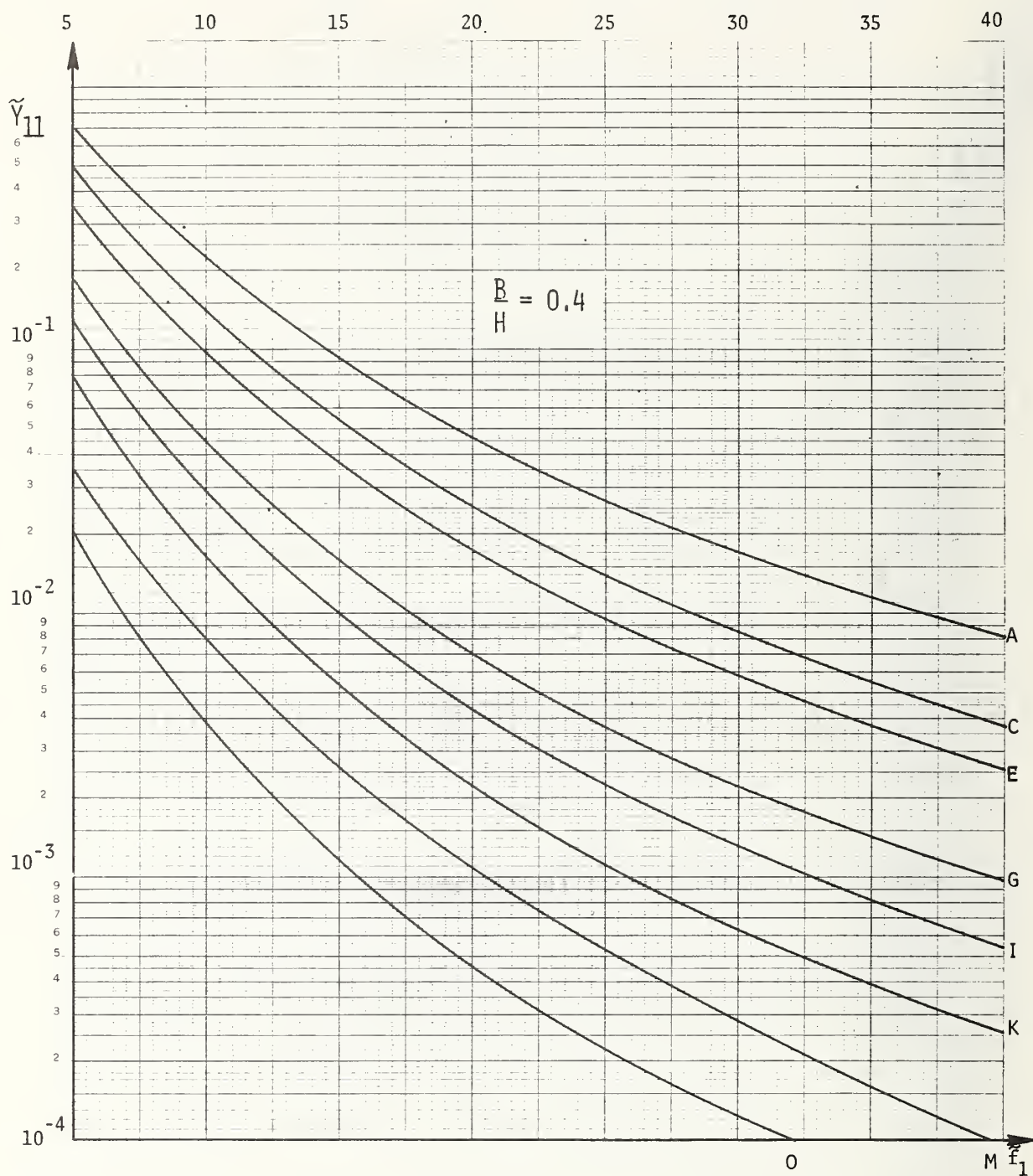


Fig. 4.11 Function \tilde{Y}_{11} , $B/H = 0.4$, $C_z = 6.3$, $C_y = 10$

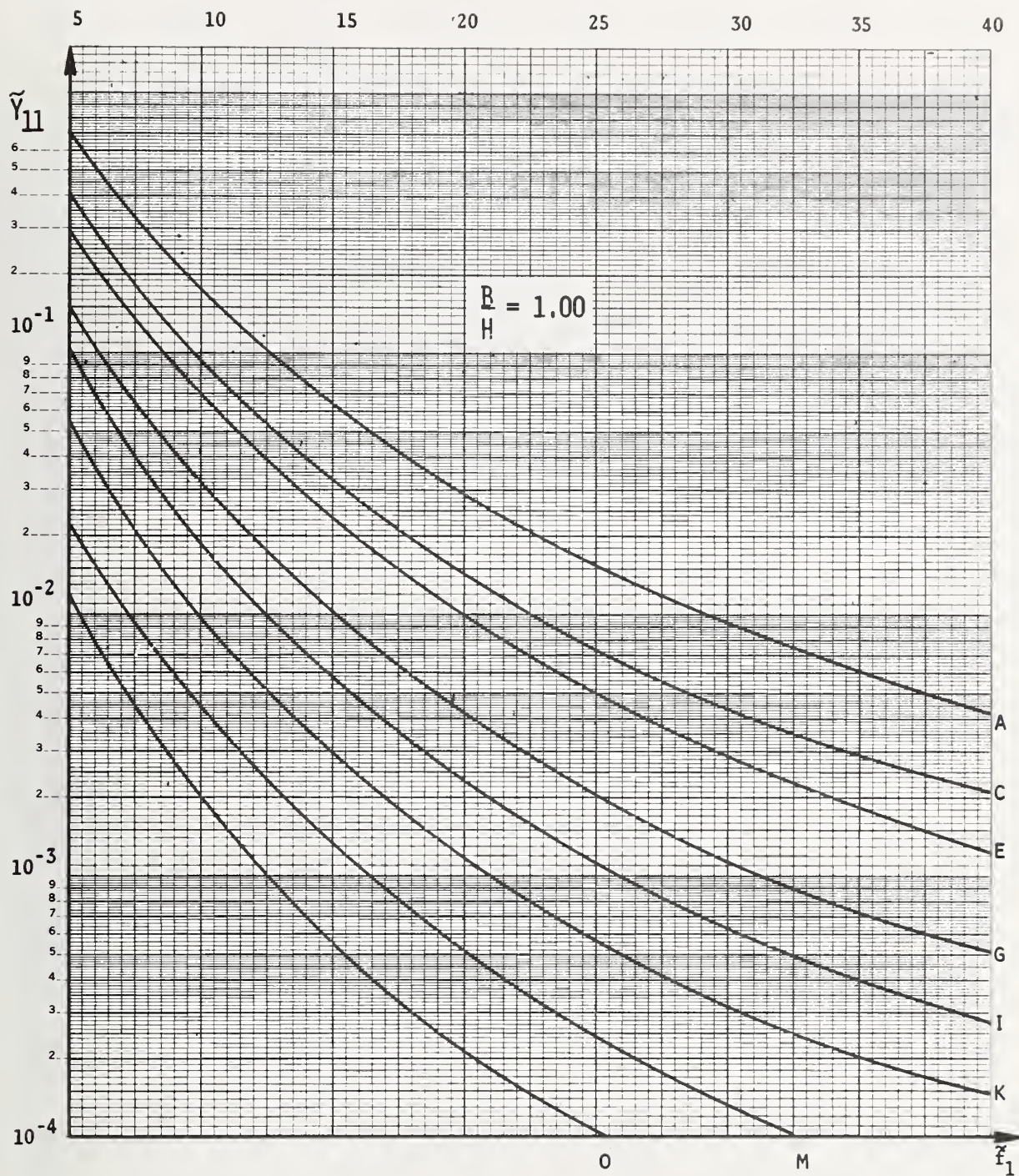


Fig. 4.12 Function \tilde{y}_{11} , $B/H = 1.0$, $C_z = 6.3$, $C_y = 10$

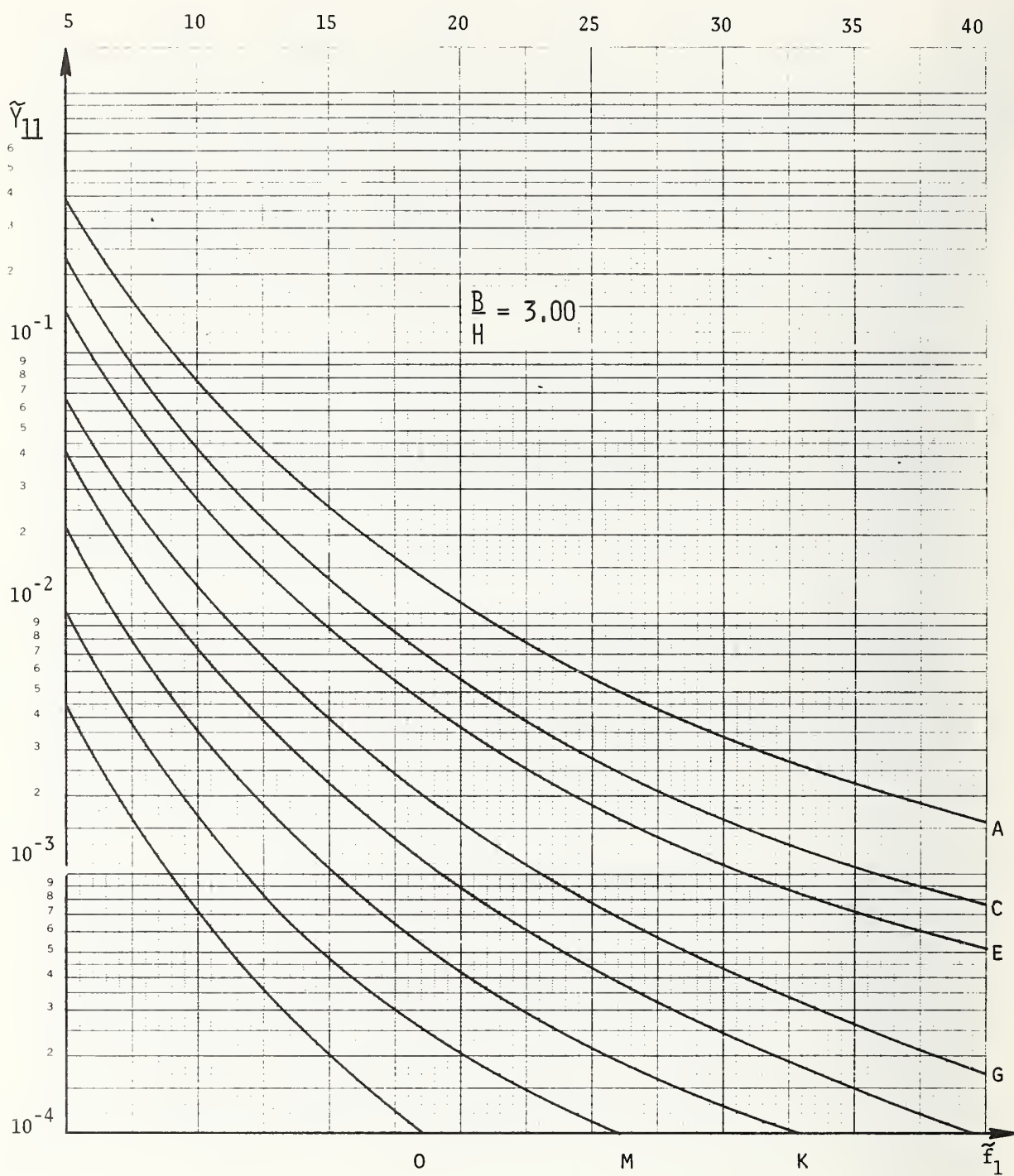


Fig. 4.13 Function \tilde{Y}_{11} , $B/H = 3.0$, $C_z = 6.3$, $C_y = 10$

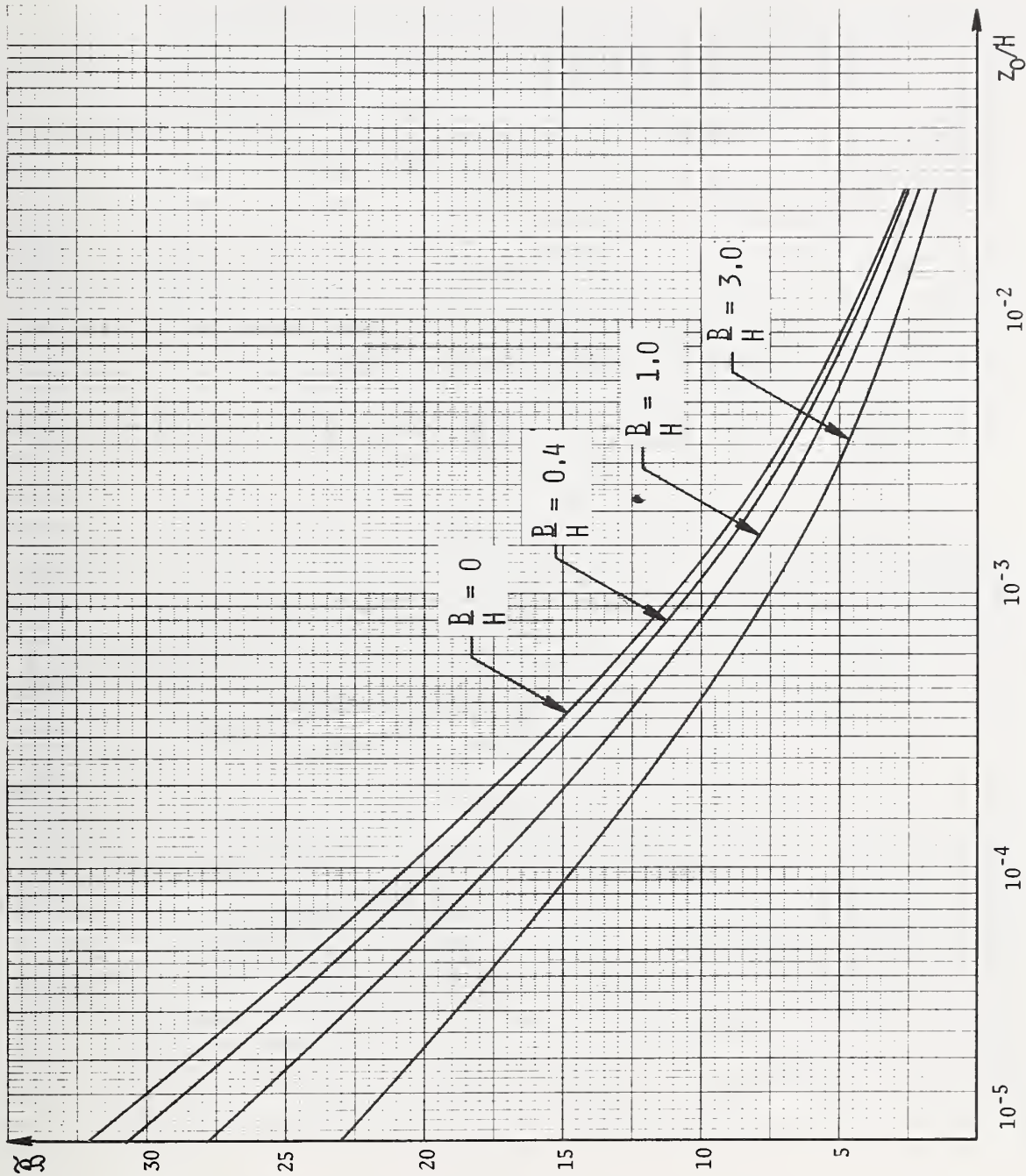


Fig. 4.14 Function α_y $C_z = 4.0$, $C_y = 6.4$

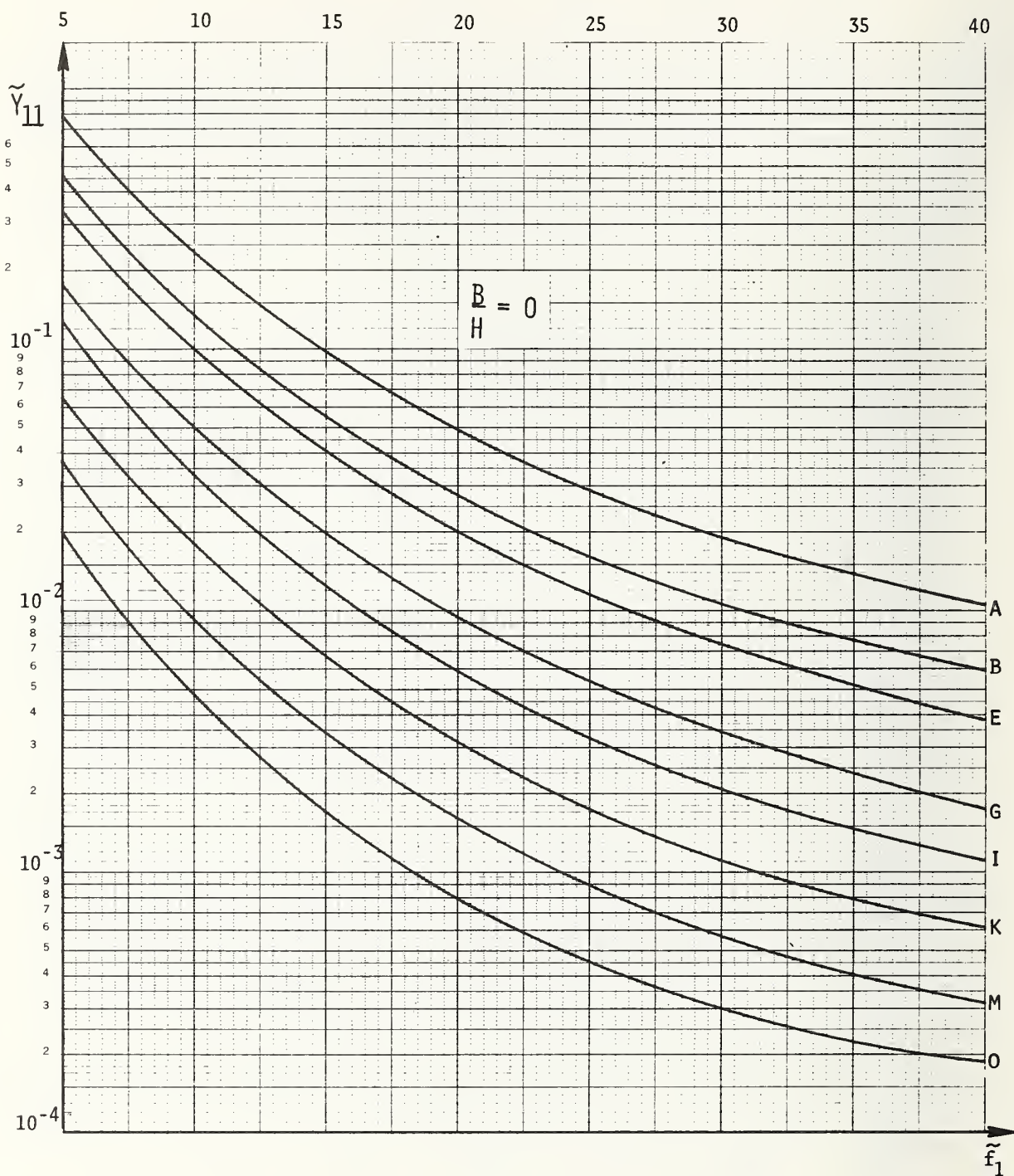


Fig. 4.15 Function \tilde{y}_{11} , $B/H = 0$, $C_z = 4.0$, $C_y = 6.4$

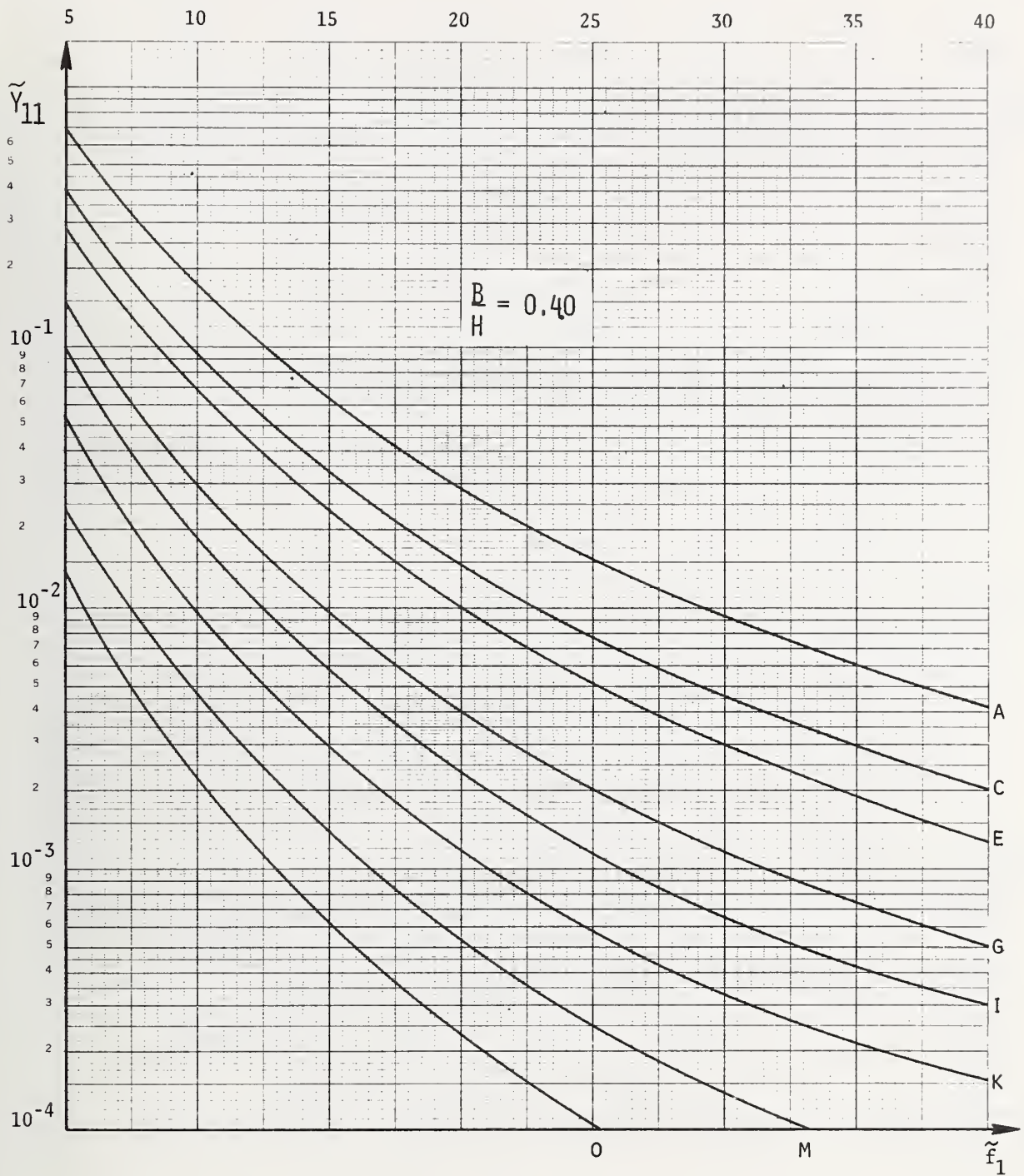


Fig. 4.16 Function $\tilde{\gamma}_{11}$, $B/H = 0.4$, $C_z = 4.0$, $C_y = 6.4$

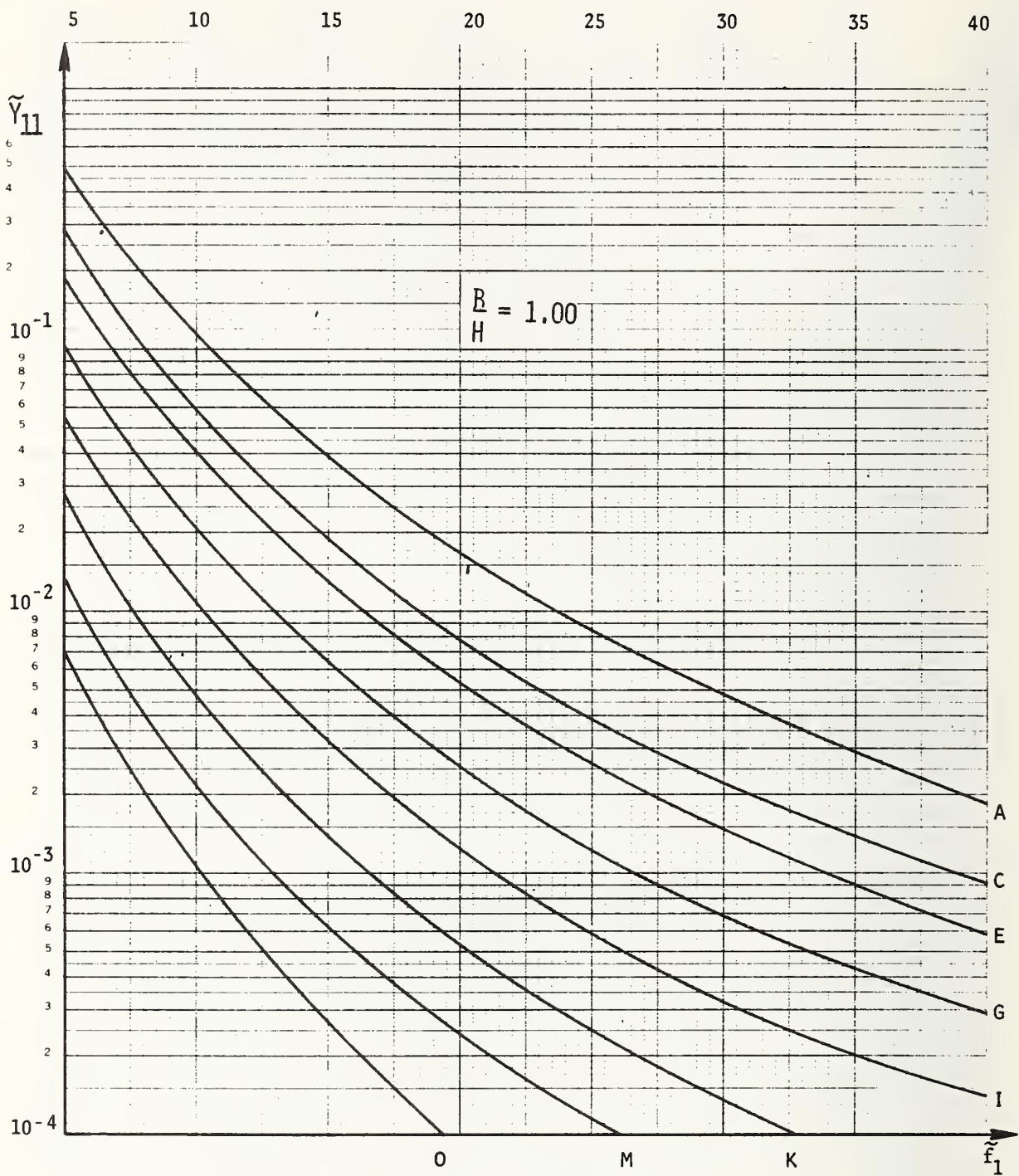


Fig. 4.17 Function $\tilde{\gamma}_{11}$, $B/H = 1.0$, $C_z = 4.0$, $C_y = 6.4$

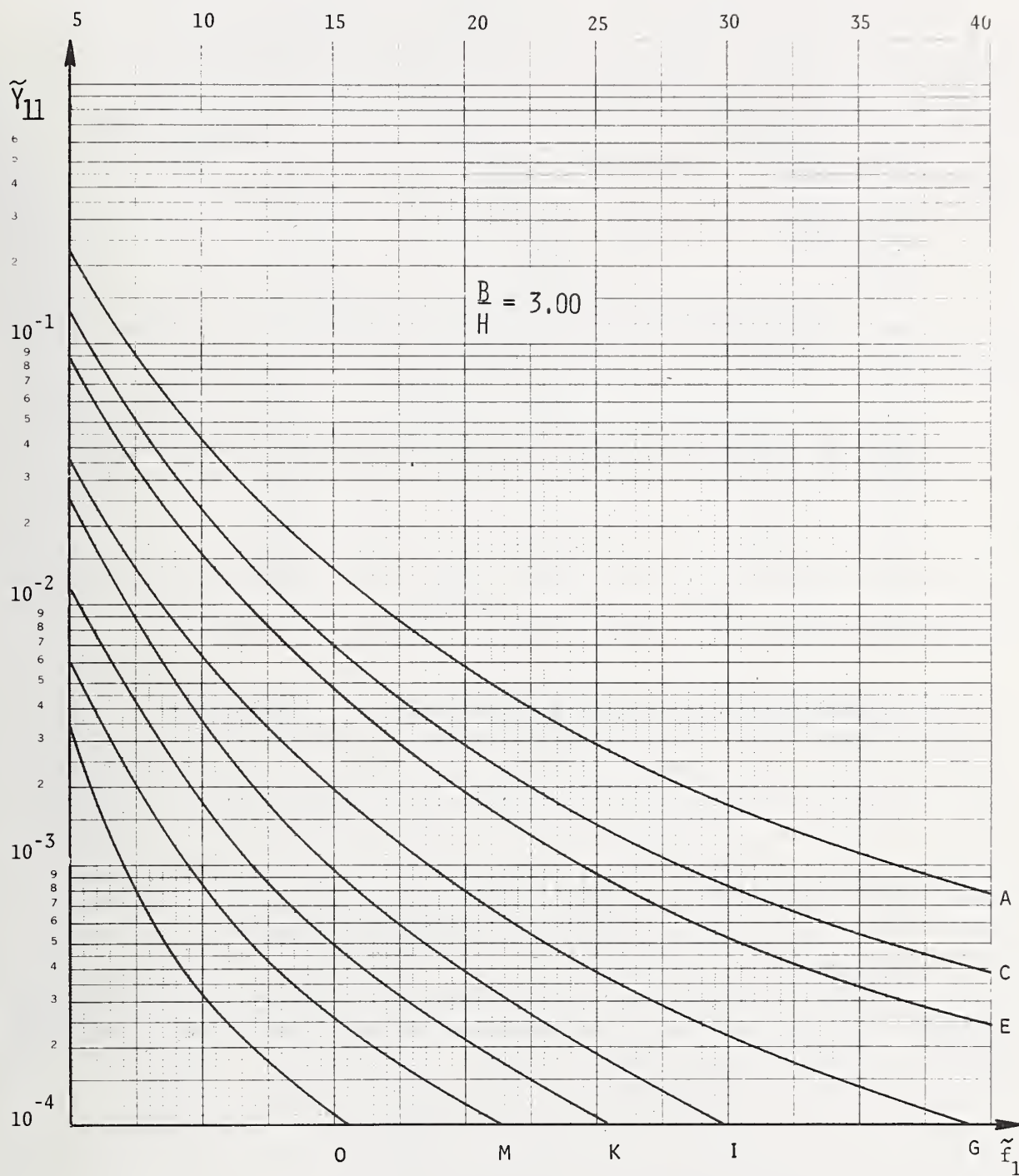


Fig. 4.18 Function \tilde{Y}_{11} , $B/H = 3.0$, $C_z = 4.0$, $C_y = 6.4$

In this chapter results of numerical calculations are presented on the basis of which estimates can be made of the errors associated with uncertainties regarding certain features and parameter values of the models employed. The calculations were carried out for three typical buildings selected as case studies and described in Table 5.1. The wind speed at 10 m above ground in open terrain ($z_o = 0.07\text{m}$) was assumed to be $v_f = 75\text{ mph}$, where v_f = fastest mile of wind.

Table 5.1

Description of Buildings Selected as Case Studies

Building	H	B meters	D	N_1 Hertz	η_1	w Newton/meter ³
1	365	60	45	0.10	0.01	1,500
2	150	60	45	0.20	0.01	1,500
3	45	45	45	1.00	0.01	1,500

Note: 1 Newton $\approx \frac{1}{4.25}$ lb

5.1 Contribution of Higher Vibration Modes to the Response

The root mean square of the fluctuating deflection and of the accelerations were calculated for buildings 2 and 4 in open exposure ($z_o = 0.07\text{ m}$, $z_d = 0$) and city exposure ($z_o = 0.80\text{m}$, $z_d = 21\text{m}$). The exponential decay coefficients assumed in the calculations were $C_z = 10$, $C_y = 16$. The assumed modal shapes in the first three modes are represented in Fig. 5.1. The damping ratios were assumed to be $\eta_1 = \eta_2 = \eta_3 = 0.01$. Calculations were carried out separately for the cases $n_2/n_1 = 1.2$, $n_3/n_1 = 1.5$ and $n_2/n_1 = 2.5$, $n_3/n_1 = 5$. The contributions of the higher (i.e., of the second and third) modes of vibration to the response are listed in Table 5.2.

The contribution of the cross-mode product terms was also included in Table 5.2. This contribution represented about one half of the amounts shown in columns (1) and (5) and was altogether negligible in all other cases.

It is seen that for the larger values of the ratios n_2/n_1 , n_3/n_1 in Table 5.2 - which are comparable to those encountered in practice in the case of typical tall buildings - the contribution of the higher modes to the fluctuating deflections is negligible. However, the contribution to the accelerations may be of the order of 10%.

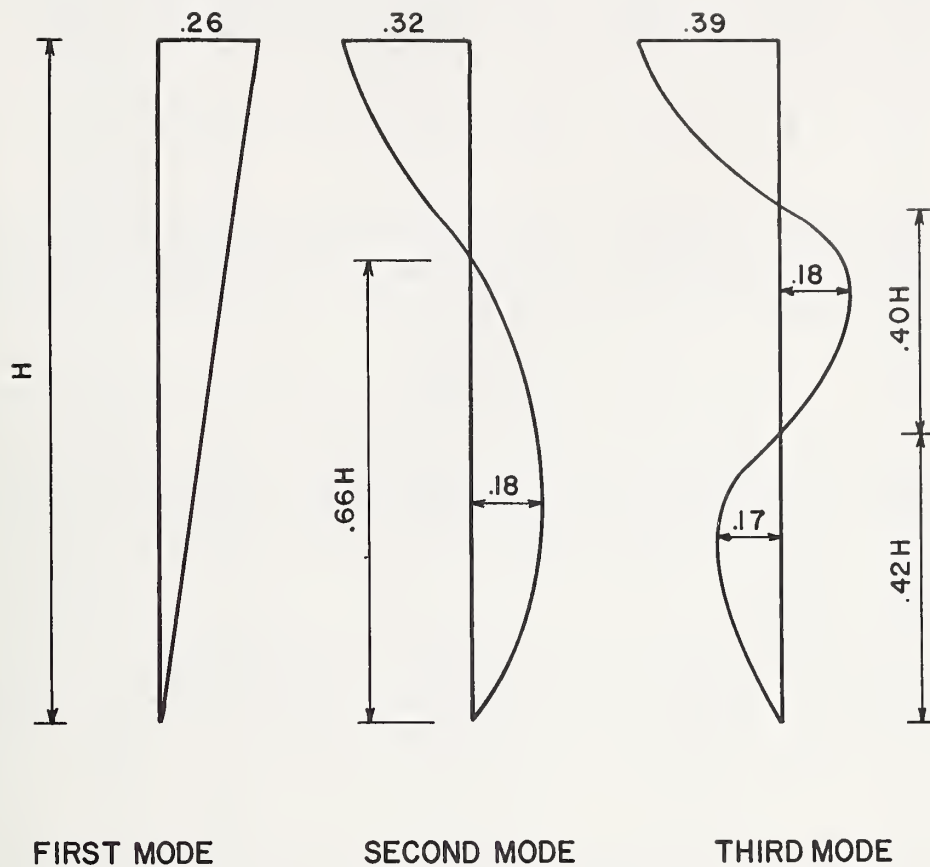


Fig. 5.1 - Modal Shapes

Table 5.2
Percent Contribution of Higher Modes of Vibration to
Root Mean Square of Fluctuating Response

Building	Open Exposure				Center of Large City			
	$n_2/n_1=1.2; n_3/n_1=1.5$		$n_2/n_1=2.5; n_3/n_1=5$		$n_2/n_1=1.2; n_3/n_1=1.5$		$n_2/n_1=2.5; n_3/n_1=5$	
	Defl. (1)	Accel. (2)	Defl. (3)	Accel. (4)	Defl. (5)	Accel. (6)	Defl. (7)	Accel. (8)
1	5	14	0.1	10	7	8	0.1	7
2	8	20	0.1	10	14	9	2	8

5.2 Influence upon Calculated Response of the Deviation from a Straight Line of Fundamental Modal Shape

A convenient means for estimating the influence upon response of the shape of the fundamental mode of vibration is provided by the expression

$$\frac{\overline{a^2}^{1/2}}{\bar{a}} = \frac{1 + \gamma + 2\alpha}{1 + \gamma + \alpha} Q \quad (5.1)$$

derived by Vickery [3] on the basis of the assumptions that the power law (Eq. 2.9) holds, that the spectra of the turbulent velocity fluctuations are independent of height and that the fundamental modal shape is described as follows:

$$\mu_1(z) = \left(\frac{z}{H}\right)^\gamma \quad (5.2)$$

where γ is a constant. In Eq. 5.1, $\overline{a^2}^{1/2}$ = r.m.s. of the fluctuating deflection, \bar{a} = mean deflection, Q = function of geometrical, mechanical and environmental parameters, independent of γ . It may be assumed, roughly, that α can vary between 0.10 for open exposure and 0.40 for centers of large cities. It follows from Eq. 5.1 that, for $\alpha = 0.10$, the ratios $\overline{a^2}^{1/2}/\bar{a}$ calculated assuming $\gamma = 0.5$ and $\gamma = 1.5$ differ by less than 1% from that calculated assuming $\gamma = 1$ (i.e., a linear fundamental modal shape). For $\alpha = 0.4$, the corresponding differences are of about 3%. It is thus seen that deviations from a straight line of the fundamental modal shape have an insignificant effect upon the calculated ratio $\overline{a^2}^{1/2}/\bar{a}$.

5.3 Influence Upon Calculated Response of Errors in the Estimation of the Roughness Length

To estimate the magnitude of the error associated with uncertainties regarding the actual value of the roughness length, the response of buildings 1,2,3 was calculated for coastal ($z_0 = 0.005-0.01m$), open ($0.03-0.08m$), suburban ($z_0 = 0.20-0.30 m$), center of town ($z_0 = 0.40 m$) and center of large city ($z_0 = 0.60-0.80 m$) exposures. The zero plane displacement was in all cases assumed to be zero. The results of the calculations are shown in Table 5.3.

It is seen from Table 5.3 that the sensitivity of the results to even large errors in the estimation of the roughness lengths is tolerably small. It is also noted that the alongwind deflections and, consequently, the design wind loads are higher by about 15% in the case of the coastal, than in the case of the open exposure.

5.4 Spectra in the Lower Frequency Range and Alongwind Response

It was shown in Section 2.2.5 that no universal relation exists that describes the shape of the spectral curve in the lower frequency range and that the peak similarity coordinate appears to vary strongly between sites and between atmosphere and laboratory. To estimate the effect of this variation, the response of buildings 1,2,3 was calculated in

Table 5.3 - Deflections and Accelerations for Various Roughness Lengths

		Exposure									
		Coastal	Open	Suburban	Town	Center of Large City					
Building 1	z_o^a	0.005	0.01	0.03	0.08	0.20	0.30	0.40	0.60	0.80	1.00
	u_*^b	1.85	1.92	2.05	2.20	2.34	2.38	2.44	2.51	2.56	2.61
	g_a	3.51	3.51	3.51	3.50	3.49	3.47	3.47	3.47	3.46	3.46
	G.F.	1.58	1.63	1.69	1.75	1.83	1.86	1.89	1.93	1.97	2.00
	$a_{\max}^{(H)^a}$	1.74	1.69	1.59	1.48	1.37	1.30	1.27	1.22	1.16	1.14
Building 2	g_a	0.020	0.020	0.019	0.019	0.018	0.017	0.016	0.016	0.015	0.015
	G.F.	3.69	3.69	3.68	3.67	3.67	3.66	3.65	3.64	3.63	3.61
	$a_{\max}^{(H)^a}$	1.62	1.68	1.74	1.81	1.87	1.95	1.97	2.03	2.08	2.13
	g_a	.37	.36	.33	.30	.27	.26	.25	.23	.22	.21
	$\ddot{a}_{\max}^{(H)^c}$	0.017	0.017	0.016	0.016	0.014	0.013	0.012	0.011	0.011	0.010
Building 3	g_a	3.94	3.89	3.89	3.87	3.85	3.84	3.83	3.80	3.78	3.76
	G.F.	1.55	1.59	1.69	1.79	1.93	2.03	2.10	2.21	2.27	2.38
	$a_{\max}^{(H)^a}$.0111	.0102	.0093	.0081	.0073	.0065	.0063	.0057	.0052	.0050
	g_a						4.18				
	$\ddot{a}_{\max}^{(H)^c}$.0061	.0050	.0050	.0043	.0040	.0035	.0034	.0030	.0023	.0026

Note: ^a meters; ^b meters/second; ^c units of g (g = acceleration of gravity)

the cases $z_o = 0.07m$, $z_d = 0$ and $z_o = 0.80m$, $z_d = 20m$ assuming values of the peak similarity coordinate $f_1 = 0.03$ (Eq. 2.14) and $f_1 = 0.01$, $f_1 = 0.10$, $f_1 = 0.19$ (Eqs. 2.15, 2.16). The ratios $[a_{max}]_{f_1} / [a_{max}]_{0.033}$ of the maximum probable response calculated using the values of the peak similarity coordinate f_1 and 0.033, respectively, are given in Table 5.4.

Table 5.4
Ratios $[a_{max}]_{f_1} / [a_{max}]_{0.03}$

Exposure	Building 1		Building 2		Building 3	
	Open	Large City	Open	Large City	Open	Large City
$f_1 = 0.01$	1.00	1.00	1.00	1.00	1.00	1.00
$f_1 = 0.10$.98	.97	.97	.94	.95	.91
$f_1 = 0.19$.97	.96	.96	.93	.93	.87

The results of Table 5.4 suggest that Eq. 2.14 (to which there corresponds $f_1 = 0.03$) is slightly conservative. As was mentioned in Section 2.2.5, according to available measurement results, between $z = 3m$ and $z = 60m$, $f_1 \approx 0.02-0.08$; the occurrence, in the case of building 3, of a fluctuating response corresponding to $f_1 = 0.10$ or $f_1 = 0.19$ is therefore believed to be unlikely. It is also noted that, in view of Eq. 4.14, the influence of the spectral curve shape in the lower frequency range upon the value of the accelerations is negligible.

5.5 Acrosswind Correlation of the Pressures and Alongwind Response

As indicated in Sect. 2.2.5, the exponential decay coefficients C_y , C_z appear to depend upon terrain roughness, height above ground and wind speed. For example, in the case of moderate wind speeds - such as usually occur during full-scale measurements of structural response - the values of C_y , C_z appear to be considerably lower than those corresponding to high winds. Values as low as $C_z = 4$ have been reported in the literature [50].

In view of the uncertainties with regard to the actual values of the coefficients C_y , C_z , it is of interest to estimate the errors in the calculated alongwind response that correspond to possible errors in the assumed values of those coefficients. The alongwind response of buildings 1, 2, 3 in open ($z_o = 0.07m$, $z_d = 0$), and large city ($z_o = 0.80m$, $z_d = 0$) exposures was therefore calculated separately for $C_z = 10$, $C_y = 16$ (case 1), for $C_z = 4$, $C_y = 6.4$ (case 6) and for four intermediate cases in which C_z , C_y were assumed either constant throughout the frequency range (case 4) or to have lower values at low frequencies and higher values near and beyond the fundamental frequency n_1 , (cases 2, 3, 5).

The ratios $r_i = [a_{\max}]_i / [a_{\max}]_1$, $\tilde{r}_i = [\ddot{a}_{\max}]_i$ in which cases 1 and i are denoted by the indices 1 and i, respectively ($i = 2, 3, 4, 5, 6$), are given in Table 5.5. It is seen that even a considerable change in the values of C_z , C_y in the lower frequency range affects little the calculated response (cases 1, 2, 3). However, large decreases in these values near the fundamental frequency of the structure do increase the total response, by as much as almost 10-20% in the case of the deflection and 160% in the case of the acceleration.

Table 5.5 - Ratios of Response for Various Values C_z , C_y to Response Calculated Using $C_z = 10$, $C_y = 16$

Case	C_z	C_y	Interval	Building 1			Building 2			Building 3		
				Open		Large City	Open		Large City	Open		Large City
				r_i	\tilde{r}_i		r_i	\tilde{r}_i		r_i	\tilde{r}_i	
1	10	16	$0 < n < \infty$	1.	1.	1.	1.	1.	1.	1.	1.	1.
2	6.3	10	$0 < n < .9n_1$	1.01	1.	1.01	1.	1.01	1.	1.01	1.	1.01
		16	$.9n_1 < n < \infty$									
3	4	6.4	$0 < n < .9n_1$	1.02	1.	1.02	1.	1.03	1.	1.02	1.	1.02
		16	$.9n_1 < n < \infty$									
4	6.3	10	$0 < n < \infty$	1.05	1.2	1.06	1.3	1.10	1.4	1.03	1.7	1.04
5	4	6.4	$0 < n < .9n_1$	1.06	1.2	1.07	1.3	1.13	1.4	1.06	1.4	1.05
		10	$.9n_1 < n < \infty$									
6	4	6.4	$0 < n < \infty$	1.12	1.5	1.11	1.5	1.17	1.3	1.08	2.1	1.10
												2.6

In this work practical procedures for calculating alongwind deflections and accelerations have been presented, which incorporate recent advances in the state of the art and are therefore believed to provide improved estimates of alongwind response. The procedures presented herein account for the variation of wind spectra with height and make allowance for the imperfect correlation of pressures acting on the windward and leeward building faces. Numerical examples are given, and the gust response factors obtained are compared to those calculated using procedures described in current codes and standards.

For structures with unusual modal shapes or for which the influence of vibration modes is significant the computer program presented in Chapter 3 and listed in the Appendix should be employed. In the case of typical tall structures, for which the ratios of higher to fundamental frequencies are not unusually low (e.g., for which $n_2/n_1 > 2$) and for which the fundamental modal shape may be expressed as $\mu_1(z) \approx (z/H)^\gamma$, where $0.5 < \gamma < 1.5$, the simplified procedure presented in Chapter 4 may be used.

Results of numerical calculations have been presented which show that the sensitivity of the results to even large errors in the estimation of the terrain roughness is tolerably small. It was noted, however, that the alongwind deflections and, consequently, the design wind loads may be higher by about 15% or so in the case of coastal, than in the case of open exposure. It was found that the effect upon the response of possible variations of the frequency, n , for which the reduced spectrum $n S(n)/u_*^2$ reaches a maximum is small. An investigation was also carried out of the effect upon the response of changes in the assumed values of the exponential decay coefficients C_y , C_z in the expression for the acrosswind cross-correlation of the fluctuating pressures. It was concluded that even a considerable change in the values of C_y , C_z in the lower frequency range has a negligible effect on the response. However, large decreases in these values near the fundamental frequency do significantly increase the calculated accelerations. The sensitivity of the calculated accelerations to changes in the values of the exponential decay coefficients suggests that measurements of accelerations, which are relatively simple and inexpensive, might offer useful information on the actual magnitude of these coefficients.

It was noted that additional research is desirable to improve current aerodynamic models describing the relation between wind speed fluctuations and the associated fluctuating pressures. It was also noted that according to full-scale measurements reported in the literature, the exponential decay coefficients C_y , C_z - which are a measure of the spatial cross-correlation of the wind speed and of the pressure fluctuations - depend upon terrain roughness, height above ground and wind intensity. In particular, the values of C_y , C_z , under moderate wind conditions, appear to be considerably lower than those corresponding to high winds. Therefore, full-scale measurements of alongwind structural response - particularly measurements of alongwind accelerations - can be useful for validating design procedures only to the extent that information on the dependence of C_y , C_z on the aforementioned parameters becomes available. Additional theoretical and experimental research aimed at obtaining such information is therefore believed to be necessary.

REFERENCES

1. Davenport, A.G., "Gust Loading Factors", Journal of the Structural Division, ASCE, Vol. 93, No. ST3, Proc. Paper 5255, June 1967, pp. 11-34.
2. Vellozzi, J. and Cohen, E., "Gust Response Factors", Journal of the Structural Division, ASCE, Vol. 94, No. ST6, Proc. Paper 5980, June 1968, pp. 1295-1313.
3. Vickery, B.J., "On the Reliability of Gust Loading Factors", Civil Engineering Transactions, April 1971, pp. 1-9.
4. American National Standard Building Code Requirements for Minimum Design Loads in Buildings and other Structures, American National Standards Institute, New York, New York, 1972.
5. National Building Code of Canada, National Research Council, Ottawa, 1970.
6. Canadian Structural Design Manual, Supplement No. 4 to the National Building Code of Canada, National Research Council of Canada, 1970.
7. Simiu, E. and Marshall, R.D., "Wind Loading and Modern Building Codes", Meeting Preprint 2268, ASCE National Structural Engineering Meeting, Cincinnati, Ohio, April 22-26, 1974.
8. Simiu, E., "Gust Factors and Alongwind Pressure Correlations", Journal of the Structural Division, ASCE, Vol. 99, No. ST4, Proc. Paper 9686, April 1973, pp. 773-783.
9. Simiu, E., "Wind Spectra and Dynamic Alongwind Response", Journal of the Structural Division, ASCE, Vol. 100, No. ST9, Proc. Paper 10815, Sept. 1974, pp. 1897-1910.
10. Hurty, W.C. and Rubinstein, M.F., Dynamics of Structures, Prentice Hall, Inc., Englewood Cliffs, N.J., 1964.
11. Southern Standard Building Code, Southern Building Code Congress, Birmingham, Alabama, 1965.
12. Patel, V.C. and Nash, J.F., "Numerical Study of the Hurricane Boundary-Layer Mean-Wind Profiles", Final Report, prepared by Sybucon, Inc., for U.S. Department of Commerce, National Bureau of Standards, Washington, D.C., June 30, 1974.
13. Teunissen, H.W., "Characteristics of the Mean Wind and Turbulence in the Planetary Boundary Layer", UTIAS Review No. 32, Institute for Aerospace Studies, University of Toronto, October, 1970.
14. Sacre, C., "Influence d'une Colline sur la Vitesse du Vent dans la Couche Limite de Surface", Centre Scientifique et Technique du Bâtiment, Section Climatologie, Nantes, France, June, 1973.
15. Panofsky, H.A., and Townsend, A.A., "Change of Terrain Roughness and the Wind Profile", Quarterly Journal of the Royal Meteorological Society, Vol. 90, 1964, pp. 147-155.
16. Taylor, P.A., "On Wind and Shear Stress Profiles above a Change in Surface Roughness", Quarterly Journal of the Royal Meteorological Society, Vol. 95, 1969, pp. 77-91.
17. Peterson, E.W., "Modification of Mean Flow and Turbulent Energy by a Change in Surface Roughness under Conditions of Neutral Stability", Quarterly Journal of the Royal Meteorological Society, Vol. 95, 1969, pp. 569-575.
18. Csanady, G.T., "On the Resistance Law of a Turbulent Ekman Layer", Journal of the Atmospheric Sciences, Vol. 24, Sept. 1967, pp. 467-471.

19. Tennekes, H., "The Logarithmic Wind Profile", Journal of the Atmospheric Sciences, Vol. 30, 1973, pp. 234-238.
20. Simiu, E., "Logarithmic Profiles and Design Wind Speeds", Journal of the Engineering Mechanics Division, ASCE, Vol. 99, No. EM5, Proc. Paper 10100, October, 1973, pp. 1073-1083.
21. Carl, D.M., Tarbell, T.C., Panofsky, H.A., "Profiles of Wind and Temperature from Towers over Homogeneous Terrain", Journal of the Atmospheric Sciences, Vol. 30, July, 1973, pp. 788-794.
22. Helliwell, N.C., "Wind Over London", Proceedings, Third International Conference of Wind Effects on Building and Structures, Tokyo, Japan, 1971.
23. Shellard, H.C., "Results of Some Recent Special Measurements in the United Kingdom Relevant to Wind Loading Problems", Proceedings, Wind Effects on Buildings and Structures, Ottawa, Vol. 1, University of Toronto Press, 1968.
24. Pasquill, F., "Wind Structure in the Atmospheric Boundary Layer", Philosophical Transactions of the Royal Society of London, A. 269, 1971, pp. 439-456.
25. Owen, P.R., "Buildings in the Wind", Quarterly Journal of the Royal Meteorological Society, Vol. 97, 1971, pp. 296-413.
26. Singer, I.A., Busch, N.E. and Frizzola, J.A., "The Micrometeorology of the Turbulent Flow Field in the Atmospheric Boundary Surface Boundary Layer", Proceedings, Wind Effects on Buildings and Structures, Ottawa, Vol. I, University of Toronto Press, 1968.
27. Busch, N.E. and Panofsky, H.A., "Recent Spectra of Atmospheric Turbulence", Quarterly Journal of the Royal Meteorological Society, Vol. 94, 1968, pp. 132-148.
28. Kaimal, J.C., et al., "Spectral Characteristics of Surface-Layer Turbulence", Quarterly Journal of the Royal Meteorological Society, Vol. 98, 1972, pp. 563-589.
29. Lumley, J.L. and Panofsky, H.A., "The Structure of Atmospheric Turbulence", John Wiley & Sons, 1964.
30. Fichtl, G., and McVehil, G., "Longitudinal and Lateral Spectra of Turbulence in the Atmospheric Boundary Layer", NASA TN D-5584, Washington, D.C., 1970.
31. Panofsky, H.A. and Singer, I.A., "Vertical Structure of Turbulence", Quarterly Journal of the Royal Meteorological Society, Vol. 91, July, 1965, pp. 339-344.
32. Vickery, B.J., and Kao, K.H., "Drag of Along-Wind Response of Slender Structures", Journal of the Structural Division, ASCE, Vol. 98, No. ST 1, Proc. Paper 8635, January 1972, pp. 21-36.
33. Kao, K.H., "Measurements of Pressure/Velocity Correlation on a Rectangular Prism in Turbulent Flow", Engineering Science Research Report BLWT-2-20, University of Western Ontario, London, Canada, 1971.
34. Bearman, P.W., "Some Measurements of the Distortion of Turbulence Approaching a Two-Dimensional Body", Journal of Fluid Mechanics, Vol. 53, part 3, pp. 451-467, 1972.
35. Petty, D.G., "The Distortion of Turbulence by a Circular Cylinder", Symposium on External Flows, University of Bristol, 4-6, July, 1972.
36. Batchelor, G.K., "The Theory of Homogeneous Turbulence", Cambridge University Press, Cambridge, England, 1953.
37. Vaicaitis, R., Shinozuka, M., and Takeno, M., "Response Analysis of Tall Buildings to Wind Loading", Technical Report No. 1, Department of Civil Engineering and Engineering Mechanics, Columbia University, July 1973, New York, p. 74.

38. Dalglish, W.A., "Statistical Treatment of Peak Gusts on Cladding", Journal of the Structural Division, ASCE, Vol. 97, No. ST 9, Proc. Paper 8356, Sept. 1971, pp. 2173-2187.
39. Van Koten, H., "The Fluctuating Wind Pressures on the Cladding and Inside a Building", Symposium on Full Scale Measurements of Wind Effects on Tall Buildings, The University of Western Ontario, June 23-29, 1974.
40. Lam Put, R., "Dynamic Response of a Tall Building to Random Wind Loads", Proceedings, International Conference on Wind Effects on Buildings and Structures, Tokyo, Japan, 1971, pp. III - 4.1 - 11.
41. Hunt, J.C.R., "A Theory of Turbulent Flow Over Bodies", Journal of Fluid Mechanics, Vol. 61, part 4, Dec. 1973, pp. 625-706.
42. Marshall, R.D., "Surface Pressure Fluctuations Near an Axisymmetric Stagnation Point", NBS Technical Note 563, National Bureau of Standards, August, 1971.
43. Sadeh, W.Z., and Cermak, J.E., "Turbulence Effects on Wall Pressure Fluctuations", Journal of the Engineering Mechanics Division, ASCE, Vol. 98, EM6, Proc. Paper 9445, Dec. 1972, pp. 1365-1379.
44. Sadeh, W.Z., Cermak, J.E. and Hsi, G., "A Study of Wind Loading on Tall Structures -- Atlantic Richfield Plaza Building, Colorado State University Research Report CER68-69W25-JEC-GH-36, Fort Collins, Colorado, Aug. 1969.
45. Newberry, C.W., Eaton, K.J., and Mayne, J.R., "Wind Loading of a Tall Building in an Urban Environment", Building Research Station Garston, Watford, England, 1968.
46. Fujii, K., Hibi, K., Kaneko, T., "The Full-Scale Measurement of Wind Pressures on a Tall Building - Further Results from the Asaki-Takai Building", Symposium of Full Scale Measurements of Wind Effects on Tall Buildings and Other Structures, The University of Western Ontario, Canada, June 23-29, 1974.
47. Holmes, J.D., "Characteristics of Pressure Fluctuations on the Windward Face of a Large Building", Symposium on Full Scale Measurements of Wind Effects on Tall Buildings and Other Structures, The University of Western Ontario, Canada, June 23-29, 1974.
48. Ishizaki, H., and Yoshikawa, Y., "On the Wind Pressure and Wind Flow around a Tall Building", Symposium on Full Scale Measurements of Wind Effects on Tall Buildings and Other Structures, The University of Western Ontario, Canada, June 23-29, 1974.
49. Kato, B. et al., "Wind Pressure Responses of a Tall Building", Symposium on Full-Scale Measurements of Wind Effects on Tall Buildings and Other Structures, The University of Western Ontario, Canada, June 23-29, 1974.
50. Newberry, C.W., Eaton, K.J., and Mayne, J.R., "Wind Loading on Tall Buildings - Further Results from the Royex House", Industrial Aerodynamics Abstracts 4, July-August, 1973, pp. 1-16.
51. Baines, W.D., "Effects of Velocity Distribution on Wind Loads and Flow Patterns on Buildings", Proceedings, Wind Effects on Buildings and Structures, Teddington, 1963, Her Majesty's Stationery Office, London, 1965.
52. Robson, J.D., An Introduction to Random Vibration, Elsevier Publishing Co., 1964, p. 91.
53. Haber, S., "A Modified Monte Carlo Quadrature", II, Mathematics of Computation, Vol. 21, 1967, pp. 388-397.
54. Meirovitch, L., Analytical Methods in Vibrations, The MacMillan Company, Collier-MacMillan Canada, Ltd., Toronto, 1967, p. 505.

55. Blume, J.A., Newmark, N.M, and Corning, L.H., Design of Multistory Reinforced Concrete Buildings for Earthquake Motions, Portland Cement Association, Chicago, Ill., 1961.
56. Durst, C.S., "Wind Speeds over Short Periods of Time", Meteorological Magazine, Vol. 89, 1960.
57. Byers, H.R., and Graham, R.R., The Thunderstorm, United States Department of Commerce, Washington, D.C., 1949.
58. Deacon, E.L., "Gust Variation with Height up to 150 m," Quarterly Journal of the Royal Meteorological Society, Vol. 91, 1955, pp. 562-573.
59. Frost, R., "The Velocity Profile in the Lowest 400 ft.", Meteorological Magazine, Vol. 81, pp. 14-17.
60. Harris, R.I. "Measurements of Wind Structure at Heights up to 598 ft above Ground Level", Proceedings, Symposium on Wind Effects on Buildings and Structures, Loughborough University of Technology, Leicestershire, England, 1968.
61. Holmes, J.D., "Pressure Fluctuations on a Large Building and Along-wind Structural Loading", International Journal of Industrial Aerodynamics, (to be published).
62. Taoka, G. et al., "Ambient Response of Some Tall Structures," Journal of the Structural Division, ASCE, Vol. 101, No. ST 1, Proc. Paper 11051, January, 1975, pp. 49-55.
63. Shiotani, M., Structure of Gusts in High Winds, Interim Report, Parts 1-4, The Physical Sciences Laboratory, Nihon University, Furabashi, Chiba, Japan, 1967-1971.
64. Shiotani, M., and Iwatani, Y., "Correlations of Wind Velocities in Relation to the Gust Loading", Proceedings, Third International Conference on Wind Effects on Buildings and Structures, Tokyo, 1971.



A P P E N D I X

COMPUTER PROGRAM LISTING

SAMPLE INPUT AND OUTPUT


```

C/**/WINDLOAD
      INTEGER R,RVAL,SVAL,PLIM
      DIMENSION PSUM(4),WP(4),FACTOR(4),WEIGHT(4),TERM(4),TERMV(4),
      ISIGMA(4),PSUU(4),WEIGHU(4),TERU(4),XJH(4)
      COMMON/BLOCK2/H,BCON,DCON,XMASS,EN(8),ZETA(8),Z0,CZ,CY,BETACN,
      IF1,FS,USTAR,T,CW,CL,XN,RHO,IREP,IPRINT,RLIM
      COMMON/BLOCK1/KOUNT
      COMMON/BLOCK3/FTILDA(200),ATILDA(200),M,NF(4),NN(4)
      COMMON/BLOCK5/RVAL,SVAL
      COMMON/BLOCK6/XMUINT(8),GINT(8)
200  CONTINUE
      KOUNT=0
      CALL INPUT
      TFAC1=CW*CW+2.0*CW*CL+CL*CL
      TFAC2=CW*CW+XN*2.0*CW*CL+CL*CL
C   SEE EQ.2.59 OF THIS REPORT FOR OCCURRENCE OF THIS FACTOR.
      TCRIT=0.9*EN(1)*H/USTAR
      DO 202 J=1,4
      XJH(J)=0.0
202  CONTINUE
      GH=0.0
      DO 250 R=1,RLIM
      RVAL=R
      SVAL=RVAL
      CALL INIT
C   PERFORM FOUR-DIMENSIONAL INTEGRATION.
      DO 205 J=1,4
      PSUU(J)=0.0
      SIGMA(J)=0.0
205  PSUM(J)=0.0
      N=NN(1)
C   M IS NUMBER OF STEPS IN FTILDA INTEGRATION
      DO 230 I=1,M
      IF (I.GT.NF(1)) N=NN(2)
      IF (I.GT.NF(1)+NF(2)) N=NN(3)
      IF (I.GT.NF(1)+NF(2)+NF(3)) N=NN(4)
      W=FTILDA(I)
      CALL TRIPLE(N,W,Z,E)
      IF (IPRINT.EQ.2) GO TO 212
      IF (MOD(I-1,5).EQ.0) WRITE (6,210) RVAL,SVAL
      WRITE (6,211) Z,E
210  FORMAT(19H1INTEGRAL FOR R,S =,I2,1H,,I2)
211  FORMAT(/26H0AVG OF TRIPLE INTEGRALS =,E12.5,4X,9HERR EST =,E12.5)
      GO TO 214
212  IF (I.LT.M) GO TO 214
      WRITE (6,210) RVAL,SVAL
      WRITE (6,211) Z,E
214  CONTINUE
      WP(1)=1.0
      WP(2)=W*W
      WP(3)=WP(2)*WP(2)
      WP(4)=WP(3)*WP(2)
      PHISTR=FISTAR(W)
      TFAC=TFAC1
      IF (W.GE.TCRIT) TFAC=TFAC2

```

```

DO 215 J=1,4
  FACTOR(J)=WP(J)*PHISTR
  WEIGHT(J)=ATILDA(1)*FACTOR(J)
  TERM(J)=Z*WEIGHT(J)
  PSUM(J)=PSUM(J)+TFAC*TERM(J)
C   PSUM IS 1 SUB RRL (EQ. 2.54 OF THIS REPORT).
  TERMV(J)=(WEIGHT(J)*E)*(WEIGHT(J)*E)
  SIGMA(J)=SQRT(SIGMA(J)*SIGMA(J)+TERMV(J))
  WEIGHU(J)=ATILDA(1)*WP(J)
  TERU(J)=Z*WEIGHU(J)
  PSUU(J)=PSUU(J)+TERU(J)
C   PSUU IS 1 SUB RRL (EQ. 2.54) WITH FISTAR AND TFAC2 EQUAL UNITY.
215 CONTINUE
  IF (IPRINT.EQ.2 .AND. 1.LT.M) GO TO 230
  WRITE(6,220)
220 FORMAT(/19X,12HMECH. ADMITT,9X,6HWEIGHT,11X,4HTERM,4X,11HPARTIAL
  ISUM,6X,9HTERM VAR.,10X,5HSIGMA,9X,4HTERU,1X,12HPARTIAL SUMU )
  WP(1)=FTILDA(1)
  DO 225 J=1,4
    WRITE(6,221) WP(J),FACTOR(J),WEIGHT(J),TERM(J),PSUM(J),TERMV(J),
    1SIGMA(J),TERU(J),PSUU(J)
221 FORMAT(1X,7E15.8,2E13.8)
225 CONTINUE
230 CONTINUE
  DO 240 J=1,4
    XJH(J)=XJH(J)*XJH(J)
    XJH(J)=XJH(J)+XMU(RVAL,1.0)*XMU(SVAL,1.0)*PSUM(J)/
    1(XMUINT(RVAL)*XMUINT(SVAL)*(EN(RVAL)*EN(SVAL)*(H/USTAR)**2)**2)
    XJH(J)=SQRT(XJH(J))
240 CONTINUE
    GH=GH+XMU(R,1.0)*GINT(R)/(XMUINT(R)*(EN(R)*H/USTAR)**2)
    DEF=0.5*(CW+CL)*RHO*BCON*H*H*GH/(39.478418*XMASS)
    RMSDEF=RHO*BCON*H*H*XJH(1)/(39.478418*XMASS)
    RMSACC=RHO*BCON*USTAR*USTAR*XJH(3)/XMASS
    XX=SQRT(2.0*ALOG(USTAR*XJH(2)*T/(H*XJH(1))))
    PEAKDF=XX+0.577/XX
    XXX=SQRT(2.0*ALOG(USTAR*XJH(4)*T/(H*XJH(3))))
    PEAKAC=XXX+0.577/XXX
    WRITE(6,280) DEF,RMSDEF,RMSACC,PEAKDF,PEAKAC
280 FORMAT(29H1MEAN ALONGWIND DEFLECTION...,E16.8/
  134H0RMS OF FLUCTUATING DEFLECTIONS...,E16.8/
  224H0RMS OF ACCELERATIONS...,E16.8/
  330H0PEAK FACTOR FOR DEFLECTION...,E16.8/
  432H0PEAK FACTOR FOR ACCELERATION...,E16.8)
250 CONTINUE
  GO TO 200
END
C /* INPUT
  SUBROUTINE INPUT
C   INPUT OF PARAMETERS FROM CARDS, SEE CHAP. 3 OF THIS REPORT.
  INTEGER RLIM
  COMMON/BLOCK2/H,BCON,DCON,XMASS,EN(8),ZETA(8),Z0,CZ,CY,BETACN,
  1F1,FS,USTAR,T,CW,CL,XN,RHO,IREP,IPRINT,RLIM
  READ(5,1) IREP,IPRINT,RLIM
  IF (IREP.EQ.0) GO TO 30

```

```

1      FORMAT(3I2)
      READ (5,2) H,BCON,XMASS
      READ (5,2) (EN(I),I=1,RLIM)
      READ (5,2) (ZETA(I),I=1,RLIM)
      IF (IREP.EQ.1) READ (5,2) Z0,CZ,CY,DCON,BETACN
      IF (IREP.EQ.2) READ (5,2) Z0,CZ,Y,DCON,BETACN,F1,FS
      READ (5,2) USTAR,T
      READ (5,2) CW,CL,XN,RHO
2      FORMAT(8F6.0)
      WRITE (6,11) IREP,IPRINT,RLIM
11     FORMAT(1H1,35X,26HVALUES OF INPUT PARAMETERS//
119H0CONTROL PARAMETERS/
114H0      IREP =,I3/
214H      IPRINT =,I3/
314H      RLIM =,I3)
      WRITE (6,12) H,BCON,XMASS
12     FORMAT(/22H0STRUCTURAL PARAMETERS/
114H0      H =,F12.3/
114H      BCON =,F12.3/
314H      XMASS =,F12.3)
      WRITE (6,13) (EN(I),I=1,RLIM)
13     FORMAT(22H      (EN(I),I=1,RLIM)...,8F10.3)
      WRITE (6,14) (ZETA(I),I=1,RLIM)
14     FORMAT(22H      (ZETA(I),I=1,RLIM)...,8F10.3)
      WRITE (6,15) Z0,CZ,CY,DCON,BETACN
15     FORMAT(/31H0MICROMETEOROLOGICAL PARAMETERS/
114H0      Z0 =,F12.3/
114H      CZ =,F12.3/
214H      CY =,F12.3/
214H      DCON =,F12.3/
314H      BETACN =,F12.3)
      IF (IREP.EQ.2) WRITE (6,16) F1,FS
16     FORMAT(14H      F1 =,F12.3/
114H      FS =,F12.3)
      WRITE (6,17) USTAR,T
17     FORMAT(/26H0CLIMATOLOGICAL PARAMETERS/
114H0      USTAR =,F12.3/
114H      T =,F12.3)
      WRITE (6,18) CW,CL,XN,RHO
18     FORMAT(/23H0AERODYNAMIC PARAMETERS/
114H0      CW =,F12.3/
114H      CL =,F12.3/
214H      XN =,F12.3/
314H      RHO =,F12.3)
      RETURN
30     WRITE (6,31)
31     FORMAT(///47H0NORMAL EXIT, END-OF-FILE ENCOUNTERED ON INPUT.)
      STOP
      END
C/*/INIT
      SUBROUTINE INIT
C   THIS SUBROUTINE SETS UP THE INTEGRATION PARAMETERS FOR THE CURRENT
C   VALUE OF RVAL. NOTE THIS INTEGRATION SCHEME IS VALID ONLY FOR THE
C   CASE RVAL=SVAL. SEE CHAP. 3 OF THIS REPORT FOR DESCRIPTION
C   OF HOW THE PARAMETERS NF AND NN MAY BE CHOSEN.

```



```

      INTEGER RLIM,RVAL,SVAL
      COMMON/BLOCK2/H,BCON,DCON,XMASS,EN(8),ZETA(8),Z0,CZ,CY,BETACN,
      IF1,FS,USTAR,T,CW,CL,XN,RHO,IREF,IPRINT,RLIM
      COMMON/BLOCK3/FTILDA(200),ATILDA(200),M,NF(4),NN(4)
      COMMON/BLOCK5/RVAL,SVAL
      NF(1)=10
      NF(2)=10
      NF(3)=20
      NF(4)=10
      NN(1)=5
      NN(2)=6
      NN(3)=6
      NN(4)=6
      FPEAK=EN(RVAL)*H/USTAR
      M=1
      STEPOL=0.
      DO 110 I=1,4
      IF (1.EQ.1) FTILDA(M)=0.
      IF (1.EQ.2) FTILDA(M) = (FPEAK-2.)/30.
      IF (1.EQ.3) FTILDA(M)=FPEAK-2.
      IF (1.EQ.4) FTILDA(M)=FPEAK+2.
      IF (1.EQ.1) STEPNU=((FPEAK-2.)/30.)/FLOAT(NF(1))
      IF (1.EQ.2) STEPNU=((29.*FPEAK-58.)/30.)/FLOAT(NF(2))
      IF (1.EQ.3) STEPNU=4./FLOAT(NF(3))
      IF (1.EQ.4) STEPNU=(2.*FPEAK)/FLOAT(NF(4))
      ATILDA(M)=(STEPOL+STEPNU)/2.
      MM=NF(I)-1
      DO 101 J=1,MM
      MJ=M+J
      FTILDA(MJ)=FTILDA(M)+FLOAT(J)*STEPNU
101  ATILDA(MJ)=STEPNU
      M=M+MM+1
110  STEPOL=STEPNU
      M=M-1
      ATILDA(M)=ATILDA(M)+(2.*FPEAK-STEPOL)*3./20.
      WRITE (6,115) RVAL,SVAL,M,NF,NN,FPEAK
115  FORMAT(44HVALUES OF INTEGRATION PARAMETERS FOR R,S = ,I2,IH,,I2/
      19H0      M =,I4/
      217H0(NF(I),I=1,4)...,4I4/
      317H0(NN(I),I=1,4)...,4I4/
      49H0 FPEAK =,F12.3)
      WRITE (6,116) (FTILDA(I),I=1,M)
116  FORMAT(21H0(FTILDA(I),I=1,M)...,10F8.3/(21X,10F8.3))
      WRITE (6,117) (ATILDA(I),I=1,M)
117  FORMAT(21H0(ATILDA(I),I=1,M)...,10F8.3/(21X,10F8.3))
      RETURN
      END
C/ */TRIPLE
      SUBROUTINE TRIPLE(N,W,Z,E)
C   TRIPLE INTEGRAL EVALUATED BY A MONTE CARLO METHOD.
C   INTEGRAL EVALUATED IS I SUB R,S OF FTILDA. (EQ. 2.57 OF THIS REPORT.
C   SEE CHAP. 3 IN WHICH THE QUADRUPLE INTEGRAL IS TRANSFORMED INTO
C   A TRIPLE INTEGRAL.)
C   INPUT...W, THE CURRENT VALUE OF FTILDA
C           N, THE NUMBER OF SUBDIVISIONS TO TAKE ON EACH EDGE OF

```

```

C      THE UNIT CUBE FOR THE MONTE CARLO QUADRATURE
C      R AND S ARE IN LABELLED COMMON AND ARE NEEDED ONLY IN
C      THE FUNCTION SUBROUTINE F THAT EVALUATES THE INTEGRAND
C      OF THE TRIPLE INTEGRAL
C      OUTPUT...Z, THE APPROXIMATION TO THE TRIPLE INTEGRAL
C      E, AN ERROR ESTIMATE FOR Z
C      DOUBLE PRECISION D,DFRA,DK,DKSQ,DPRIME
C      COMMON/BLOCK1/KOUNT
C      DIMENSION D(3),DPRIME(3),Q(3),X(3),XPRIME(3),P(3),R(3),RPRIME(3),
C      IS(3),SPRIME(3)
C
C      SIX SEQUENCES OF PSEUDO-RANDOM NUMBERS ARE GENERATED
C      FOR THE MONTE CARLO QUADRATURE. THEY ARE OF THE FORM
C
C      X SUB K = FRACT. PART OF (K**2)*SQRT(P)
C
C      WHERE P TAKES THE PRIME VALUES 2,3,5,7,11 AND 13.
C      VALUES OF K AND K**2 ARE STORED IN DOUBLE PRECISION
C      TO ALLOW THE LARGEST POSSIBLE VALUE OF K**2. THE
C      FOLLOWING ARITHMETIC STATEMENT FUNCTION CONTAINS
C      A NON-STANDARD INTRINSIC FUNCTION, DMOD, TO PERMIT
C      THE DOUBLE PRECISION FRACTIONAL PART TO BE TAKEN.
C      DFRA(D)=DMOD(D,1.0D0)
C      IF (KOUNT.GT.0) GO TO 10
C      DK=0.0D0
C      D(1)=DFRA(DSQRT(2.0D0))
C      D(2)=DFRA(DSQRT(3.0D0))
C      D(3)=DFRA(DSQRT(5.0D0))
C      DPRIME(1)=DFRA(DSQRT(7.0D0))
C      DPRIME(2)=DFRA(DSQRT(11.0D0))
C      DPRIME(3)=DFRA(DSQRT(13.0D0))
10  CONTINUE
C      XN=N
C      RXN=1.0/XN
C      RXNH=0.5*RXN
C      N3=N*N*N
C      XN3=XN3
C      RXN3=1.0/XN3
C      RXN3H=0.5*RXN3
C      Y=0.0
C      YPRIME=0.0
C      E=0.0
C      DO 30 K3=1,N
C      DO 30 K2=1,N
C      DO 30 K1=1,N
C      DK=DK+1.0D0
C      DKSQ=DK*DK
C      Q(1)=K1-1
C      Q(2)=K2-1
C      Q(3)=K3-1
C      DO 15 I=1,3
C      X(I)=DFRA(DKSQ*D(I))
C      XPRIME(I)=DFRA(DKSQ*DPRIME(I))
15  CONTINUE
C      DO 20 I=1,3

```

```

      Q(I)=Q(I)*RXN
      P(I)=Q(I)+RXNH
      R(I)=Q(I)+RXN*X(I)
      RPRIME(I)=Q(I)+RXN*XPRIME(I)
      PI2=2.0*P(I)
      S(I)=PI2-R(I)
      SPRIME(I)=PI2-RPRIME(I)
20  CONTINUE
      FR=F(R,W)
      FS=F(S,W)
      G=FR+FS
      FRPRIM=F(RPRIME,W)
      FSPRIM=F(SPRIME,W)
      GPRIME=FRPRIM+FSPRIM
      Y=Y+G
      YPRIME=YPRIME+GPRIME
      E=E+(G-GPRIME)**2
30  CONTINUE
      Y=Y*RXN3H
      YPRIME=YPRIME*RXN3H
      Z=0.5*(Y+YPRIME)
      E=0.25*RXN3*SQRT(E)
      RETURN
      END
C / * / F
      FUNCTION F(V,W)
C      CALCULATION OF INTEGRAND FOR TRIPLE INTEGRAL
C      Y SUB R,S OF FTILDA
C (EQ. 2.57 OF THIS REPORT, WHICH IS TRANSFORMED INTO A TRIPLE
C INTEGRAL BY A CHANGE OF VARIABLE. SEE CHAP. 3.)
C THE PROGRAM VARIABLE W STANDS FOR FTILDA. THE VALUES
C OF R AND S ARE STORED IN COMMON BLOCK /BLOCK5/.
C THE VARIABLE KOUNT IN /BLOCK1/ IS SET TO ZERO WHEN
C NEW INPUT PARAMETERS ARE READ BY SUBROUTINE INPUT. IT IS INCREASED
C BY ONE EACH TIME THIS SUBROUTINE IS EXECUTED, SO AT THE END OF THE
C WHOLE FOUR-DIMENSIONAL INTEGRATION, IT CONTAINS THE NUMBER OF TIMES
C THE INTEGRAND FOR THE TRIPLE INTEGRAL WAS CALCULATED.
      INTEGER RLIM,RVAL,SVAL
      DIMENSION V(3)
      COMMON/BLOCK1/KOUNT
      COMMON/BLOCK2/H,BCON,DCON,XMASS,EN(8),ZETA(8),Z0,CZ,CY,BETACN,
      IF1,FS,USTAR,T,CW,CL,XN,RHO,IREF,IPRINT,RLIM
      COMMON/BLOCK5/RVAL,SVAL
      IF (KOUNT.GT.0) GO TO 2000
C      INITIALIZATION.
      CON1=2.0*CZ
      CON2=CY*BCON/(CZ*H)
2000  CONTINUE
      Z1=V(1)
      Z2=V(2)
      TT=V(3)
      UT1=UTILDA(Z1)
      UT2=UTILDA(Z2)
      ALPHA=(1.0-TT)*XMU(RVAL,Z1)*XMU(SVAL,Z2)*UT1*UT2
      ALPHA=ALPHA*SQRT(STILDA(W,Z1,UT1)*STILDA(W,Z2,UT2))

```

```

      BETA=CON1*SQR((Z1-Z2)**2+(CON2*TT)**2)/(UT1+UT2)
      F=ALPHA*EXP(-BETA*W)
      KOUNT=KOUNT+1
      RETURN
      END
C/ */XMU
      FUNCTION XMU(I,Z)
C    COMPUTATION OF MODAL SHAPES.
      COMMON/BLOCK1/KOUNT
      COMMON/BLOCK6/XMUINT(8),GINT(8)
      DIMENSION XMUTAB(15,8)
C    FIRST MODAL SHAPE
      DATA XMUTAB(1,1),XMUTAB(2,1),XMUTAB(3,1),XMUTAB(4,1),XMUTAB(5,1),
1        XMUTAB(6,1),XMUTAB(7,1),XMUTAB(8,1),XMUTAB(9,1),XMUTAB(10,1),
2    XMUTAB(11,1),XMUTAB(12,1),XMUTAB(13,1),XMUTAB(14,1),XMUTAB(15,1)/
3    .00000, .01857, .03714, .05571, .07429,
4    .09286, .11143, .13000, .14857, .16714,
5    .18571, .20429, .22286, .24143, .26000/
C    SECOND MODAL SHAPE
      DATA XMUTAB(1,2),XMUTAB(2,2),XMUTAB(3,2),XMUTAB(4,2),XMUTAB(5,2),
1        XMUTAB(6,2),XMUTAB(7,2),XMUTAB(8,2),XMUTAB(9,2),XMUTAB(10,2),
2    XMUTAB(11,2),XMUTAB(12,2),XMUTAB(13,2),XMUTAB(14,2),XMUTAB(15,2)/
3    .00000,-.05377,-.10620,-.14350,-.17210,
4    -.18310,-.16310,-.12920,-.08235,-.02325,
5    .05252, .12850, .22520, .29870, .32350/
C    THIRD MODAL SHAPE
      DATA XMUTAB(1,3),XMUTAB(2,3),XMUTAB(3,3),XMUTAB(4,3),XMUTAB(5,3),
1        XMUTAB(6,3),XMUTAB(7,3),XMUTAB(8,3),XMUTAB(9,3),XMUTAB(10,3),
2    XMUTAB(11,3),XMUTAB(12,3),XMUTAB(13,3),XMUTAB(14,3),XMUTAB(15,3)/
3    .00000,-.07302,-.13360,-.16530,-.16940,
4    -.11011, .02515, .10890, .16540, .18120,
5    .10110,-.04585,-.19280,-.30800,-.37660/
C    HIGHER MODAL SHAPES NOT USED IN PRESENT SUBROUTINE.
      IF (KOUNT.GT.0) GO TO 5
C    INITIALIZATION.
      DO 10 J=4,8
      DO 10 K=1,15
10    XMUTAB(K,J)=0.0
C    COMPUTE INTEGRALS OF XMU(I,Z)**2 AND OF XMU(I,Z)*UTILDA(Z)**2.
C    THESE ARE DENOTED BY XMUINT AND GINT, RESPECTIVELY, AND THE
C    VALUES ARE RETURNED IN COMMON BLOCK /BLOCK6/.
      DO 2 J=1,3
      S=0.0
      T=0.0
      DO 1 K=2,14
      S=S+XMUTAB(K,J)*UTILDA(FLOAT(K-1)/14.0)**2
1    T=T+XMUTAB(K,J)**2
      S=S+0.5*XMUTAB(15,J)*UTILDA(1.0)**2
      T=T+0.5*XMUTAB(15,J)**2
      GINT(J)=S/14.0
2    XMUINT(J)=T/14.0
      DO 3 J=4,8
      GINT(J)=0.0
3    XMUINT(J)=0.0
5    CONTINUE

```



```

      Y=14.0*Z
      J=Y
      IF (J.EQ.14) GO TO 30
      XMU=XMUTAB(J+1,I)+(Y-FLOAT(J))*(XMUTAB(J+2,I)-XMUTAB(J+1,I))
      RETURN
30    XMU=XMUTAB(J+1,I)
      RETURN
      END
C/ */UTILDA
      FUNCTION UTILDA(Z)
C    NONDIMENSIONALIZED MEAN WIND SPEED AT ELEVATION Z.
      INTEGER RLIM
      COMMON/BLOCK1/KOUNT
      COMMON/BLOCK2/H,BCON,DCON,XMASS,EN(8),ZETA(8),Z0,CZ,CY,BETACN,
      IF1,FS,USTAR,T,CW,CL,XN,RHO,IREP,IPRINT,RLIM
      IF (KOUNT.GT.0) GO TO 1
C    INITIALIZATION.
      ZA=(10.0+DCON)/H
      UCONST=2.5*ALOG(10.0/Z0)
      DTILDA=DCON/H
      HOZ0=H/Z0
1     CONTINUE
      UTILDA=UCONST
      IF (Z.GT.ZA) UTILDA=2.5*ALOG((Z-DTILDA)*HOZ0)
      RETURN
      END
C/ */STILDA
      FUNCTION STILDA(W,Z,UT)
C    THIS FUNCTION IS RELATED TO THE ASSUMED REPRESENTATION
C    OF THE SPECTRUM OF LONGITUDINAL WIND FLUCTUATIONS. STILDA
C    IS THE EXPRESSION
      N*S(Z,N)/(FTILDA*USTAR**2)
C    THAT APPEARS IN EQ. 2.57 OF THIS REPORT.
C
C    TWO REPRESENTATIONS OF STILDA ARE CODED HERE, ONE A
C    MODIFICATION OF A FORMULA (EQ. 2.14 OF THIS REPORT)
C    OF KAIMAL, THE OTHER A FORMULA (EQS. 2.15, 2.16 AND 2.11 OF
C    THIS REPORT) DEVISED TO STUDY THE DEPENDENCE ON
C    THE PARAMETER F1, THE PEAK SIMILARITY COORDINATE. THE FIRST
C    OR SECOND REPRESENTATION WILL BE SELECTED ACCORDING AS
C    IREP IS 1 OR 2.
      INTEGER RLIM
      COMMON/BLOCK1/KOUNT
      COMMON/BLOCK2/H,BCON,DCON,XMASS,EN(8),ZETA(8),Z0,CZ,CY,BETACN,
      IF1,FS,USTAR,T,CW,CL,XN,RHO,IREP,IPRINT,RLIM
      IF (KOUNT.GT.0) GO TO 20
      GO TO (11,12),IREP
C
C    INITIALIZATION FOR MODIFIED KAIMAL FORMULA.
11    ZA=(DCON+10.0)/H
      DTILDA=DCON/H
      GO TO 20
C
C    INITIALIZATION FOR FORMULA DEPENDENT ON THE PARAMETER F1.
12    BETAI=0.39*FS**(-2.0/3.0)

```

```

      BETA2=(2.0/3.0)*BETA1
      BETA3=BETACN-BETA1
      BETA4=FS-2.0*F1
      BETA5=0.5*FS-2.0*F1
      C2=(BETA4*BETA3-BETA2*BETA5)/((1.5+ALOG(FS/F1))*BETA4-BETA5)
      IF (BETA4) 16,15,16
15    B2=2.0*(BETA2*(1.5+ALOG(2.0))-BETA3)/(FS*FS)
      GO TO 17
16    B2=(BETA2-C2)/(FS*BETA4)
17    B1=B2-C2/(F1*F1)
      DTILDA=DCON/H
      ZA=(10.0+DCON)/H
20    GO TO (100,200),IREP
C
C   MODIFIED KAIMAL FORMULA
100   CONTINUE
      ZZ=AMAX1(Z,ZA)
      ZZF=(ZZ-DTILDA)/UT
      STILDA=200.0*ZZF/((1.+50.0*W*ZZF)**1.67)
      RETURN
C
C   FORMULA DEPENDENT ON THE PARAMETER F1.
200   CONTINUE
      ZZ=AMAX1(Z,ZA)
      ZUT=(ZZ-DTILDA)/UT
      A=W*ZUT
      IF (A.GE.FS) GO TO 202
      IF (A.GE.F1) GO TO 201
      STILDA=B1*ZUT*(A-2.0*F1)
      GO TO 205
201   STILDA=B2*ZUT*(A-2.0*F1)+C2/W
      GO TO 205
202   STILDA=0.26/(W*A**0.666667)
205   RETURN
      END
C/ */FISTAR
      FUNCTION FISTAR(W)
C   CALCULATION OF THE FUNCTION PHI STAR OF FTILDA.
C   SEE EQ.2.56 OF THIS REPORT.
C   W STANDS FOR FTILDA.
      INTEGER RLIM,RVAL,SVAL
      COMMON/BLOCK2/H,BCON,DCON,XMASS,EN(8),ZETA(8),Z0,CZ,CY,BETACN,
      IF1,FS,USTAR,T,CW,CL,XN,RHO,IREP,IPRINT,RLIM
      COMMON/BLOCK5/RVAL,SVAL
      A=(W/EN(RVAL))*(USTAR/H)
      E=(W/EN(SVAL))*(USTAR/H)
      G=2.*ZETA(RVAL)*A
      D=2.*ZETA(SVAL)*E
      A=1.-A*A
      E=1.-E*E
      FISTAR=(A*E+G*D)/((A*A+G*G)*(E*E+D*D))
      RETURN
      END

```

VALUES OF INPUT PARAMETERS

CONTROL PARAMETERS

IREP = 1
IPRINT = 2
RLIN = 3

STRUCTURAL PARAMETERS

H = 365.000
BCON = 61.000
XMASS = 415000.000
(EN(I),I=1,RLIN)... .100 .300 .500
(ZETA(I),I=1,RLIN)... .010 .010 .010

MICROMETEOROLOGICAL PARAMETERS

Z0 = .070
CZ = 10.000
CY = 16.000
DCON = .000
BETACN = 6.000

CLIMATOLOGICAL PARAMETERS

USTAR = 2.200
T = 3600.000

AERODYNAMIC PARAMETERS

CV = .800
CL = .500
XN = .000
RHO = 1.250

VALUES OF INTEGRATION PARAMETERS FOR VIBRATION MODES R,S = 1, 1

M = 50

(NF(1),1=1,4)... 10 10 20 10

(NN(1),1=1,4)... 5 6 6 6

PEAK = 16.591

(FTILDA(1),1=1,M)... .000

.486 1.697 .849 .097 .146 .195 .243 .292 .340 .389 .438

14.591 14.791 14.991 15.191 15.391 15.591 15.791 15.991 16.191 16.391

16.591 16.791 16.991 17.191 17.391 17.591 17.791 17.991 18.191 18.391

18.591 21.989 25.227 28.545 31.864 35.182 38.500 41.818 45.136 48.455

(ATILDA(1),1=1,M)... .024 .049 .049 .049 .049 .049 .049 .049 .049 .049

.730 1.410 1.410 1.410 1.410 1.410 1.410 1.410 1.410 1.410

.605 .200 .200 .200 .200 .200 .200 .200 .200 .200

.200 .200 .200 .200 .200 .200 .200 .200 .200 .200

1.759 3.318 3.318 3.318 3.318 3.318 3.318 3.318 3.318 3.318

INTEGRAL FOR R,S = 1, 1

AVG OF TRIPLE INTEGRALS = .56557-03 ERR EST = .48887-04

MECH. ADMITT	WEIGHT	TERM	PARTIAL SUM	TERM VAR.	SIGMA	TERU PARTIAL SUMU
.48454545+02	.17637218-01	.13753022+00	.77782385-04	.54764725+02	.44101278-02	.16208044+02
.23478429+04	.41409417+02	.32289933+03	.18262082+00	.24918138-03	.10354287+02	.18643361+03
.55123661+07	.97222804+05	.75811689+06	.42876498+03	.13735790+04	.24310239+05	.10573708+06
.12942169+11	.22826386+09	.17799393+10	.10066728+07	.75716703+10	.69050655+07	.57076619+08
RESPONSE BASED ON FIRST MODE OF VIBRATION						.14767325+09
MEAN ALONGWIND DEFLECTION...	.89357486+00					
RMS OF FLUCTUATING DEFLECTIONS...	.19185240+00					
RMS OF ACCELERATIONS...	.52426819-01					
PEAK FACTOR FOR DEFLECTION...	.34990751+01					
PEAK FACTOR FOR ACCELERATION...	.36010870+01					

VALUES OF INTEGRATION PARAMETERS FOR VIBRATION MODES R,S = 2, 2

M = 50
 (NF(1),I=1,M)... 10 10 20 10
 (NN(1),I=1,M)... 5 6 6 6
 FPEAK = 49.773
 (FTILDA(1),I=1,M)...
 .000 .159 .318 .478 .637 .796 .955 1.115 1.274 1.433
 1.592 6.210 10.828 15.447 20.065 24.683 29.301 33.919 38.537 43.155
 47.773 49.973 50.173 50.373 50.573 50.773 50.973 51.173 51.373 51.573
 51.773 61.727 71.682 81.636 91.591 101.545 111.500 121.455 131.409 141.364
 .080 .159 .159 .159 .159 .159 .159 .159 .159 .159
 2.389 4.618 4.618 4.618 4.618 4.618 4.618 4.618 4.618 4.618
 2.409 .200 .200 .200 .200 .200 .200 .200 .200 .200
 .200 .200 .200 .200 .200 .200 .200 .200 .200 .200
 5.077 9.955 9.955 9.955 9.955 9.955 9.955 9.955 9.955 9.955 23.393
 INTEGRAL FOR R,S = 2, 2

AVG OF TRIPLE INTEGRALS = .19159-04 ERR EST = .37513-05

MECH. ADMITT	WEIGHT	TERM	PARTIAL SUM	TERM VAR.	SIGMA	TERU PARTIAL SUMU
.14136364+03	.20023794-01	.46842026+00	.89743887-05	.30876221-11	.10704430+00	.44818623-03 .20904499+01
.19983677+05	.40014904+03	.93607593+04	.17934129+00	.12330337-02	.22914555+03	.89564090+01 .20777059+03
.39934736+09	.79964494+07	.18706239+09	.35838984+04	.18921042+08	.49240875+06	.57318354+06 .17898199+06 .72491870+06
.79804289+13	.15979846+12	.37381945+13	.71619470+08	.47602896+11	.19664214+15	.14418791+10 .35767183+10 .80102925+10

RESPONSE BASED ON FIRST 2 MODES OF VIBRATION
 MEAN ALONGWIND DEFLECTION... .89726889+00
 RMS OF FLUCTUATING DEFLECTIONS... .19202385+00
 RMS OF ACCELERATIONS... .55985111-01
 PEAK FACTOR FOR DEFLECTION... .35010167+01
 PEAK FACTOR FOR ACCELERATION... .36949763+01

VALUES OF INTEGRATION PARAMETERS FOR VIBRATION MODES R,S = 3, 3

M = 50
 (NF(1),I=1,4)... 10 10 20 10
 (NN(1),I=1,4)... S 6 6 6
 FPEAK = 82.955
 (FTILDA(1),I=1,M)...
 .000 .270 .540 .810 1.079 1.349 1.619 1.889 2.159 2.429
 2.698 10.524 18.350 26.175 34.001 41.827 49.652 57.478 65.303 73.129
 80.955 81.155 81.355 81.555 81.755 81.955 82.155 82.355 82.555 82.755
 82.955 83.155 83.355 83.555 83.755 83.955 84.155 84.355 84.555 84.755
 84.955 101.545 118.136 134.727 151.318 167.909 184.500 201.091 217.682 234.273
 .135 .270 .270 .270 .270 .270 .270 .270 .270 .270
 (ATILDA(1),I=1,M)...
 4.048 7.826 7.826 7.826 7.826 7.826 7.826 7.826 7.826 7.826
 4.013 .200 .200 .200 .200 .200 .200 .200 .200 .200
 .200 .200 .200 .200 .200 .200 .200 .200 .200 .200
 8.395 16.591 16.591 16.591 16.591 16.591 16.591 16.591 16.591 16.591
 INTEGRAL FOR R,S = 3, 3

AVG OF TRIPLE INTEGRALS = .16586-05 ERR EST = .11659-05

MECH. ADMITT	WEIGHT	TERM	PARTIAL SUM	TERM VAR.	SIGMA	TERU PARTIAL SUMU
.23427272+03	.20549871-01	.80121142+00	.13288951-05	.57398974+01	.16326273+00	.64666834-04 .27593338+01
.54883709+05	.11278531+04	.43973454+05	.72934690-01	.77063400+04	.59254307+03	.35491557+01 .16968150+03
.30122215+10	.61900762+08	.24134263+10	.40029263+04	.52190050+08	.42000973+07	.19479083+06 .11927321+07
.16532189+15	.33973434+13	.13245778+15	.21969544+09	.36352050+12	.29842047+11	.10690843+11 .34658360+11

RESPONSE BASED ON FIRST 3 MODES OF VIBRATION
 MEAN ALONGWIND DEFLECTION... .91435113+00
 RMS OF FLUCTUATING DEFLECTIONS... .19204729+00
 RMS OF ACCELERATIONS... .57469588-01
 PEAK FACTOR FOR DEFLECTION... .35013228+01
 PEAK FACTOR FOR ACCELERATION... .37570624+01

U.S. DEPT. OF COMM. BIBLIOGRAPHIC DATA SHEET		1. PUBLICATION OR REPORT NO. NBS BSS-74	2. Gov't Accession No.	3. Recipient's Accession No.
4. TITLE AND SUBTITLE The Buffeting of Tall Structures by Strong Winds			5. Publication Date October 1975	
			6. Performing Organization Code	
7. AUTHOR(S) Emil Simiu and Daniel W. Lozier			8. Performing Organ. Report No.	
9. PERFORMING ORGANIZATION NAME AND ADDRESS NATIONAL BUREAU OF STANDARDS DEPARTMENT OF COMMERCE WASHINGTON, D.C. 20234			10. Project/Task/Work Unit No.	
			11. Contract/Grant No.	
12. Sponsoring Organization Name and Complete Address (Street, City, State, ZIP) Same as No. 9			13. Type of Report & Period Covered BSS	
			14. Sponsoring Agency Code	
15. SUPPLEMENTARY NOTES Library of Congress Catalog Card Number: 75-30727				
16. ABSTRACT (A 200-word or less factual summary of most significant information. If document includes a significant bibliography or literature survey, mention it here.) <p>Certain shortcomings of current procedures for computing alongwind structural response have been shown to result in unrealistic estimates of tall building behavior under the action of strong winds. Differences between predictions of fluctuating response based on various such procedures may be as high as 200%. In recent years, advances in the state of the art have been made which provide a basis for significantly improved alongwind response predictions. The purpose of the present work is to present a procedure for calculating alongwind response which incorporates and utilizes these advances. The basic structural, meteorological and aerodynamic models employed are described, and expressions for the alongwind deflections and accelerations, consistent with those models, are derived. A computer program is presented for calculating the alongwind response of structures with unusual modal shapes or for which the contribution of the higher modes to the response is significant. For more common situations, a simple procedure is presented which makes use of graphs and on the basis of which rapid manual calculations of the alongwind deflections and accelerations can be performed. Numerical examples are given to illustrate the use of the computer program and of the graphs. Results of numerical calculations are used to discuss some of the approximations and errors inherent in the models employed.</p>				
17. KEY WORDS (six to twelve entries; alphabetical order; capitalize only the first letter of the first key word unless a proper name; separated by semicolons) <p>Accelerations; buffeting; building codes; buildings; deflections; dynamic response; gust factors; structural engineering; wind engineering; wind loads.</p>				
18. AVAILABILITY <input checked="" type="checkbox"/> Unlimited <input type="checkbox"/> For Official Distribution. Do Not Release to NTIS <input checked="" type="checkbox"/> Order From Sup. of Doc., U.S. Government Printing Office Washington, D.C. 20402, SD Cat. No. C13. 29:2774 <input type="checkbox"/> Order From National Technical Information Service (NTIS) Springfield, Virginia 22151		19. SECURITY CLASS (THIS REPORT) X UNCLASSIFIED		21. NO. OF PAGES 90
		20. SECURITY CLASS (THIS PAGE) UNCLASSIFIED		22. Price \$ 1.55

(cut here)

**ANNOUNCEMENT OF NEW PUBLICATIONS IN
BUILDING SCIENCE SERIES**

Superintendent of Documents,
Government Printing Office,
Washington, D.C., 20402

Dear Sir:

Please add my name to the announcement list of new publications to be
issued in the series: National Bureau of Standards Building Science Series.

Name.....

Company.....

Address.....

City.....State.....Zip Code.....

(Notification key N-339)



NBS TECHNICAL PUBLICATIONS

PERIODICALS

JOURNAL OF RESEARCH reports National Bureau of Standards research and development in physics, mathematics, and chemistry. It is published in two sections, available separately:

• **Physics and Chemistry (Section A)**

Papers of interest primarily to scientists working in these fields. This section covers a broad range of physical and chemical research, with major emphasis on standards of physical measurement, fundamental constants, and properties of matter. Issued six times a year. Annual subscription: Domestic, \$17.00; Foreign, \$21.25.

• **Mathematical Sciences (Section B)**

Studies and compilations designed mainly for the mathematician and theoretical physicist. Topics in mathematical statistics, theory of experiment design, numerical analysis, theoretical physics and chemistry, logical design and programming of computers and computer systems. Short numerical tables. Issued quarterly. Annual subscription: Domestic, \$9.00; Foreign, \$11.25.

DIMENSIONS/NBS (formerly Technical News Bulletin)—This monthly magazine is published to inform scientists, engineers, businessmen, industry, teachers, students, and consumers of the latest advances in science and technology, with primary emphasis on the work at NBS. The magazine highlights and reviews such issues as energy research, fire protection, building technology, metric conversion, pollution abatement, health and safety, and consumer product performance. In addition, it reports the results of Bureau programs in measurement standards and techniques, properties of matter and materials, engineering standards and services, instrumentation, and automatic data processing.

Annual subscription: Domestic, \$9.45; Foreign, \$11.85.

NONPERIODICALS

Monographs—Major contributions to the technical literature on various subjects related to the Bureau's scientific and technical activities.

Handbooks—Recommended codes of engineering and industrial practice (including safety codes) developed in cooperation with interested industries, professional organizations, and regulatory bodies.

Special Publications—Include proceedings of conferences sponsored by NBS, NBS annual reports, and other special publications appropriate to this grouping such as wall charts, pocket cards, and bibliographies.

Applied Mathematics Series—Mathematical tables, manuals, and studies of special interest to physicists, engineers, chemists, biologists, mathematicians, computer programmers, and others engaged in scientific and technical work.

National Standard Reference Data Series—Provides quantitative data on the physical and chemical properties of materials, compiled from the world's literature and critically evaluated. Developed under a world-wide

program coordinated by NBS. Program under authority of National Standard Data Act (Public Law 90-366).

NOTE: At present the principal publication outlet for these data is the *Journal of Physical and Chemical Reference Data* (JPCRD) published quarterly for NBS by the American Chemical Society (ACS) and the American Institute of Physics (AIP). Subscriptions, reprint, and supplements available from ACS, 1155 Sixteenth St. N.W., Wash. D.C. 20036.

Building Science Series—Disseminates technical information developed at the Bureau on building materials, components, systems, and whole structures. The series presents research results, test methods, and performance criteria related to the structural and environmental functions and the durability and safety characteristics of building elements and systems.

Technical Notes—Studies or reports which are complete in themselves but restrictive in their treatment of a subject. Analogous to monographs but not so comprehensive in scope or definitive in treatment of the subject area. Often serve as a vehicle for final reports of work performed at NBS under the sponsorship of other government agencies.

Voluntary Product Standards—Developed under procedures published by the Department of Commerce in Part 10, Title 15, of the Code of Federal Regulations. The purpose of the standards is to establish nationally recognized requirements for products, and to provide all concerned interests with a basis for common understanding of the characteristics of the products. NBS administers this program as a supplement to the activities of the private sector standardizing organizations.

Federal Information Processing Standards Publications (FIPS PUBS)—Publications in this series collectively constitute the Federal Information Processing Standards Register. Register serves as the official source of information in the Federal Government regarding standards issued by NBS pursuant to the Federal Property and Administrative Services Act of 1949 as amended, Public Law 89-306 (79 Stat. 1127), and as implemented by Executive Order 11717 (38 FR 12315, dated May 11, 1973) and Part 6 of Title 15 CFR (Code of Federal Regulations).

Consumer Information Series—Practical information, based on NBS research and experience, covering areas of interest to the consumer. Easily understandable language and illustrations provide useful background knowledge for shopping in today's technological marketplace.

NBS Interagency Reports (NBSIR)—A special series of interim or final reports on work performed by NBS for outside sponsors (both government and non-government). In general, initial distribution is handled by the sponsor; public distribution is by the National Technical Information Service (Springfield, Va. 22161) in paper copy or microfiche form.

Order NBS publications (except NBSIR's and Bibliographic Subscription Services) from: Superintendent of Documents, Government Printing Office, Washington, D.C. 20402.

BIBLIOGRAPHIC SUBSCRIPTION SERVICES

The following current-awareness and literature-survey bibliographies are issued periodically by the Bureau: Cryogenic Data Center Current Awareness Service

A literature survey issued biweekly. Annual subscription: Domestic, \$20.00; foreign, \$25.00.

Liquefied Natural Gas. A literature survey issued quarterly. Annual subscription: \$20.00.

Superconducting Devices and Materials. A literature

survey issued quarterly. Annual subscription: \$20.00. Send subscription orders and remittances for the preceding bibliographic services to National Technical Information Service, Springfield, Va. 22161.

Electromagnetic Metrology Current Awareness Service. Issued monthly. Annual subscription, \$100.00 (Special rates for multi-subscriptions). Send subscription order and remittance to Electromagnetics Division, National Bureau of Standards, Boulder, Col. 80502.

U.S. DEPARTMENT OF COMMERCE
National Bureau of Standards
Washington, D.C. 20234

OFFICIAL BUSINESS

Penalty for Private Use, \$300

POSTAGE AND FEES PAID
U.S. DEPARTMENT OF COMMERCE
COM-215

SPECIAL FOURTH-CLASS RATE
BOOK

